

Activation of the trigeminal system in the animal models of migraine

Klaudia Flóra Laborc M.D.

Ph.D. thesis

Supervisor: Árpád Párdutz M.D., Ph.D.



Doctoral School of Clinical Medicine
Experimental and Clinical Neuroscience Program
Department of Neurology
Albert Szent-Györgyi Medical School
University of Szeged
Szeged, 2023

Original publications directly related to the Ph.D. thesis:

I.

Klaudia Flóra Laborc, Eleonóra Spekker, Zsuzsanna Bohár, Mónika Szűcs, Gábor Nagy-Grócz, Annamária Fejes-Szabó, László Vécsei, Árpád Párdutz

“Trigeminal activation patterns evoked by chemical stimulation of the dura mater in rats”

The Journal of Headache and Pain 2020 Aug 15;21(1):101

IF: **7.277**

II.

Gábor Nagy-Grócz, Zsuzsanna Bohár, Annamária Fejes-Szabó, **Klaudia Flóra Laborc**, Eleonóra Spekker, Lilla Tar, László Vécsei, Árpád Párdutz

Nitroglycerin increases serotonin transporter expression in rat spinal cord but anandamide modulated this effect

Journal of Chemical Neuroanatomy 2017 Nov;85:13-20

IF: **2.162**

Cumulative impact factor of the publications directly related to the thesis: 9.439

Publications not directly related to the Ph.D. thesis:

I.

Gábor Nagy-Grócz, Lilla Tar, Zsuzsanna Bohár, Annamária Fejes-Szabó, **Klaudia Flóra Laborc**, Eleonóra Spekker, László Vécsei, Árpád Párdutz

The modulatory effect of anandamide on nitroglycerin-induced sensitization in the trigeminal system of the rat

Cephalalgia 2016 Aug;36(9):849-61

IF: **3.609**

II.

Gábor Veres, Annamária Fejes-Szabó, Dénes Zádori, Gábor Nagy-Grócz, Anna M László, Attila Bajtai, István Mándity, Márton Szentirmai, Zsuzsanna Bohár, **Klaudia Laborc**, István Szatmári, Ferenc Fülöp, László Vécsei, Árpád Párdutz

A comparative assessment of two kynurenic acid analogs in the formalin model of trigeminal activation: a behavioral, immunohistochemical and pharmacokinetic study

Journal of Neural Transmission 2017 Jan;124(1):99-112

IF: **3.886**

III.

Gábor Nagy-Grócz, **Klaudia Flóra Laborc**, Gábor Veres, Attila Bajtai, Zsuzsanna Bohár, Dénes Zádori, Annamária Fejes-Szabó, Eleonóra Spekker, László Vécsei, Árpád Párdutz

The effect of systemic nitroglycerin administration on the kynurenine pathway in the rat

Frontiers in Neurology 2017 Jun 14;8:278

IF: **3.508**

IV.

Scott J Denstaedt, Joanna L Spencer-Segal, Michael W Newstead, **Klaudia Laborc**, Anne P Zhao, Alexander Hjelmaas, Xianying Zeng, Huda Akil, Theodore J Standiford, Benjamin H Singer

S100A8/A9 Drives Neuroinflammatory Priming and Protects against Anxiety-like Behavior after Sepsis.

Journal of Immunology 2018 May 1;200(9):3188-3200

IF: **4.718**

V.

Annamária Fejes-Szabó, Eleonóra Spekker, Lilla Tar, Gábor Nagy-Grócz, Zsuzsanna Bohár, **Klaudia Flóra Laborc**, László Vécsei, Árpád Párdutz

Chronic 17 β -estradiol pretreatment has pronociceptive effect on behavioral and morphological changes induced by orofacial formalin in ovariectomized rats.

Journal of Pain Research 2018 Sep 25;11:2011-2021

IF: **2.236**

VI.

Scott J Denstaedt, Joanna L Spencer-Segal, Michael Newstead, **Klaudia Laborc**, Xianying Zeng, Theodore J Standiford, Benjamin H Singer

Persistent Neuroinflammation and Brain Specific Immune Priming in A Novel Survival Model of Murine Pneumosepsis.

Shock 2020 Jul;54(1):78-86

IF: **3.454**

VII.

Joanna L. Spencer-Segal, Benjamin H. Singer, **Klaudia Laborc**, Khyati Somayaji, Stanley J. Watson, Theodore J. Standiford, Huda Akil

“Sepsis survivor mice exhibit a behavioral endocrine syndrome with ventral hippocampal dysfunction”

Psychoneuroendocrinology 2020 Jul;117:104679

IF: **4.732**

VIII.

Eleonóra Spekker, **Klaudia Flóra Laborc**, Zsuzsanna Bohár, Gábor Nagy-Grócz, Annamária Fejes-Szabó, Mónika Szűcs, László Vécsei, Árpád Párdutz

“Effect of dural inflammatory soup application on activation and sensitization markers in the caudal trigeminal nucleus of the rat and the modulatory effects of sumatriptan and kynurenic acid”

The Journal of Headache and Pain 2021 Mar 31;22(1):17.

IF: **8.592**

IX.

Swapnill Gavade, Qiang Wie, Colin Johnson, Savannah Kounelis-Wuillaume, **Klaudia Laborc**, Salisha Baranwal, Huda Akil, Joanna L. Spencer-Segal

Forebrain glucocorticoid receptor overexpression alters behavioral encoding of hippocampal CA1 pyramidal cells in mice

eNeuro 2022 Dec 9;9(6):ENEURO.0126-22.2022

IF: **4.363** (2021)

Cumulative impact factor of publications not directly related to the thesis: 39.098

Total impact factor: 48.537

Table of contents

List of abbreviations:	2
Summary.....	4
Introduction	5
Aims	16
Materials and methods:.....	17
I. The effect of NTG and AEA on the expression of SERT	17
II. Activation patterns following chemical stimulation of the dura	20
Results	24
I. The effect of NTG and AEA on the expression of SERT	24
II. Activation patterns following chemical stimulation of the dura	29
Discussion.....	39
I. The effect of NTG and AEA on the expression of SERT	39
II. Activation patterns following chemical stimulation of the dura	41
Conclusion.....	46
Acknowledgement.....	47
References	48

List of abbreviations:

<i>5-HT</i>	– serotonin
<i>5-HTergic</i>	– serotonergic
<i>5HTTLPR</i>	– serotonin transporter-linked promoter region
<i>ACEA</i>	– arachidonoyl-2'-chloroethylamide
<i>AEA</i>	– anandamide
<i>CFA</i>	– Complete Freund's Adjuvant
<i>cGMP</i>	– cyclic guanosine monophosphate
<i>CGRP</i>	– calcitonin gene-related polypeptide
<i>CSD</i>	– cortical spreading depression
<i>ECs</i>	– endocannabinoid system
<i>FAAH</i>	– fatty acid amide hydrolase
<i>GAPDH</i>	– glyceraldehyde 3-phosphate dehydrogenase
<i>i.p.</i>	– intraperitoneal / intraperitoneally
<i>IL-1β</i>	– interleukin 1 β
<i>iNOS</i>	– inducible nitric oxide synthase
<i>IR</i>	– immunoreactive
<i>IS</i>	– inflammatory soup
<i>nNOS</i>	– neuronal nitric oxide synthase
<i>NO</i>	– nitric oxide
<i>NOS</i>	– nitric oxide synthase
<i>NTG</i>	– nitroglycerin
<i>PBS</i>	– phosphate-buffered saline
<i>PBS-T</i>	– PBS containing 1% Triton-X-100
<i>PET</i>	– positron emission tomography
<i>PFA</i>	– 4% paraformaldehyde in phosphate-buffered saline
<i>PGE₂</i>	– prostaglandin E ₂
<i>PHYS</i>	– physiological saline
<i>s.c.</i>	– subcutaneous / subcutaneously
<i>S.E.M.</i>	– standard error of mean
<i>SERT</i>	– serotonin transporter

<i>SIF</i>	– synthetic interstitial fluid
<i>SP</i>	– substance P
<i>TG</i>	– trigeminal ganglion
<i>TRPV1</i>	– transient receptor potential cation channel subfamily V member 1

Summary

Migraine is one of the most common primary headaches, affecting up to 10% of the Hungarian population. The exact pathogenesis is still not fully understood, but the activation of the trigeminovascular system and neurogenic inflammation have a role in its pathomechanism. Serotonin is also strongly involved in the process, and its metabolite level is increased in the urine during migraine attacks. Serotonin transporter is the protein responsible for the reuptake of this transmitter from the synaptic cleft and extracellular space, and increased levels of its expression were found in the brainstem of migraineurs, showing that it might have a function in the pathomechanism of the disease. The cannabinoid system has a role in descending pain modulation, and its receptors are found in the trigeminal system as well. Anandamide is an endocannabinoid with antinociceptive properties, and it can decrease the activation and sensitization markers in the trigeminal system in the animal model of migraine. There are growing numbers of studies that suggest a connection between the endocannabinoid and the serotonin system, therefore, we aimed to (i) examine the serotonin transporter levels in the caudal trigeminal nucleus (TNC) of rats in the nitroglycerin model of migraine and (ii) study the effect of systemic anandamide treatment. Using immunohistochemistry and Western blot, we found increased levels of serotonin transporter after both nitroglycerin and anandamide injection, while the combined treatment did not change its expression in the TNC, probably through feedback mechanisms.

The application of chemical irritants on the surface of the dura mater is also often used to model migraine. In our second study, we wanted to examine the detailed effect of dural administration of two irritants, Complete Freund's Adjuvant and inflammatory soup, on the c-Fos expression in the TNC using immunohistochemistry. Short-term application of Complete Freund's Adjuvant did not substantially change the c-Fos expression in the TNC; however, research studies suggest that it might be used to model the chronification of migraine. Inflammatory soup significantly increased the number of c-Fos immunoreactive cells in the same area, suggesting that this method might mimic acute attacks in a more precise way.

In conclusion, our findings show evidence of a relationship between serotonin and the endocannabinoid system and offer a better method to examine changes in the trigeminal system in the animal model of migraine, providing insight into the pathomechanism of the disorder.

Introduction

Epidemiology, the importance of migraine

Migraine is one of the most common primary headaches, affecting one billion people worldwide with a rising prevalence (1,2). International Headache Society's classification defines migraine as an episodic headache that usually lasts 4-72 hours. During a migraine attack, four stages can be distinguished, which may overlap or missing in some cases. The prodrome appears with symptoms like fatigue, irritability, and increased yawning that precedes the headache in 67-77% of the patients (3,4). Usually, the patients have the same symptoms; thus, they can predict their migraine attacks reliably (5). The aura manifests as a transient neurological symptom, which develops before or during the headache in 20-30% of the patients, consisting mainly of visual disturbances like flashing lights, zig-zag lines, scotoma, and sometimes sensory or motor signs (6). The headache itself in migraine is moderate or severe in intensity and described as unilateral, throbbing, and aggravated by physical activity like climbing stairs, walking, or bending over. It can be accompanied by photophobia, phonophobia, nausea, vomiting, and allodynia. This is followed by postdrome symptoms, e.g., fatigue, weakness, and cognitive dysfunction (1).

Although epidemiologic studies show that migraine affects 1 out of 10 people, the actual number of patients can be much higher (2). Migraine is often under or misdiagnosed; many people do not seek medical care, making it harder to determine the actual number of patients (7,8). Besides the high prevalence, its severity also places an enormous economic burden on societies. The total cost of migraine was estimated at €50 billion to €111 billion per year in Europe (2012) (9) and \$78 billion in the US annually (2017) (10). Apart from the direct cost of regular medical care for these patients, the indirect cost is also enormous, e.g., productivity loss, contributing to reduced life quality (11). Migraine, especially chronic migraine, is often comorbid with depression, anxiety, addiction, and suicide; altogether, they increase the risk of disabilities and reduce the quality of life (12,13). Also, it is well known that migraine patients are often under- or mistreated or do not have access to proper medication (7). Although more and more migraine-specific therapeutic options are available, therapy efficacy is still around 60%, which might result in poorer patient adherence (14). Acute treatment aims to stop or reverse the progression of the headache, while preventive therapy intends to decrease the

headache frequency or reduce the severity of the migraine attacks. Acute therapy drugs include non-steroid anti-inflammatory agents like acetaminophen, ibuprofen, and naproxen; migraine-specific drugs involve ergot alkaloids, triptans, and the new calcitonin gene-related peptide (CGRP) antagonists. A large scale of medications is used as a preventive therapy, including antiepileptics, antidepressants, beta-blockers, and antibodies against CGRP or its receptor (15,16). Due to the limited effectiveness of the drugs, there is a high demand for further development, however, the lack of knowledge about the exact pathogenesis sets back the advancement of putative therapeutics.

Pathomechanism

The pathomechanism of migraine is still unclear, but it is known that the activation and sensitization of the trigeminal system have a crucial role. The latter is composed of the ophthalmic nerve (V/1), the maxillary nerve (V/2), and the mandibular nerve (V/3); all three branches give sensory fibers to the dura mater and the face. The V/1 is predominantly responsible for the innervation of the meninges, but the V/2 and V/3 nerves also supply the cranial vessels and the dura (17). A plexus of nerve fibers run in the dural - and pial vessel walls; vasodilation of these vessels can activate the first-order neurons in the trigeminal ganglion (TG) (18). Once activated, neurons release multiple vasoactive mediators like CGRP and substance-P (SP), which in turn increases the responsiveness of these ganglion cells to stimuli. This process is called peripheral sensitization, and it contributes to the throbbing nature of the headache and its intensification after physical activity (19). The persistent overactivation of first-order neurons and the released mediators also affect the second-order sensory neurons, leading to the so-called central sensitization in the TNC, where the most important symptom is the appearance of allodynia (20,21). Besides the inflammatory mediators, the ionotropic glutamate receptors (N-methyl-D-aspartate receptors – NMDA, α -amino-3-hydroxy-5-methyl-4-isoxazole propionic acid receptor – AMPA), and nitric oxide synthase (NOS) also play a role in this phenomenon (20,21).

The initial cause of the activation and sensitization process is not fully understood, despite the growing number of studies. Although migraine is a multifactorial disease, genetic predisposition is mainly responsible for the development of the condition (22). After examining the genetic material of patients with and without aura, it was suggested that the two types of

migraine might have a different backgrounds (23). Despite the evidence, researchers could only identify the responsible gene in rare monogenic migraine disorders, like familial hemiplegic migraine (24). Besides genetics, environmental and internal factors also have a role in pathomechanism. This is also indicated by the fact that women are disproportionally affected by migraine; it is assumed that changes in estrogen levels increase hyperexcitability of the brain and makes women more susceptible to headaches (25,26).

Several hypotheses emerged about the processes that could initiate the activation in the trigeminovascular system. The vascular theory is based on Wolff's observations that vasodilation of cranial vessels causes pain, and the vasoconstrictor ergot alkaloids alleviate this pain. Thus, it was assumed that the ischemia caused by vasoconstriction is the main culprit for the aura (27). However, this concept failed to explain the other aspects of the disease, like the prodrome symptoms or allodynia. According to Moskowitz's neurogenic theory, migraine is primarily the result of neural activation followed by the release of vasoactive neuropeptides that induce vascular changes. The neuropeptides like CGRP, SP, and neurokinin A cause vasodilation, plasma extravasation, and mast cell degranulation, which triggers the release of additional proinflammatory substances, thus producing neurogenic inflammation on the meninges (28). Parasympathetic fibers from the sphenopalatine ganglion can also contribute to this process via the release of acetylcholine, vasoactive intestinal polypeptide, and nitric oxide (NO) (29).

The connection between cortical spreading depression (CSD) and migraine with aura was first suggested by Leão and Morison (30). CSD is a slowly spreading depolarization that develops when the extracellular potassium concentration reaches ~40-50 mM (31). High potassium (K^+) levels may activate adjacent brain areas; thus, this depolarization spreads with 2-6 mm/minute velocity, followed by hyperpolarization. Characteristic changes in blood flow accompany this process; a study using laser-Doppler has demonstrated that after the initial hyperemia in the occipital lobe, the blood flow is reduced by 40-90%, and oligemia occurs; these changes last for approximately an hour (32). Imaging studies confirmed that CSD could be correlated to the aura symptoms in migraineurs; during this phase, brain oxygen level-dependent signal propagated with a similar speed as the CSD and was consistent with the retinotopy of the visual percept (33). CSD is also able to activate the trigeminal system and trigger headaches; it is

assumed that during the depolarization phase of the CSD, K^+ , H^+ , and glutamate release can induce neuronal activation of the perivascular fibers (34).

The theory of migraine generators arose after the findings of Weiler et al. in 1995. Using positron emission tomography (PET) scan, they found that multiple brain regions were active during and after a spontaneous migraine attack, including nucleus raphe magnus (NRM), dorsal raphe (DR), periaqueductal grey (PAG), rostroventro-medial medulla (RVM), and locus coeruleus (35). These structures are part of the descending pain modulation system and give efferent innervation to the dorsal horn of the spinal cord and medulla through the dorsolateral funiculus. Dysfunction or lesion of these brain areas might have a role in the etiology of migraine; however, it is still unclear if the activation of these regions initiates the attack or if it is just an epiphenomenon (36).

Serotonin system and pain

Serotonin (5-HT) is a monoamine neurotransmitter involved in many physiological and pathological processes, including migraine (37,38). Most (~90%) of the 5-HT synthesis occurs in the enteric nervous system, while only 1-2% of the 5-HT is produced in the brain, mainly in the serotonergic (5-HTergic) neurons of the raphe nuclei (39). 5-HT has a complex role in nociception; depending on the site of action, receptor subtype, and cell type, 5-HT can facilitate pain as a proinflammatory mediator, while the descending pain modulatory system can either reduce or enhance spinal pain transmission (40).

5-HT acts as a pronociceptive mediator in the periphery after nerve injury or inflammation that can activate and sensitize nociceptors. Endogenous inflammatory agents, including 5-HT, are released after thermal injury or inflammation, causing sensitization of the neurons, which in turn can increase pain-related behavior in animals (41,42). Furthermore, when 5-HT was injected into the skin of volunteers, 5-HT caused increased excitability of C fibers and, consequently, pain perception and hyperalgesia (43). In summary, the 5-HT can activate and decrease the threshold of nociceptors and play a role in inflammation and nerve injury.

The descending pain modulatory system consists of multiple, widely distributed brain structures that alter the activity of nociceptors primarily by releasing monoamine transmitters. (35). The dorsal horn of the spinal cord and medulla receives input from PAG-RVM through the dorsolateral funiculus; they can either decrease or increase spinal nociceptive transmission.

Electrical stimulation of the so-called migraine generator structures, like PAG, RVM, and NRM, produces antinociception and 5-HT release in the spinal cord, and the pretreatment with a nonselective 5-HT antagonist blocked this effect (44). It has been known for a long time that 5-HT has a role in migraine pathogenesis, after Sicuteri et al. detected increased urinary levels of its breakdown product, hydroxy-indoleacetic acid, during migraine attacks (45). This hypothesis is supported by the observation that 5-HT depletion by reserpine was able to trigger migraine-like headaches, which might indicate that migraine can be a consequence of decreased 5-HTergic transmission (46). An animal model of migraine showed similar findings; 5-HT-depleted rats showed an increased number of c-Fos immunoreactive (IR) cells in the TNC after chemical stimulation of the dura. Consequently, a low 5-HT state might facilitate trigeminal pain transmission, but the exact role of the 5-HT is unclear in migraine headache. (47).

Serotonin transporter (SERT) is a protein responsible for the reuptake of the 5-HT, thus playing a pivotal role in regulating its level in the synaptic cleft and extracellular space. Approximately 10% of the released 5-HT is lost, while most of it is taken up by monoamine transporters, including SERT (48). SLC6A4 gene codes SERT; polymorphism of the promoter region (serotonin transporter linked promoter region - 5HTTLPR) of the gene is associated with several neuropsychiatric diseases, including migraine with aura (49). 5HTTLPR alleles usually consist of fourteen (short allele – s) or sixteen (long allele – l) repeated elements. Previous studies indicate that the s allele is associated with less effective transcription of the gene promoter and, consequently, decreased SERT expression and reduced reuptake of 5-HT (50). Kotani et al. found that 5HTTLPR polymorphism affects the frequency of migraine headaches, patients with the s/s genotype had more migraine attacks than patients with either l/l or l/s genotypes (51). Additionally, an imaging study showed that migraine patients had increased SERT availability interictally in the mesopontine brainstem compared to healthy volunteers, which might be the result of constitutional upregulation of the transporter or compensatory overexpression due to altered 5-HT neurotransmission (52).

Taken together, 5-HT regulates inflammation and pain transmission in a complex manner; increasing amount of data suggests that altered 5-HT neurotransmission can play a role in migraine.

c-Fos

c-Fos is a proto-oncogene, its protein, Fos, is expressed in many cell types, including neurons and glial cells, and it is a frequently used activation marker to map functional pain pathways (53–55). c-Fos is considered an immediate early gene, the expression of the gene starts a few minutes after depolarization, and it can be detected until the stimulus ceases with a half-life of two hours (56). In general, measuring its expression levels is used for (i) neural circuitry mapping, (ii) to examine the sensitivity and receptive field changes in sensitization processes, and (iii) to investigate the effect of potential drugs in pharmacological studies. Research examining the activation of the trigeminal system provided valuable insight into the pathomechanism of migraine. In an animal model of migraine, electrical stimulation of the superior sagittal sinus induced c-Fos expression in PAG and hypothalamus, allowing to map additional pathways that can be involved in migraine (57,58). In addition, it was shown that injection of inflammatory soup (IS) to the dura mater caused trigeminal sensitization, and consequently, increased touch-evoked c-Fos expression was detected on day 8 compared to day 1 in the dorsal horns of TNC and spinal cord (59). In a pharmacological study, sumatriptan was able to reduce the number of c-Fos IR cells in the trigeminal system after chemical stimulation of the dura, so it can be stated that this study successfully predicted the clinical effectiveness of sumatriptan in migraine (60).

Although mapping c-Fos IR cells is a simple and widely used method to examine activation in pain processing pathways, it has its own shortcomings. Not all activated neurons become immunopositive for c-Fos, and not all of them are neurons (55). In addition, the detection of the c-Fos signal often requires intense stimulation, which exceeds the physiological level; thus, the lack of immunopositive cells does not mean the lack of neural activation (61). c-Fos is also thought to be unspecific since a wide variety of effects might increase its level. To get an accurate picture of activation patterns, we must also consider the timeline and the half-life of c-Fos. The level of its mRNA peaks at approximately 30 minutes, while the protein level culminates roughly two hours after the stimulus. However, the onset of the maximal signal intensity can vary across different species or after different altering factors; therefore, the timing of the experiments is essential (58,62). Another pitfall of the technique is the assessment of the c-Fos positive cells. Cell counting can be subjective, but a well-established counting guideline was introduced to reduce observer-dependent bias (63). In summary, measuring the c-Fos

expression either by in situ hybridization or immunohistochemistry is an easy and widely accepted technique to study activation patterns and identify pain pathways in the trigeminal system. Meticulous control of the experiment provides a reliable method to compare the effects of different stimuli and test putative pain relief drugs in animals.

Animal models

Nitroglycerin model

Nitroglycerin (NTG), or glyceryl trinitrate, is a drug that has been used in clinical practice since the 1800s (64). Due to its lipophilic properties, it can diffuse freely through membranes and reaches the CNS through the blood-brain barrier. NTG has a short half-life in plasma (1-4 minutes), but it accumulates in lipophilic tissues, including the brain, which can prolong its metabolism (65,66). NTG is rapidly converted to NO within cells by enzymes like mitochondrial aldehyde dehydrogenase or nonenzymatic catabolism (66–68). NO can activate guanylate cyclase, which will increase the cyclic guanosine monophosphate (cGMP) level (69). NO is a potent vasodilator, the increasing level of cGMP potentiates the myosin dephosphorylation that results in smooth muscle relaxation in blood vessels (70).

NO donors have a well-known side effect, they can trigger headaches in healthy subjects, but in 80% of migraine patients, NTG has a biphasic effect (71,72). In addition to the immediate headache, a delayed migraine-like headache develops after 4-6 hours, fulfilling the International Classification of Headache Disorders' criteria (71). Based on this observation, systemic administration of NTG is often used as a human migraine model. As vasodilators (including NTG) can cause headaches, and NTG-induced immediate headaches were associated with its vasoactive properties, but imaging studies questioned this hypothesis (73,74). Following the immediate headache, prodrome symptoms of migraine can also develop after NTG administration, along with activation of the so-called migraine generator structures like the hypothalamus and PAG (75,76). The origin of the NTG-induced delayed headache is also not fully understood, though similar to migraine, brainstem activation was detected during these headaches by a PET study (77,78). The vasoactive effects of NTG cannot explain the migraine-like attack that develops after 4-6 hours; even the half-life of its metabolites does not exceed forty minutes (79). After it was shown that increased levels of CGRP and SP in the external

jugular vein during NTG-induced headaches, it was suspected that NTG could also induce proinflammatory pathways, which was confirmed in animal experiments (80,81).

Several animal studies support that systemic administration of NTG is able to activate and sensitize the trigeminal system. Tassorelli et al. found that NTG increases c-Fos expression in various brain areas, including migraine-related structures like the PAG and TNC. Similar to the onset of the NTG-induced delayed headache in migraine patients, Fos expression in these animals reached its peak four hours after the NTG injection (82). It has also been shown that NTG treatment not only activated second-order sensory neurons in TNC, but also sensitized them to electrical stimulation of the superior sagittal sinus (83). Increasing amount of evidence indicates that NTG upregulates inflammatory processes and can play a role in the activation and sensitization of TNC neurons. For instance, systemic NTG is able to decrease the area covered by CGRP IR fibers in the TNC, indicating CGRP release, which is in line with the increased CGRP levels found in migraine patients (80,84). In addition, elevated levels of other inflammatory mediators like interleukin 1 β (IL-1 β), interleukin 6, and enhanced NO production via inducible NOS (iNOS) were shown in dural macrophages several hours after NTG injection in rats (85). In a later study, the enhanced activity of nuclear factor- κ B was detected following the iNOS expression, which has a pivotal role in inflammation (86). Besides iNOS, neuronal NOS (nNOS) levels are also increased in the TNC in rats, which was prevented by lysine-acetyl-salicylate pretreatment; this suggests the involvement of the cyclo-oxygenase pathway after NTG administration (87,88). In multiple behavior studies, NTG also induced hyperalgesia and allodynia in animals (89,90). In addition to hyperalgesia, light aversion was also observed in rats in the light-dark box paradigm, similar to photophobia in patients (91). Moreover, NTG-induced extracephalic allodynia was decreased by a migraine-specific medication, sumatriptan, in mice, confirming its validity in drug testing (92).

Chemical stimulation of the dura mater as an animal model of trigeminal activation

The idea of modeling headaches with chemical stimulation of the dura arose from the fact that subarachnoid hemorrhage caused severe headaches. Later, the use of intracisternal carrageen instead of autologous blood was proposed as a new animal model of headache, and they found that two migraine-specific drugs; sumatriptan and dihydroergotamine, successfully reduced the c-Fos IR cells in the TNC in this experimental setup (60). Other substances like capsaicin,

Complete Freund's Adjuvant (CFA), and IS were also used for chemical stimulation of the meninges in various experiments (93–95).

The IS consists of multiple inflammatory mediators: 5-HT, bradykinin, prostaglandin E₂ (PGE₂), and histamine. Strassman et al. used IS to show that it not only activates the secondary neuronal cells, but also sensitizes them to mechanical stimulation (95). This was confirmed in behavioral studies, in which IS-induced cutaneous allodynia in the face and hind paws of rats, decreased the withdrawal threshold to von Frey filament stimulation with the maximum effect after three hours (59). The inflammatory agents directly or indirectly (through the release of other mediators) activate and sensitize the trigeminal system. Hoffman et al. detected increased levels of CGRP in the blood and increased CGRP IR fibers in the TNC; additionally, they confirmed that the first-order neurons were the primary source of CGRP after cisternal IS injection (96,97).

CFA is a suspension of dried, killed *Mycobacterium tuberculosis* and is commonly used to induce inflammation in joints and skin. CFA and IS, when applied to the dura, increased mediators like IL-1 β in the TG; these data suggest the presence of neurogenic inflammation after such chemical stimulation of the meninges (94).

Migraine-specific (e.g., sumatriptan) and unspecific drugs (e.g., naproxen, ketorolac) were shown to be effective in this experimental setup; while neurokinin-1 antagonists were ineffective both in clinical trials and after chemical stimulation of the dura in rodents, demonstrating the translation potential of this model (98–101).

Taken together, although no animal model can show all the aspects of migraine, systemic use of NTG and chemical stimulation of the dura can activate and sensitize the trigeminal system and consequently present with pain- and allodynia-related behavior in rodents. These experimental paradigms successfully predicted the effectiveness of drugs; thus, they can be used to model migraine headache.

Anandamide

Cannabis has been used for alleviating pain, migraine, and nausea for a long time; its active ingredient, tetrahydrocannabinol, binds to cannabinoid receptors (102). The first endogenous agonist of the cannabinoid receptors, 2-arachidonoyl ethanolamine, also known as anandamide (AEA), was identified in 1992 (103). The endocannabinoid system (ECs) affects numerous

physiological processes; it regulates appetite and energy metabolism, immune function, memory, circadian rhythm, thermoregulation, and pain modulation (104–108). They exert their functions at the cannabinoid 1 (CB1) and cannabinoid 2 (CB2) receptors, but even in the same brain region, in different cell types, agonist binding can activate different signaling pathways (109). CB1 is mainly expressed in the nervous system, e.g., olfactory bulbs, neocortex, hippocampus, amygdala, basal ganglia, thalamus, hypothalamic nuclei, cerebral cortex, and parts of the brainstem, including the descending pain-modulating pathways (110). CB1 is found mainly presynaptically on glutamatergic and gamma-aminobutyric acidergic neurons, but in the cervical spinal cord, CB receptors have been detected both presynaptically and postsynaptically (111). CB2 is expressed primarily on the immune system cells, mainly on T cells, B cells, and macrophages. The receptor occurs only sporadically in the central nervous system, mostly on microglia (112). Cannabinoid receptors are also abundant in the periphery, dorsal root ganglions, and the skin (113,114).

The ECs play a crucial part in pain modulation. Cannabinoids administered peripherally or intrathecally were able to reduce hyperalgesia and allodynia, alleviate local edema, and decrease the activity of nociceptive neurons (115,116). When examining brain structures involved in pain transmission, Palkovics et al. found that endocannabinoids were abundant in the dorsal horn of the spinal cord and TNC (117). The antinociceptive effect of endocannabinoids, including AEA, may be related to the activation of CB1 and CB2 receptors, although the CB1 receptor has a more prominent role (118). AEA also exerts neuromodulatory effects through transient receptor potential cation channel subfamily V member 1 (TRPV1) receptors, also known as the capsaicin receptor or vanilloid receptors, which are nonselective cation channels. Two endocannabinoids, AEA and N-arachidonoyl dopamine, are agonists of TRPV1, and after activating the receptor, sodium and calcium flow into the cell, leading to depolarization (119). If prolonged or repeated, this might cause a significant increase in intracellular calcium concentration affecting multiple cell organelles. As a result of a series of different processes, the neurons can become refractory to further noxious stimulation; this phenomenon is responsible for the analgesic properties of capsaicin (120). Thus, both overactivation and inhibition of the TRPV1 receptor can reduce hyperalgesia. Like capsaicin, AEA is able to desensitize TRPV1 upon activation, which can contribute to its pain-relieving effects (121).

ECs modulates the 5-HTergic system peripherally and centrally, which can also play a role in their antinociceptive properties. A selective CB1 agonist, arachidonoyl-2'-chloroethylamide (ACEA), decreased the 5-HT level in the peripheral blood, and this effect was prevented with pretreatment with a CB1 receptor agonist, showing that cannabinoids can affect 5-HT levels in the periphery (122). Additionally, selective inhibition of CB1 reduced the firing rate of DR 5-HTergic cells in vitro, suggesting that endocannabinoids might regulate 5-HTergic DR cells tonically (123).

Russo postulated that ECs might be deficient in multiple pain-related conditions like migraine, fibromyalgia, or irritable bowel syndrome (124). This hypothesis was based on the fact that female migraineurs have higher platelet activity of fatty acid amide hydrolase (FAAH), which suggests increased breakdown of AEA in female migraine patients (125). ECs deficiency was further supported by a study that detected lower AEA levels in the cerebrospinal fluid of chronic migraineurs compared to healthy volunteers (126). Additionally, a negative correlation between cerebrospinal fluid levels of AEA–CGRP and AEA–nitrate was shown in these patients (126). When AEA was given to rats, it alleviated dural vessel dilation after CGRP, capsaicin, and a NO-donor (127). In an animal model of migraine, intraperitoneal (i.p.) AEA was also able to decrease the Fos-positive cells in the TNC after NTG administration; these studies suggest AEA can be used to modulate nociceptive transmission in the trigeminal system (128).

In summary, endocannabinoids are involved in pain modulation, and there might be a connection between ECs and the 5-HTergic system. Multiple experiments suggested an ECs deficiency in migraine, and AEA treatment was able to decrease dural vessel dilation and c-Fos immunopositive cells in migraine models. Based on these findings, further studies are needed to explore whether endocannabinoids could be used as a possible treatment option for migraine.

Aims

1. To examine the expression of SERT in the dorsal horn of TNC after systemic administration of NTG.
2. To investigate whether the AEA affects the expression of SERT in the NTG model.
3. To map the activation pattern in the dorsal horn of the TNC after chemical stimulation of the dura mater.

Materials and methods:

All procedures followed the guidelines of the Use of Animals in Research of the International Association for the Study of Pain and the directive of the European Parliament (86/609/ECC; 2010/63/EU). Committee of the Animal Research of University of Szeged (I-74-12/2012; I-74-49/2017) and the Scientific Ethics Committee for Animal Research of the Protection of Animals Advisory Board (XI./352/2012; XI./1098/2018).

I. The effect of NTG and AEA on the expression of SERT

Animals, experimental groups:

Forty-four adult male Sprague-Dawley rats weighing 200-250 g were used. The animals were raised under standard laboratory conditions, regular rat chow, and water *ad libitum*, with light cycle of 12-12h. Animals were divided into four groups, n=6 per group for immunohistochemistry and n=5 per group for Western blot (*Fig. 1.*). Rats in the first group (“Placebo”) received physiological saline (PHYS) as pretreatment and vehicle solution as treatment. PHYS and NTG were injected to the second group (“NTG”). AEA was administered as pretreatment to the third (“AEA”) and fourth (“AEA+NTG”) groups, and they received NTG or vehicle solution later. Animals were perfused four hours following the NTG or PHYS injections.

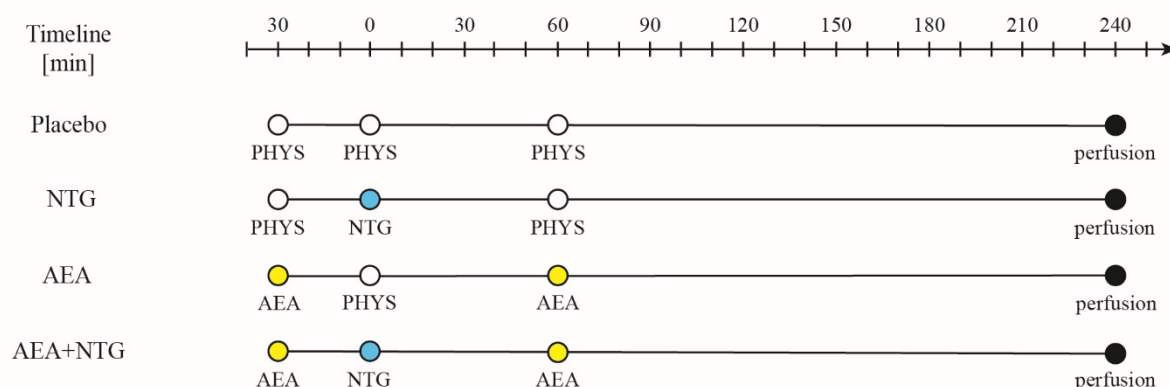


Figure 1. Schematic timeline of the experimental design. Animals in the “Placebo” group received only i.p. PHYS treatment, and NTG and PHYS were administered to the “NTG” group. Rats in “AEA” and “AEA+NTG” groups received AEA pretreatment before the vehicle or NTG injections.

Drugs:

The NTG was administered i.p. (dosage: 10 mg/kg body weight, Pohl Boskamp, Hohenlocksted, Germany), and control groups received the same volume of PHYS. AEA (Sigma-Aldrich, St. Louis, MO, USA) was dissolved in PHYS, and it was injected two times (dosage: 2×5 mg/kg, i.p.), thirty minutes before PHYS/NTG treatment and sixty minutes after, to counterbalance the short half-life of the drug (129).

Immunohistochemistry:

Animals were deeply anesthetized with chloral hydrate (dosage: 0.4 g/kg body weight) and perfused intracardially using 100 mL phosphate-buffered saline (PBS; 0.1 mM; pH 7.4) and 500 mL formaldehyde (PFA, 4% in PBS). Segments corresponding to TNC (obex -5 mm to -11 mm) were removed and postfixed overnight with formaldehyde. Cryoprotection was performed using gradient sucrose solutions (10-30%). 30 µm transverse sections were cut with a cryostat; the free-floating sections were serially collected in wells containing cold PBS with 0.1% sodium azide. Then they were rinsed in PBS, and endogenous peroxidase activity was suppressed by 0.3% H₂O₂ in PBS, followed by washing several times using PBS containing 1% Triton X-100 (PBS-T) and incubation for two nights at 4 °C in anti-SERT primary antibody (Merck Millipore; ab 9726; dilution of 1:100 000). The reaction was visualized by Vectastain (PK6101) avidin-biotin kit and using nickel ammonium sulfate-intensified 3,3'-diaminobenzidine. After mounting the sections on glass slides, they were cleared in xylene and coverslipped. The specificity of the immune reaction was verified by omitting the primary antiserum.

Using a Zeiss AxioImager microscope supplied with an AxioCam MRc Rev.3 camera (Carl Zeiss Microscopy, Jena, Germany), photomicrographs were taken of the stained sections of TNC using a 20× objective. All measurements and evaluations were implemented by an observer blind to the experimental groups. The density of the SERT IR fibers was measured by Image-Pro Plus 6.21 software (Media Cybernetics). The dorsal horn's laminae I, II, and III borders were defined manually (area of interest). In greyscale images, the background level of immunostaining intensity was assessed and used as a threshold to segment pixels with grey levels above the background. The area covered by the IR fibers was expressed as a cumulative number of pixels with densities above the threshold. The relative area innervated by

immunolabelled fibers is calculated for each lamina and shown in area fractions (%) of the corresponding structures. Background intensities in indifferent areas on the sections with non-specific staining were determined and used as inter-experimental controls to exclude any difference in staining efficiency in separate experiments. To assess the size of IR varicosities, we took photomicrographs using a higher magnification (40×) objective of the same digital system. Immunolabelled processes in focus were selected and defined as single objects. The area of IR varicosities was measured using the same method mentioned above.

Western blot:

After transcardial perfusion with 100 ml PBS, the segments corresponding to the TNC were extracted, and dorsal horns were separated and stored in cold lysis buffer containing 50 mM Tris-HCl and 150 mM NaCl at -80°C . The samples were sonicated in ice IGEPAL, 0.1% cholic acid, 2 mg/mL leupeptin, 2 mM phenylmethyl-sulphonyl fluoride, 1 mg/mL pepstatin, 2 mM EDTA and 0.1% sodium dodecyl sulfate. Following centrifugation (12000 RPM; 10 minutes; at 4°C), the supernatants were separated and stored at -20°C until use. Protein concentration was measured with BCA Protein Assay Kit, and bovine serum albumin was used as standard. The samples were mixed with sample buffer and denatured by boiling before loading. The Page Ruler Prestained Protein Ladder (Thermo Scientific; 10-170 kDa) was used to define approximate molecular weights. Protein samples (20 mg/each lane) were separated by standard SDS polyacrylamide gel electrophoresis on 10% Tris-Glycine gel and electro-transferred onto Amersham Hybond-ECL nitrocellulose membrane (0.45 mm pore size; GE Healthcare). After the transfer, membranes were blocked using Tris-buffered saline containing Tween 20 (TBST) and 5% non-fat dry milk for an hour at room temperature. Membranes were incubated in TBST containing 1% non-fat dry milk and SERT antibody (Merck Millipore; ab9726; at dilution: 1:2000) or glyceraldehyde 3-phosphate dehydrogenase (GAPDH) antibody (Cell Signaling Technologies; 8884; dilution 1:1000) overnight at 4°C or room temperature. Then membranes were immersed in TBST containing 1% non-fat dry milk and horseradish peroxidase-conjugated anti-rabbit secondary antibody (Santa Cruz Biotechnology; sc-2030) for 2 hours at room temperature. As the last step, membranes were incubated with SuperSignal West Pico Chemiluminescent Substrate. For visualization of the protein bands, we used Care-Stream Kodak Biomax Light film.

Films were scanned, then densitometric analysis was performed with Java ImageJ 1.47v analysis software (National Institute of Health). Results were normalized to GAPDH, and it also served as a control to ensure the loading of the equivalent amount of protein.

Statistical analysis:

Statistical analyses were performed in SPSS Statistics software (Version 20.0 for Windows, SPSS Inc.). One-way analysis of variance was used, followed by Fisher's Least Significant Difference post hoc test, $p < 0.05$ was considered statistically significant. We used the Shapiro-Wilk test for testing normality. Values are reported as mean + standard error of mean (S.E.M.).

II. Activation patterns following chemical stimulation of the dura

Animals, experimental groups:

Forty-eight adult male Sprague-Dawley rats (weight 240-430 g) were divided into twelve groups (*Fig. 2.*). The animals were raised and housed under standard laboratory conditions, light-dark cycle of 12-12 h, regular rat chow, and water *ad libitum*.

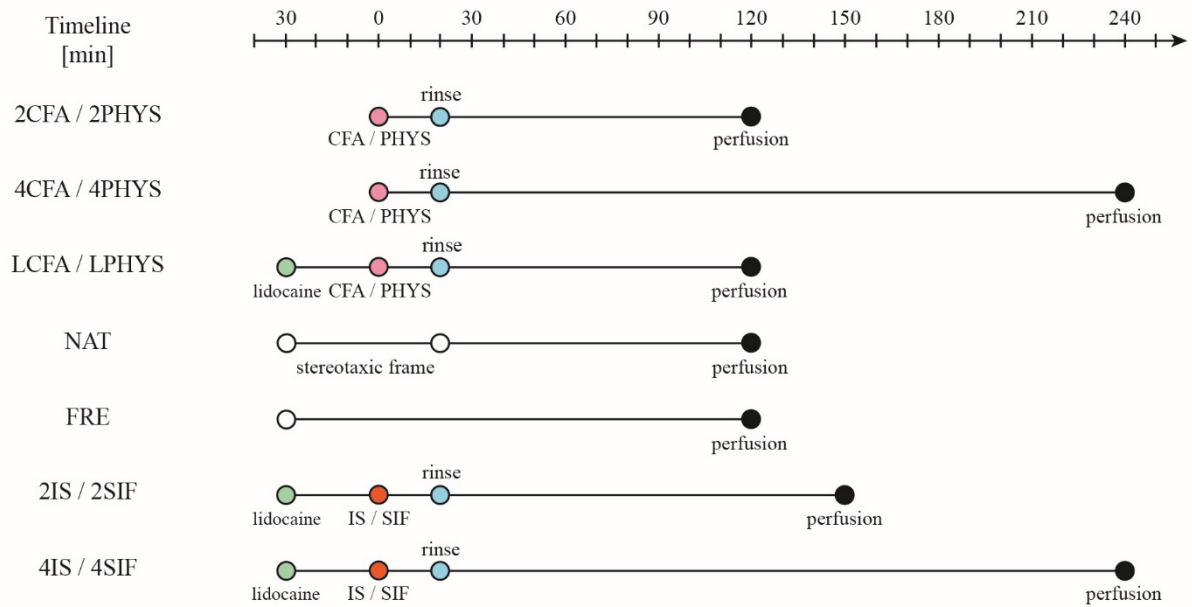


Figure 2. Schematic timeline of experimental design. The dural CFA/saline/IS/SIF application was considered the “0” time point. LCFA, LPHYS, 2IS, 2SIF, 4IS, 4SIF groups received s.c. lidocaine before the skin incision. The surface of the dura was rinsed off with either saline or SIF 20 minutes after dural treatment. Animals in NAT and FRE groups were only anesthetized and placed in a stereotaxic frame (NAT) or left on a heating pad (FRE) for the same duration as in other groups.

Two groups did not undergo craniotomy and were only anesthetized (FRE) or anesthetized and fixed in a stereotaxic instrument (NAT) for two hours. Animals in 2PHYS/2CFA and 4PHYS/4CFA groups underwent surgery, and PHYS or CFA was applied on the surface of the dura mater. Two (FRE, NAT, 2PHYS/2CFA) or four hours (4PHYS/4CFA) after the PHYS/CFA application, rats were perfused (n=3, n=3, n=4, n=4, n=3, n=3). In LPHYS/LCFA groups, rats underwent the same procedure as 2CFA/2PHYS groups, but local lidocaine was used on the scalp before the head incision (n=2, n=2). Animals in 2SIF/2IS and 4SIF/4IS groups had the same surgical procedure as LPHYS/LCFA group, but synthetic interstitial fluid (SIF) or IS was applied on the dural surface. 2.5- and 4-hour survival time was chosen to ensure we avoid any activation due to surgery (n=6/group).

Drugs:

We used two different inflammatory agents in our experiments: CFA contained dried, inactivated *Mycobacterium tuberculosis* in mineral oil (Sigma-Aldrich, St. Louis, MO, USA), and IS contained 1 mM bradykinin, 100 μ M PGE₂, 1 mM 5-HT, 1 mM histamine, (pH 5.0) in 10 mM HEPES buffer. Control groups received 0.9% PHYS or SIF (135 mM NaCl, 5 mM KCl, 1 mM MgCl₂, 5 mM CaCl₂, 10 mM glucose, in 10 mM HEPES buffer, pH 7.3). For local lidocaine anesthesia, lidocaine (20 mg/mL; Egis, Budapest, Hungary) was diluted with PHYS to have a final concentration of 10 mg/ml (1%).

Procedures:

Before each procedure, animals were deeply anesthetized using chloral hydrate (4%; 400 mg/kg; i.p.) and placed in a stereotaxic apparatus. The scalp was infiltrated with lidocaine (dosage of 4.5 mg/kg; subcutaneously [s.c.]) in LCFA, LPHYS, 2SIF, 2IS, 4SIF, and 4IS groups. A 2 mm \times 2 mm craniotomy (5 mm posterior from the bregma and 3 mm lateral of the midline, above the right hemisphere) was carefully drilled using saline for cooling, with slow speed, avoiding any injury of the dura mater. 10 μ L CFA (in groups 2CFA, 4CFA, LCFA) or IS (2IS, 4IS) was applied on the dural surface. While control groups received PHYS (2PHYS, 4PHYS, LPHYS groups) or SIF (2SIF, 4SIF). To prevent the local spreading of the chemicals, the head position was adjusted in the stereotaxic frame so the dorsal surface of the skull was horizontal. After 20 minutes, the area was washed with either physiological saline or SIF. A saline or SIF-soaked cotton ball was placed carefully on top to prevent drying out of the dura.

After the surgery, animals were placed on a heating pad, and they were kept under anesthesia. 2 hours (2PHYS, 2CFA, LPHYS, LCFA, NAT, FRE), 2.5 hours (2IS, 2SIF), or 4 hours (4PHYS, 4CFA, 4IS, 4SIF) after the treatment with inflammatory mediators, rats were transcardially perfused under deep anesthesia. 50 mL of 0.1 M PBS and 200 mL of 4% PFA were used for the perfusion. The brain with the cervical spinal cord was removed and left overnight in the same fixative for postfixation.

Immunohistochemistry:

After postfixation and cryoprotection with 30% sucrose solution, a superficial, angled rostrocaudal cut was made on the ventral, left side of the brainstem, and spinal cord. This mark allowed us to determine the correct rostrocaudal order and orientation of the free-floating sections. Cryostat free-floating sections of 30 μ m thickness were cut, and thirty serials of them were collected into ten wells starting from one millimeter rostrally to the obex. Every tenth section was used for staining; being 500 μ m apart. Then they were blocked with 0.3% H₂O₂ in PBS and after several washes with PBS-T, sections were immersed in 10% goat serum in PBS-T for an hour. The incubation with primary antibody for c-Fos (1:2000, sc-52, Santa Cruz Biotechnology, Dallas, TX, USA) was on a shaker overnight at room temperature. To visualize the reaction, we used the Vectastatin Elite avidin-biotin kit (PK6101, Vector Laboratories, Burlingame, CA, USA) with 3,3'-diaminobenzidine (Sigma-Aldrich, St. Louis, MO, USA) intensified by nickel-ammonium-sulfate. The samples were mounted on glass slides, cleared in xylene, and coverslipped. The specificity of the immune labeling was tested by omitting the primary antiserum.

An observer blind to the procedures counted the IR cells in laminae I-II of the dorsal horn and also according to the somatotopic representation of the trigeminal nerve branches (based on Strassman and Vos, 1993 (130)), for the assessment, we followed the guidelines of Hammond et al. (63). The ventral, intermediate, and dorsal parts of the dorsal horn were considered to be equivalent to the area of the V/1, V/2, and V/3 branch. Nikon Optiphot-2 light microscope (Nikon, Tokyo, Japan) under 10 \times objective was used for cell counting. Representative photographs were taken by an AxioImager M2 microscope (Carl Zeiss, Germany) using AxioCam MRc rev.3 camera with a 20 \times objective.

Statistical analysis:

The collected data were analyzed in the 2IS, 2SIF, 4IS, and 4SIF groups using IBM SPSS 24.0 (IBM Corp, Armonk, NY, USA). For all other groups, no statistical analysis was used because of the small sample size; the sample size was not further increased to minimize the number of animals used. The effects of dural treatments, distance from obex, and sides (treated or untreated) on c-Fos cell numbers were examined with the mixed-design variance of analysis (MIXED-ANOVA) models with treatment, distance, and side as repeated measures (within-subject factor) and the group as between-subject factors. Pairwise comparisons were made on estimated marginal means, considering the presence or absence of interaction; the Holm-Sidak method was performed to adjust p-values. $p < 0.05$ was considered statistically significant. Graphs were made in GraphPad Prism 8.0.1, and all figures show data as mean + S.E.M.

Results

I. The effect of NTG and AEA on the expression of SERT

Immunohistochemistry

NTG and AEA increased SERT expression in the TNC, but the combined treatment minimized this effect

We examined the transverse sections of the TNC cord under 20× objective of a microscope. We found abundant SERT-positive fibers in the dorsal horn's superficial layers (laminae I-III). The relative area covered by SERT immunolabelled fibers was significantly higher in NTG-treated animals compared to animals in the placebo group ($p < 0.01$), AEA had the same effect on the SERT fibers ($p < 0.01$; $p < 0.001$). Surprisingly, the combined NTG+AEA treated group had significantly decreased SERT area fractions ($p < 0.01$) compared to either NTG or AEA groups. Lamina I: $F(3,20)=26.556$; $p=2 \times 10^{-6}$; lamina II: $F(3,20)=92.104$; $p=2.62 \times 10^{-10}$; lamina III: $F(3,20)=45.300$; groups lamina I: $F(3,20)=26.556$; $p=2 \times 10^{-6}$; lamina II: $F=45.300$; $p=4.81 \times 10^{-8}$. *Fig. 3-6*

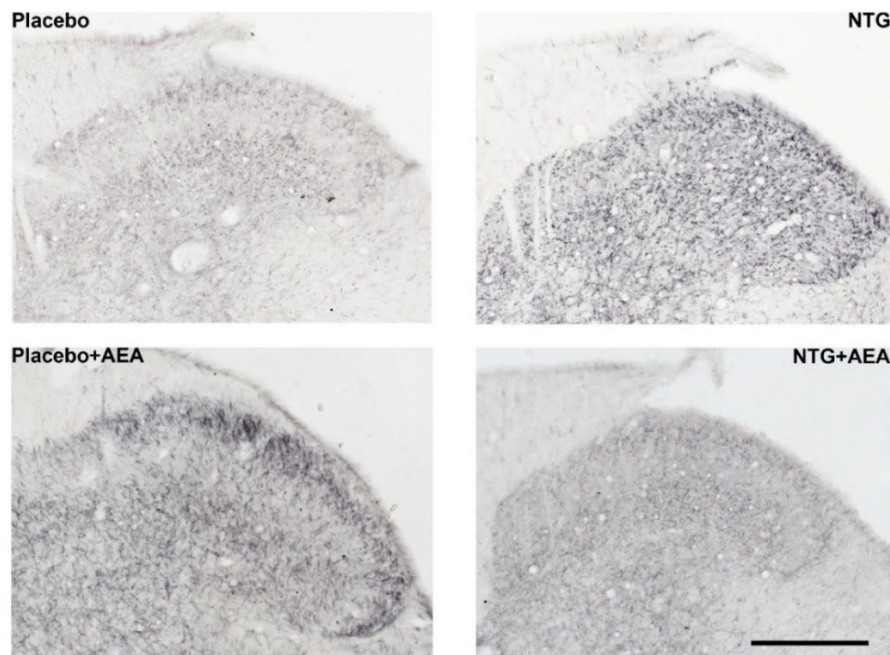


Figure 3. Representative photomicrographs of the SERT expression in the TNC from the four treatment groups. SERT expression was not homogenous across the laminae; the density of IR fibers was higher in lamina I and III than in lamina II. Scale bar: 100 μ m

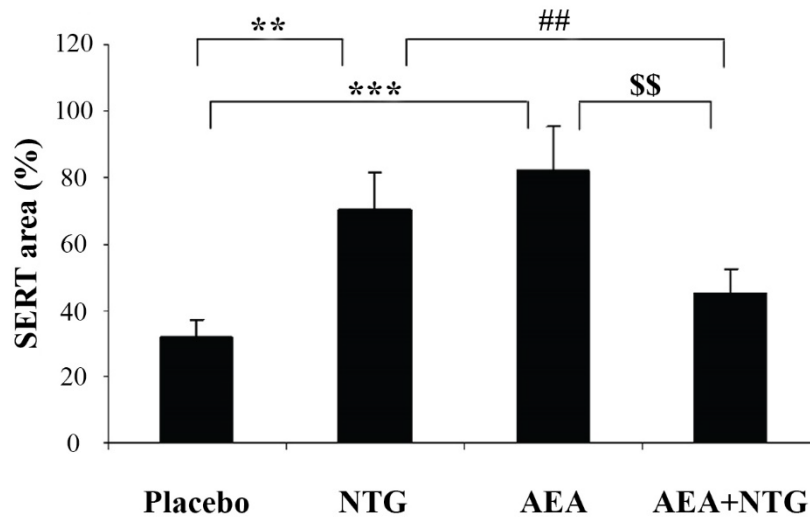


Figure 4. Diagram showing the relative area (%) covered by SERT IR fibers in the dorsal horn's lamina I in the TNC. The area fraction was significantly higher in the NTG group; AEA had the same effect on SERT immunolabelled fibers. Combined AEA+NTG treatment did not increase the relative area covered by immunolabelled fibers. Figure shows mean+S.E.M., ** $p < 0.01$, *** $p < 0.001$, ## $p < 0.01$, \$\$ $p < 0.01$.

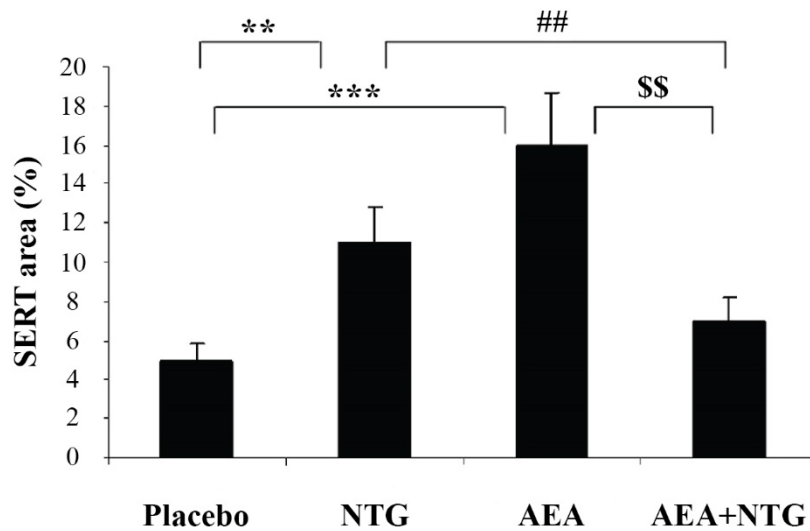


Figure 5. Diagram illustrates the relative area (%) covered by SERT IR fibers in lamina II of the dorsal horn, TNC. The area fraction was significantly higher in the NTG group; AEA had the same effect on SERT IR fibers. Combined AEA+NTG treatment did not increase the relative area covered by immunolabelled fibers. Bars show mean+S.E.M., ** $p < 0.01$, *** $p < 0.001$, ## $p < 0.01$, \$\$ $p < 0.01$.

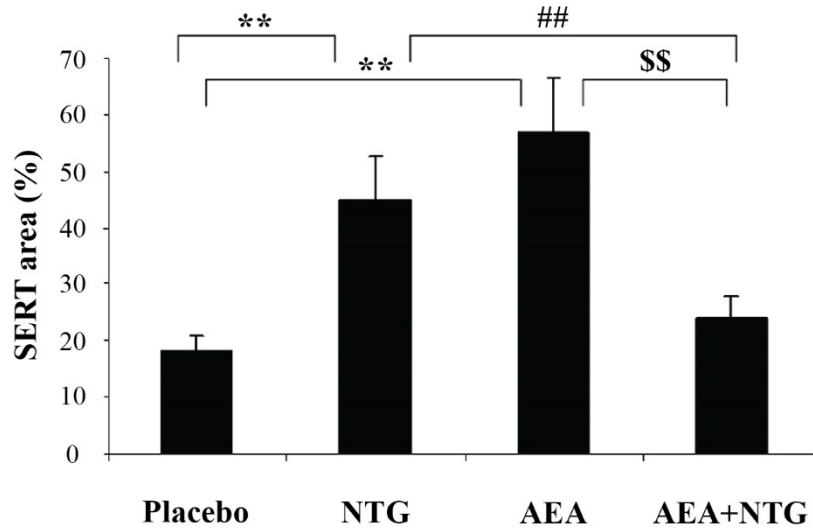


Figure 6. Diagram shows the relative area covered by SERT IR fibers in the dorsal horn's lamina III in the TNC. The area fraction was significantly higher in the NTG group; AEA had the same effect on SERT IR fibers. Combined AEA+NTG treatment did not increase the relative area covered by immunolabelled fibers. Figure shows mean+S.E.M., ** $p < 0.01$, ## $p < 0.01$, \$\$ $p < 0.01$.

The size of the SERT varicose fibers was also enhanced by NTG and AEA in the TNC, but the combined treatment reduces this effect

Using higher magnification (40× objective) of the microscope, we examined the IR processes of the dorsal horn. The average size of the fiber varicosity was significantly increased in the NTG or AEA group compared to the placebo group ($p < 0.05$). Combined NTG + AEA treatment reduced the average size of varicose fibers in comparison to NTG or AEA treatment. $F(3,20) = 12.071$; $p = 9.9 \times 10^{-5}$. Fig. 7-8

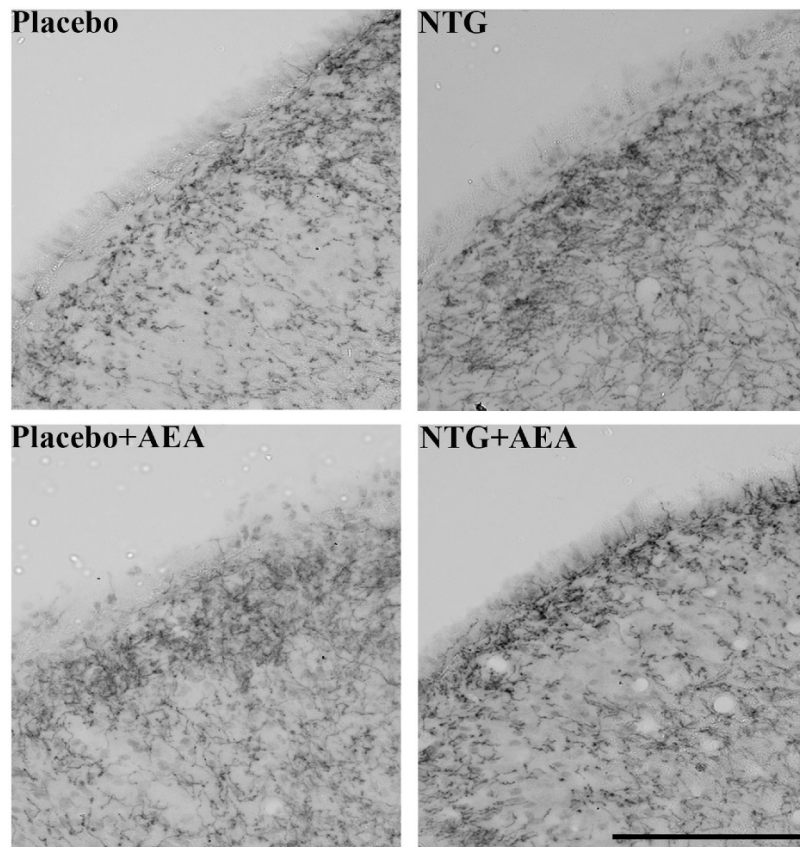


Figure 7. Representative photos showing SERT immunolabelled varicose fibers in the TNC. The size of SERT IR fiber boutons was significantly larger in NTG and AEA groups compared to placebo. Scale bar: 100 μm

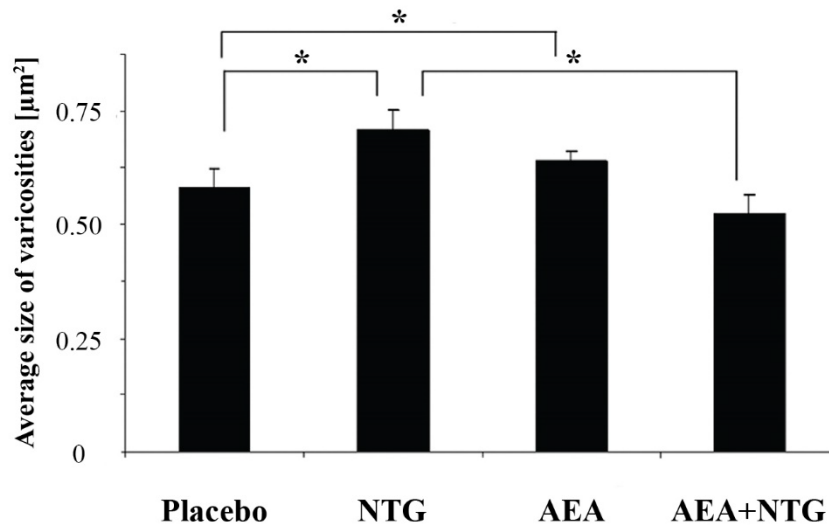


Figure 8. Diagram shows the average immunopositive fiber bouton size in the dorsal horn's laminae I-III of TNC. The average immunolabelled varicosity size was increased in the NTG- and AEA-treated groups compared to placebo group. AEA+NTG treatment prevented this effect. Figure shows mean+S.E.M., * $p < 0.05$

Western blot

Western blot analysis showed the same tendency as we obtained in SERT immunohistochemistry. A band characteristic of the SERT protein was visualized at 64 kDa. The densitometric analysis confirmed that NTG and AEA treatment caused significantly enhanced SERT protein band density ($p < 0.01$) compared to the placebo group. Compared to NTG- or AEA-treated groups, the protein band of NTG+AEA group was significantly less dense ($p < 0.05$; $p < 0.01$) in comparison to either NTG- or the AEA-treated groups. $F(3,16) = 8.088$; $p = 2 \times 10^{-3}$. *Fig. 9-10*

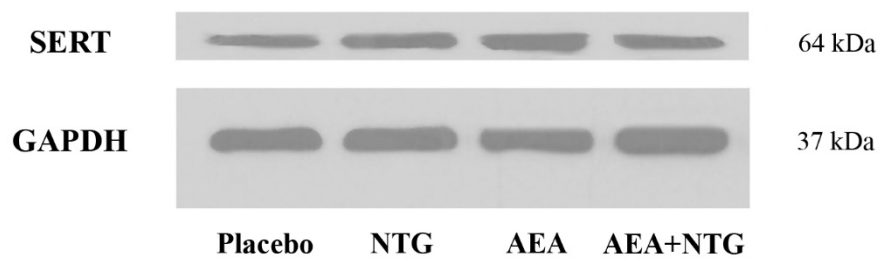


Figure 9. Western blot of SERT and GAPDH expression in the TNC

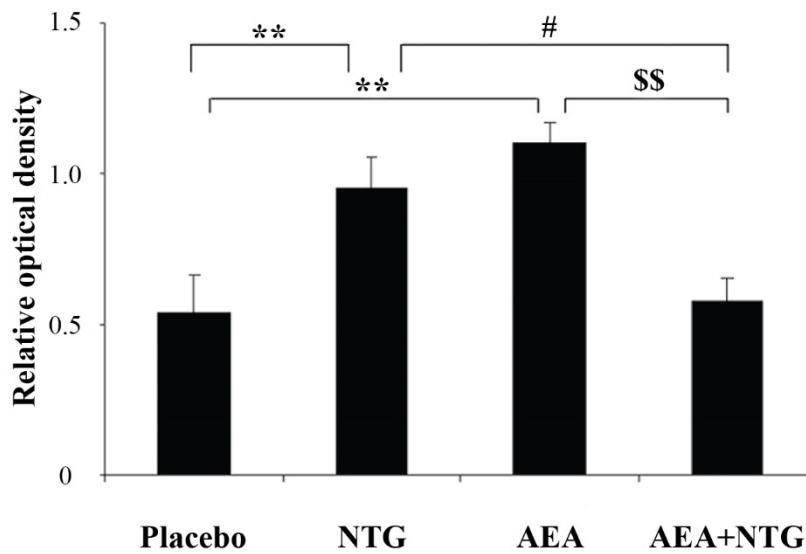


Figure 10. Bar graph showing the relative optical density of SERT-specific bands. Density was significantly higher in the NTG-treated group compared to the placebo, AEA treatment had the same effect. Compared to NTG or AEA, the protein band of the AEA+NTG group was significantly less dense. Figure shows mean+S.E.M., ** $p < 0.01$, ## $p < 0.01$, \$\$ $p < 0.01$.

II. Activation patterns following chemical stimulation of the dura

Stereotaxic frame (NAT group)

Placement of the ear bars or snout fixation caused a bilateral dense, localized increase in the number of IR cells in the somatotopic area of the V/2 nerve (maximum cell number (V/2) 24.17 ± 7.96 at obex -7.5) Fig. 11A, 12A

Anesthetic drug (chloral hydrate) and perfusion (FRE group)

The effect of chloral hydrate and the perfusion in the TNC was negligible (maximum cell number V/1: 3.83 ± 1.68 at obex -0.3). Fig. 11B, 12B

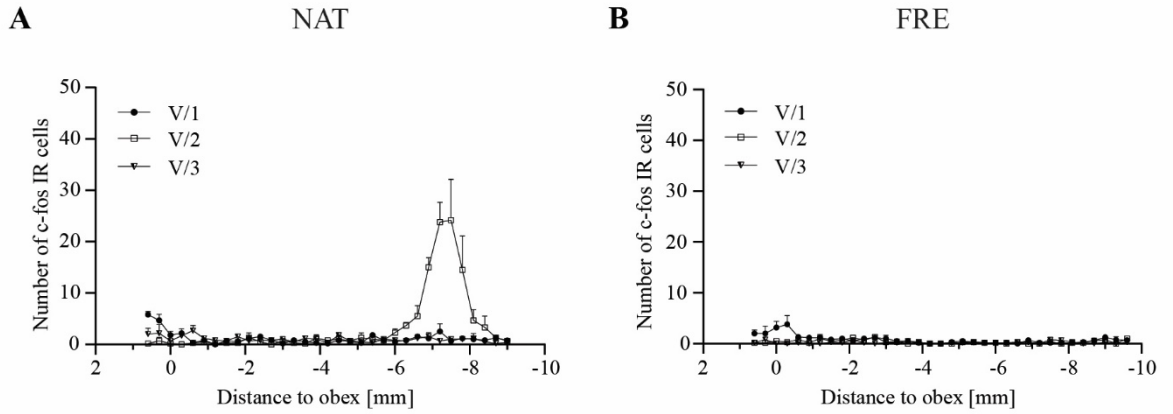


Figure 11. Diagrams show the mean number of c-Fos IR cells in NAT (A) and FRE (B) groups. In the NAT group, we found bilateral dense, localized increase in the number of IR cells in the somatotopic area of the V/2 nerve. The effect of anesthesia and perfusion was negligible in the TNC. Figure shows mean \pm S.E.M.

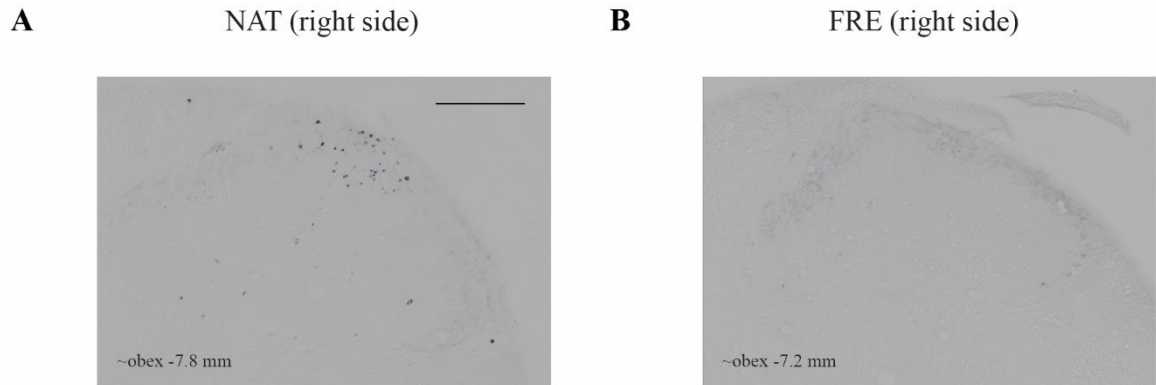


Figure 12. Representative photomicrographs from NAT (A) and FRE (B) groups showing dorsal horn. More *c-Fos* IR cells were detected in the NAT group compared to the FRE group in the area corresponding to the V/2 nerve. Scale bar: 200 μ m

Complete Freund's Adjuvant

Dural application of CFA did not cause notable increase in the number of IR cells compared to PHYS, neither two hours nor four hours after administration. We did not find difference in the number of cells between the right and left dorsal horns, neither in 2CFA nor in 2PHYS groups (Fig. 13A). Although, when the cells were counted based on the trigeminal somatotopy, a substantial increase was found in the V/2 nerve area (2CFA, 2PHYS) with substantial variance. A mild increase was observed in the V/1 nerve area without a difference between the two groups. The number of IR cells was negligible in the V/3 nerve area. Fig. 13A-D, 14A-B

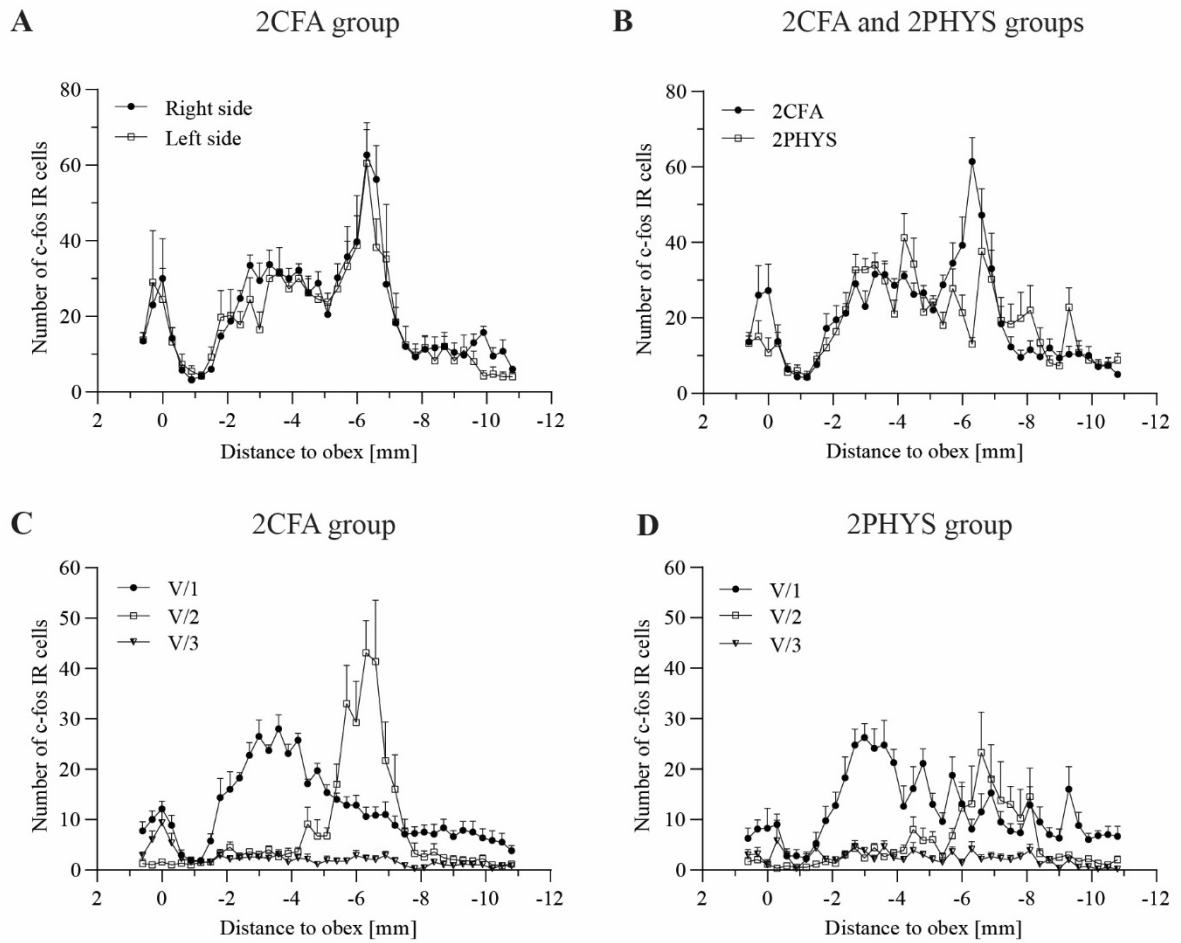


Figure 13. Diagrams showing the mean number of *c-Fos* immunolabelled cells in the TNC two hours after dural CFA or PHYS treatment. In the 2CFA group, no difference was found in the number of *c-Fos* IR cells between the right and left sides (A). Dural application of CFA did not cause notable differences between 2CFA and 2PHYS groups. When the cells were counted based on the trigeminal somatotopy (C, D), a substantial increase was found in the V/2 nerve area (2CFA, 2PHYS) with substantial variance and a mild increase in the V/1 nerve area. Figure shows mean+S.E.M.

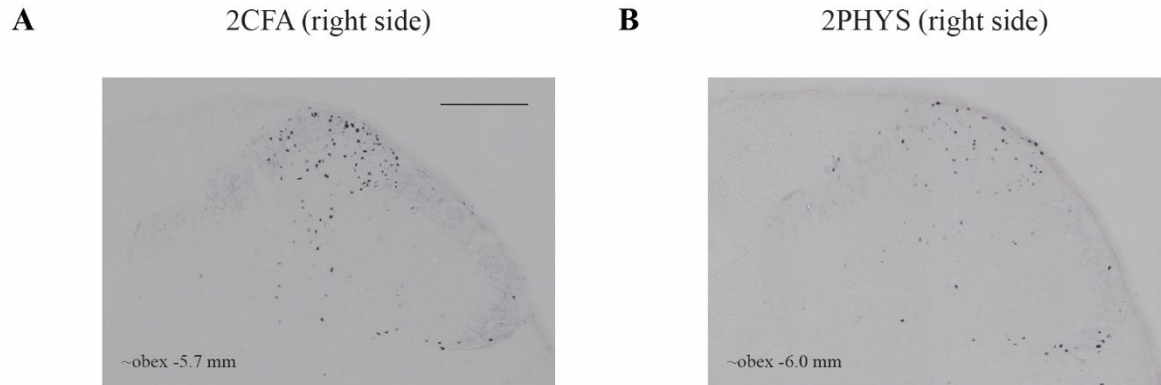


Figure 14. Representative photomicrograph of dorsal horns in TNC in 2CFA (A) and 2PHYS groups (B). Increased number of IR cells can be seen in the V/2 nerve area. Scale bar: 200 μm

No difference was found between the 4CFA and 4PHYS groups four hours after CFA application on the dura. The number of c-Fos IR cells was less after four hours compared to the two hours group, and we found the same tendency in cell distribution as in 2CFA and 2PHYS groups. *Fig. 15A-B, 16A-D*

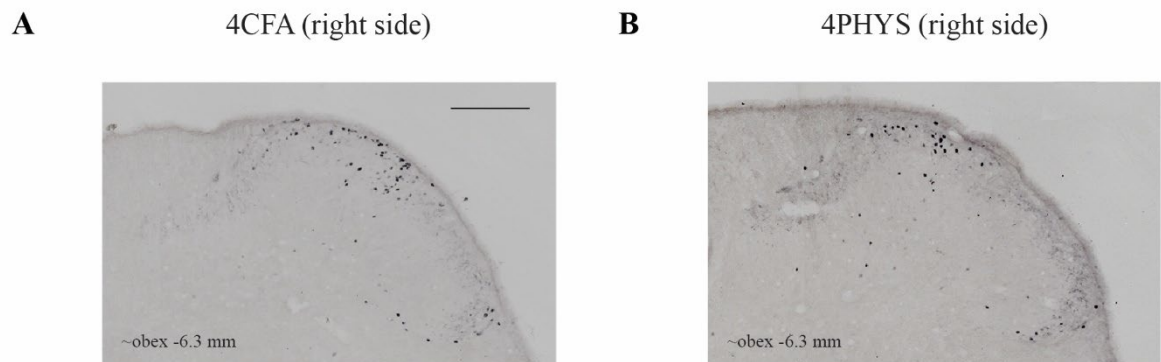


Figure 15. Representative photos showing the dorsal horns of the 4CFA (A) and 4PHYS (B) groups approximately obex -6.3 mm. We found the same tendency in cell distribution in the 4CFA and 4PHYS groups as in 2CFA and 2PHYS. Scale bar: 200 μm

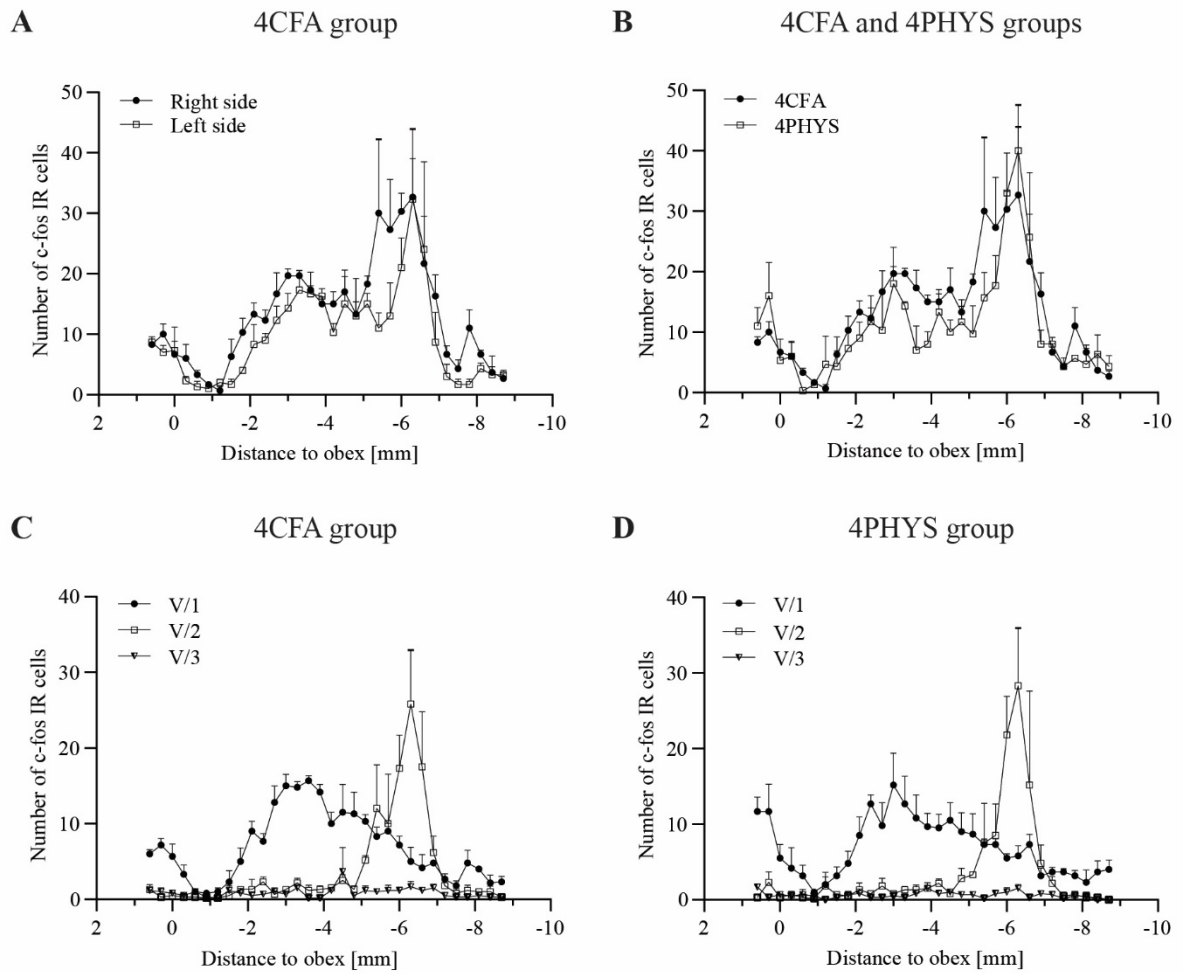


Figure 16. Diagrams illustrate the mean number of c-Fos IR cells in the TNC four hours after dural application of CFA or PHYS. We did not find a difference between the right (treated) and left (untreated) side (A), nor between 4CFA and 4PHYS groups (B). Similar cell distribution was found along the trigeminal nerve branches in both 4CFA (C) and 4PHYS (D) groups. Figure shows mean+S.E.M.

Lidocaine

S.c. applied lidocaine decreased the number of c-Fos immunopositive cells compared to the 2CFA group, particularly in the V/1 branch area. Dural application of CFA did not cause robust changes compared to PHYS in this case either. *Fig. 17A-B, 18A-B*

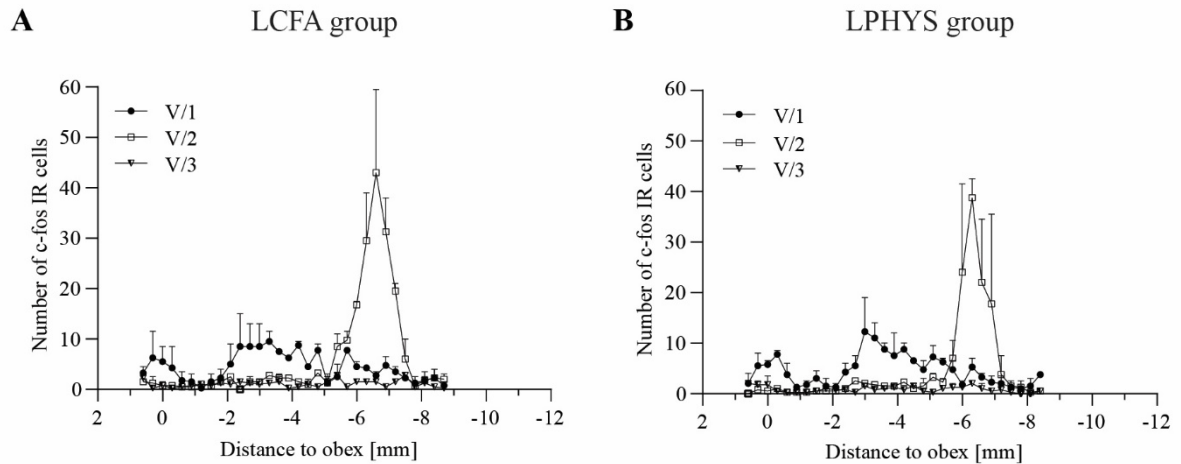


Figure 17. Diagrams illustrate the mean number of c-Fos IR cells in the TNC. No difference was found between LCFA (A) and LPHYS (B) groups. Lidocaine decreased the c-Fos IR cell number compared to 2CFA and 2PHYS groups, particularly in the area corresponding to the V/1 nerve. Figure shows mean+S.E.M.

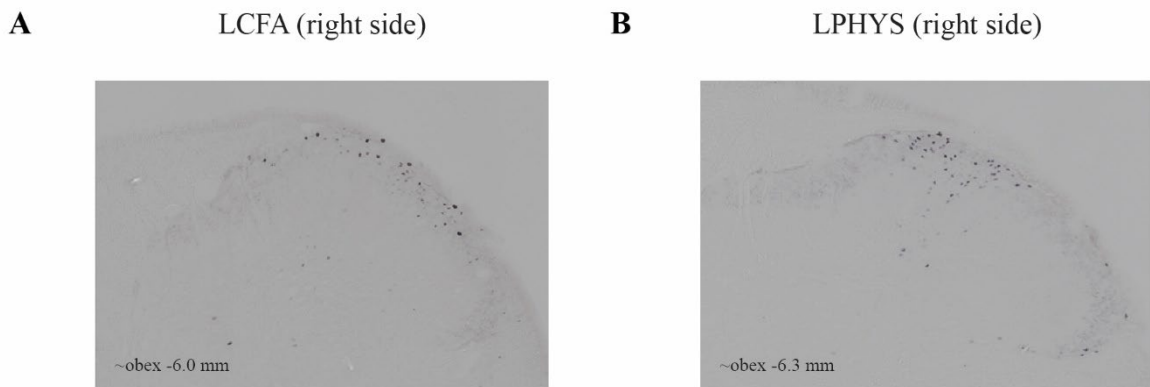


Figure 18. Representative photomicrographs show the dorsal horn of the TNC in LCFA (A) and LPHYS (B) groups two hours after CFA or PHYS treatment.

Inflammatory soup

After applying IS on the dura, animals showed significantly increased number of c-Fos immunolabelled cells in the TNC (Fig. 19, 20). These changes were more prominent in the 2IS group, especially in the somatotopic area of the V/1 nerve. Two peaks of activation were found among the rostrocaudal axis. The first peak was at the level of the obex, which follows the activation pattern of FRE, while the second was at obex (-2) – (-6) mm. This second peak in the 2IS group was significantly higher compared to the 2SIF group. In the 2IS group, we found

significant difference between the right (ipsilateral) and left (contralateral) sides at the same rostrocaudal levels. A substantial peak (at obex [-6] – [-8] mm) was seen in the sensory area of the V/2 nerve, which is consistent with the peak in the NAT group and is not different among 2IS and 2SIF. The number of IR cells in the V/3 nerve area was negligible, without any difference between the groups.

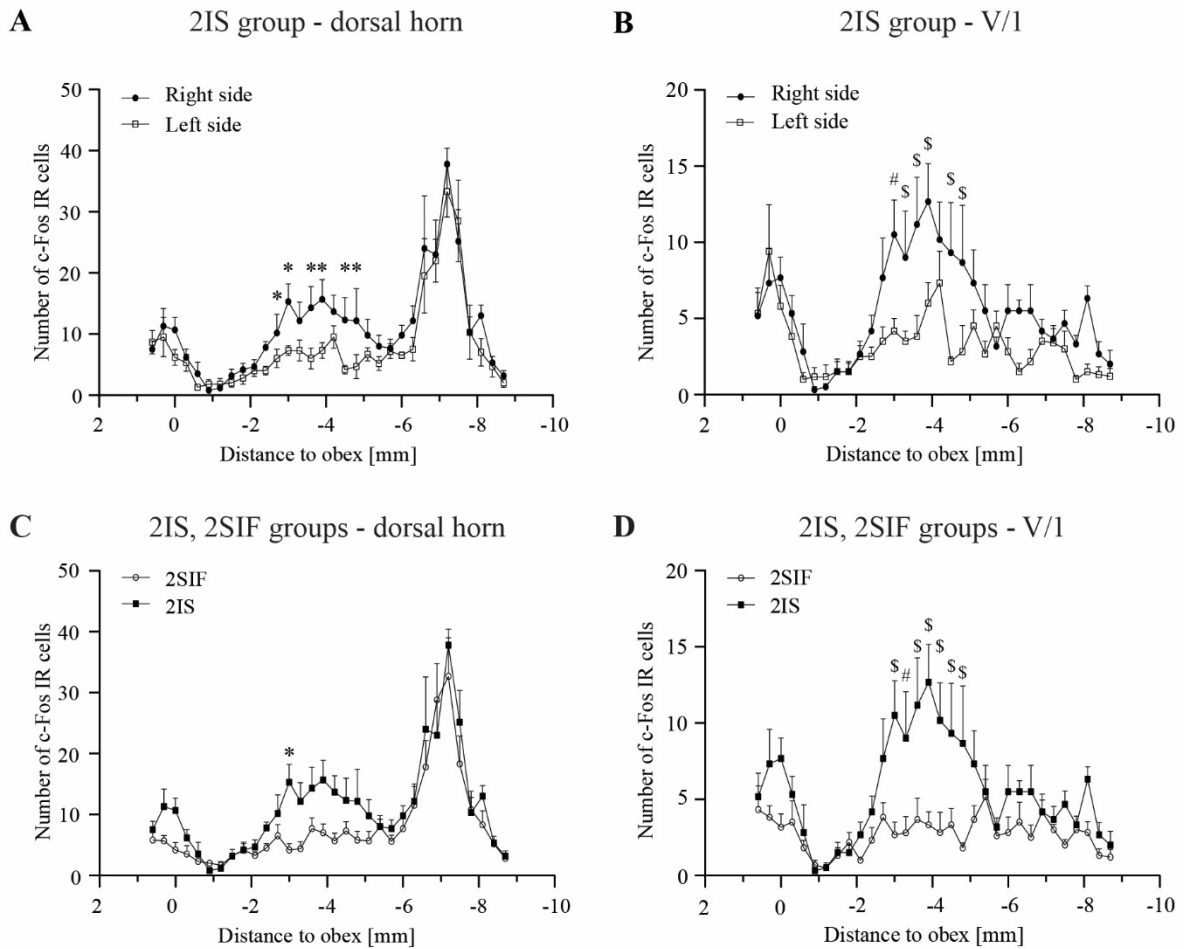


Figure 19. Diagrams showing the mean number of *c-Fos* immunolabelled cells across different levels of TNC in the whole dorsal horn (A, C) and the V/1 nerve area (B, D). A significant difference was found between the right (treated) and left (untreated) sides (A, B) and between 2IS and 2SIF groups. The difference was more pronounced when only the V/1 nerve area was analyzed. Figure shows mean+S.E.M., * $p < 0.05$, # $p < 0.01$, \$ $p < 0.001$

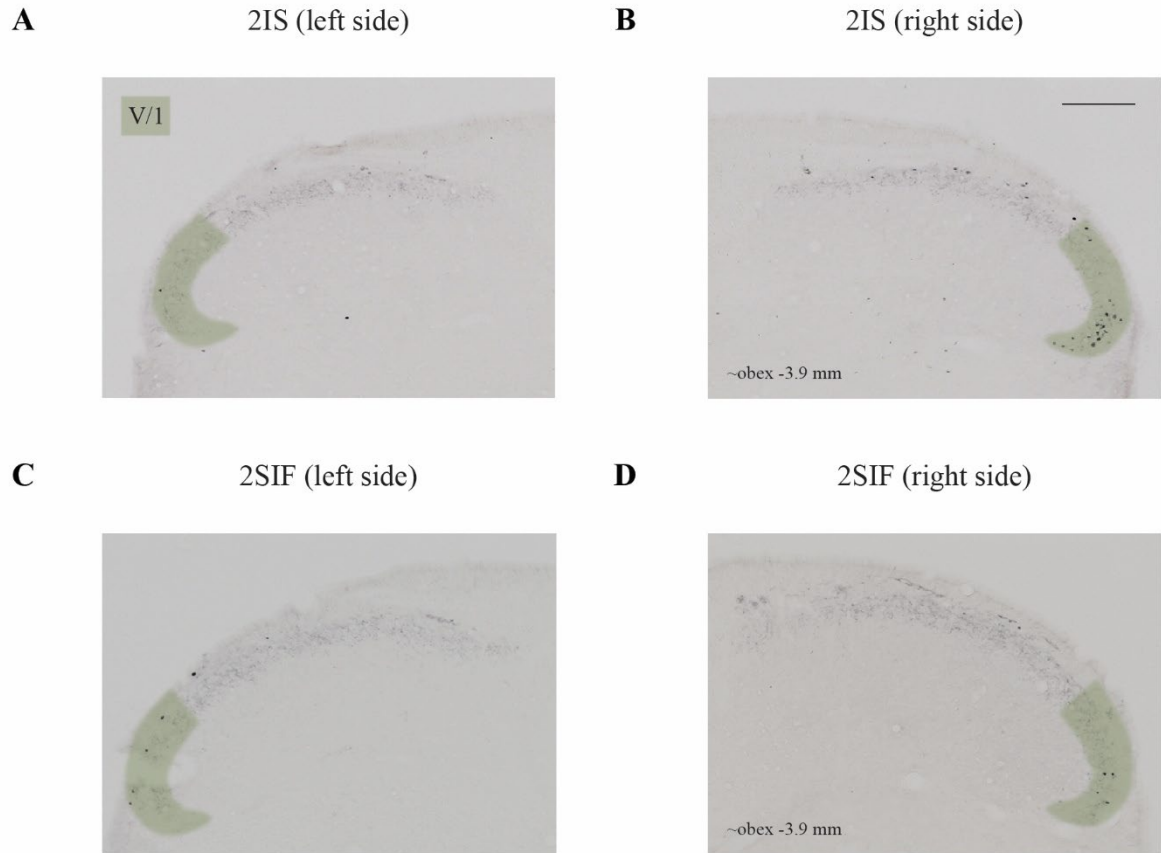


Figure 20. Representative photos of the dorsal horn of 2IS (A, B) and 2SIF groups (C, D), approximately obex -3.9 mm, 2.5 hours after dural IS or SIF application. Green highlighting shows the V/1 nerve area. IS caused an increase in the number of c-Fos IR cells on the right (treated) side (B) compared to the left (untreated) side (A). 2.5 hours after dural treatment, more cells were detected in the dorsal horn and V/1 nerve area in the IS-treated group compared to the SIF-treated group. We did not find a difference between the right (treated) and left (untreated) sides in the 2SIF group. Scale bar: 200 μ m

The cell distribution in the 4IS group is comparable to the peak seen in the 2IS group in the V/1 area; this suggests sustained stimulation of the nerve. The substantial increase in the c-Fos IR cell number in V/2 was not found in the 4-h survival groups. In the V/3 area, the number of c-Fos immunopositive cells is negligible (Fig. 22). Four hours after the IS application, we found a significant difference between the 4SIF and 4IS groups, both in the dorsal horn and V/1 area. The results from the 4SIF and 4IS groups are shown in Fig. 21.

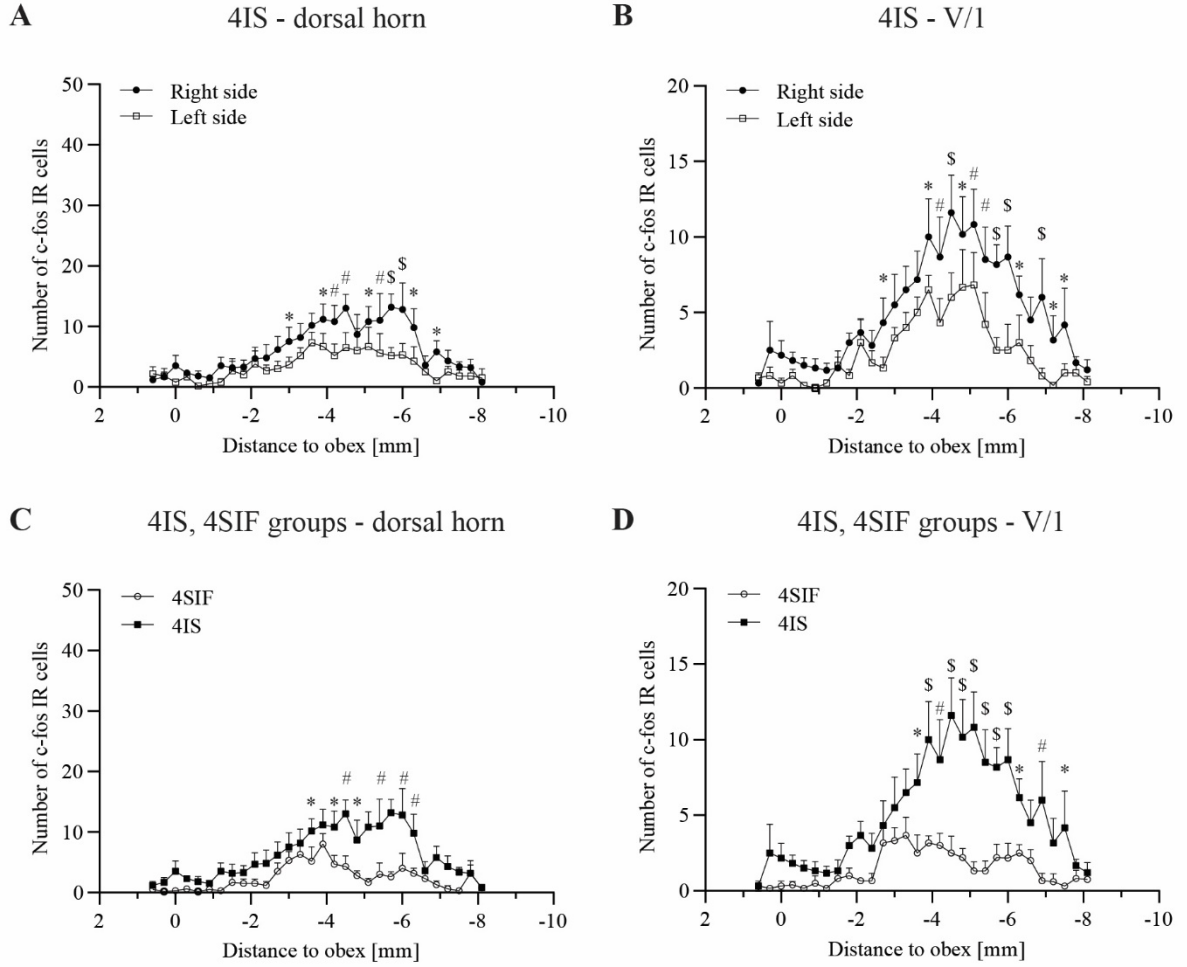


Figure 21. Diagrams illustrate the mean number of *c-Fos* IR cells along the rostrocaudal axis in the whole dorsal horn (A, C) and V/1 nerve area (B, D) four hours after application of IS or SIF on the dura mater. We found significant difference between the right (treated) and left (untreated) sides in the 4IS group; the difference was seen both in the whole dorsal horn (A) and the V/1 nerve area (B). Four hours after IS or SIF dural treatment, IS caused significant difference in the whole dorsal horn (C) and the V/1 nerve area (D) compared to SIF. Figure shows mean+S.E.M., * $p < 0.05$, # $p < 0.01$, \$ $p < 0.001$

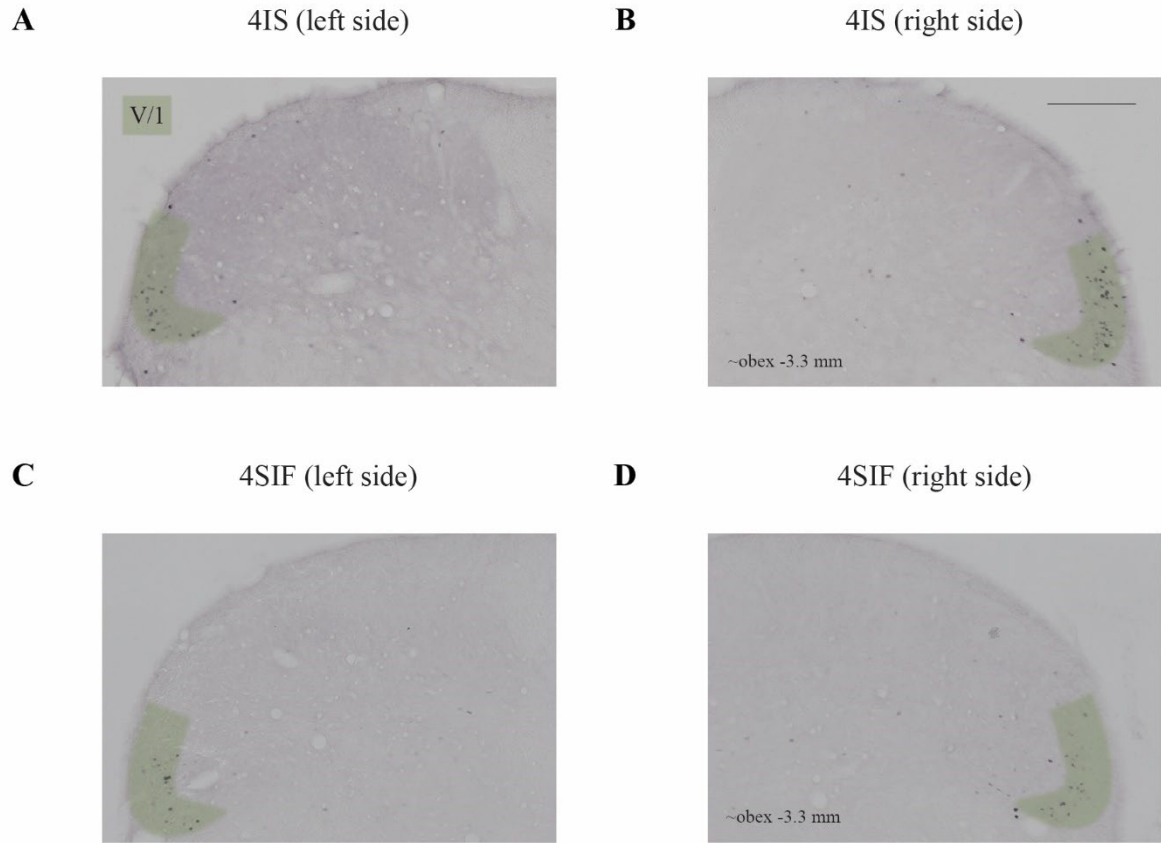


Figure 22. Representative photomicrographs of dorsal horns of 4IS and 4SIF groups at approximately obex -3.3 mm. Green highlighting shows the V/1 nerve area. An increased number of c-Fos IR cells were detected in the 4IS group on the right (treated) side (B) compared to the left (untreated) side (A). Four hours after dural treatment, more cells were found in the dorsal horn and V/1 nerve area in the IS-treated group compared to the SIF-treated group. There was no difference between the right (treated) and left (untreated) sides in the 4SIF group. Scale bar: 200 μ m.

Discussion

I. The effect of NTG and AEA on the expression of SERT

5-HT plays a complex role in the pathomechanism of migraine and pain modulation. Furthermore, inhibition of brain 5-HT synthesis has been linked to stronger migraine attacks, therefore, the transporter which regulates its levels in the synaptic cleft and extracellular space might be of interest (131). Our experiments aimed to examine the SERT expression changes in TNC after NTG, AEA, and combined NTG and AEA treatment in rats.

Examining the transsectional segments of TNC in NTG-treated rats, we found increased amount of SERT IR fibers, increased size of SERT labeled boutons, and increased protein band density compared to the control group. A previous study suggested crosstalk between NO and the 5-HTergic system; they found that the physical interaction of nNOS and SERT enables reciprocal regulation between each other (132). This was also supported by the fact that NOS inhibition was able to enhance the action of selective serotonin reuptake inhibitors (133). NTG injections increased the amount of 5-HT IR fibers in rat TNC, which can suggest reduced 5-HT release from terminals (84). Consequently, our results might indicate that NTG can increase 5-HT reuptake by SERT and 5-HT turnover at the level of the secondary sensory neurons, and this transport upregulation might contribute to the decreased 5-HTergic activity. Reduced amount of 5-HT was found in the medulla four hours after NTG administration suggesting low 5-HT transmission (134). Numerous studies proposed a hyposerotonergic state during migraine because the short-term reduction of 5-HT levels in the brain can induce more intense headaches in migraine patients; therefore, the regulation of 5-HT levels might play a role in trigeminal activation (131).

We found a similar tendency in the AEA-treated group as in the NTG group; AEA was able to increase the amount of SERT immunopositive fibers, enhance the size of SERT IR boutons, and increase the SERT protein band density in the dorsal horn of TNC. Cannabinoids can decrease 5-HT levels at peripheral sites; in vitro application of Δ^9 tetrahydrocannabinol inhibited 5-HT release from platelets incubated in plasma obtained from migraine patients (135). Supporting this idea, a later study also showed that a selective CB1 receptor agonist, ACEA, reduced the whole blood 5-HT levels, and this effect was reversed when a CB1 receptor antagonist was administered as pretreatment (122). As we assumed that NTG treatment reduced

5-HT release from terminals, and SERT expression was upregulated, by the same token, AEA, which also activates the CB1 receptor, could inhibit 5-HT release, explaining the changes seen in the AEA group. In contrast to peripheral effects, cannabinoids can increase 5-HT release in the central nervous system, which could contribute to its antinociceptive effect. CB receptors are also abundant in the central descending pain modulatory system, which also projects to the trigeminal system (136,137). Repeated injections of a CB receptor agonist and a FAAH inhibitor (which inhibits the breakdown of AEA) elevated the 5-HT release by enhancing neuronal firing in the 5-HTergic DR (138). Moreover, the descending 5-HTergic pathways might contribute to cannabinoid-induced analgesia, as the selective lesion of spinal 5-HTergic pathways or the dorsolateral funiculus was able to reduce the antinociceptive effect of cannabinoid receptor agonists (139). Based on these findings, experimental data suggest that the descending 5-HTergic pain modulatory pathways might increase the 5-HT turnover and possibly play a role in SERT expression changes that we found after AEA treatment. In summary, cannabinoids like AEA decrease 5-HT levels in the periphery, where 5-HT exerts a nociceptive effect, while centrally, they increase the amount of 5-HT via modulating the descending pain pathway. In addition, we cannot exclude the possibility of indirect actions, as endocannabinoids are also able to upregulate nNOS activity, thus increasing NO levels, this can contribute to our findings (140).

We found that the combined AEA and NTG pretreatment did not cause any significant change in the amount of SERT immunopositive fibers, size of varicosity, or SERT protein band density compared to control. Unfortunately, due to the limitation of this study, our present data do not allow us to explain this phenomenon unambiguously. We expected an additive effect, however, there is a possibility that a negative feedback mechanism takes effect in this process. It was shown that the NTG treatment was able to alter medullary and mesencephalon levels of hydrolases responsible for the breakdown of endocannabinoids, indicating that NTG might affect the ECs as well (128). Furthermore, both NTG and AEA can exert influence on NO and cGMP levels, thus, feedback mechanisms might play a role in this experimental setup (140). Apart from this, earlier research showed that NTG changed the expression of multiple inflammatory and sensitization markers, and combined treatment prevented this effect; these findings revealed that many other mechanisms are involved in this experimental setting and can contribute to our results (141).

In summary, several studies demonstrated a complex connection between the endocannabinoid and the 5-HTergic system. 5-HT can act as a nociceptive substance on the periphery, but on the other hand, it is also involved in the descending pain modulatory system; regulation of 5-HT levels by SERT can alter pain transmission. Cannabinoids, including endocannabinoids, can alter 5-HT levels both on the periphery and central sites; both processes could contribute to our results and play a role in its analgesic effect.

II. Activation patterns following chemical stimulation of the dura

Fos protein is widely used for mapping nociceptive pathways and neuronal populations in pain and headache models (142,143). In our study, we aimed to examine the effect of dural chemical stimulation using IS and CFA, and we quantified the c-Fos expression in the TNC. The expression of c-Fos can be detected after ~30 minutes following the stimulation with a half-life of two hours; thus, it is crucial to design the experiments and endpoints accordingly (144). Moreover, in the dural inflammation model, anesthesia, stereotaxic instrument, and surgical intervention can cause unspecific c-Fos activation that might interfere with accurate data analysis. Therefore, we focused on controlling the details of our experiments meticulously to enable precise mapping of the c-Fos patterns in the trigeminal system after chemical treatment of the dura mater. To learn the exact effect of these modifying factors on the expression of c-Fos, we examined the activation pattern after i.p. chloral hydrate, stereotaxic frame, and s.c. lidocaine anesthesia. The IR cells were quantified in TNC according to the rostrocaudal and somatotopic distribution of the three trigeminal branches.

Urethane increases, while pentobarbital does not substantially affect the c-Fos expression in the trigeminal system without facial stimulation (130). Therefore, first, we tested whether systemic chloral hydrate anesthesia could influence c-Fos levels in the TNC. We found that perfusion (FRE group) mildly increased the number of c-Fos positive cells in the V/1 area, without activation in the V/2 and V/3 areas, our findings agree with previous studies under pentobarbital anesthesia. Our next experiment showed that stereotaxic fixation caused robust and highly variable activation in TNC, especially in the V/2 area (NAT group). In general, the head of the animals is stabilized in a frame using the front incisors and ear bars to ensure consistency between experimental subjects and fixation of the skull for the craniotomy. V/2 is responsible for the innervation of the front incisors, while the external ear canal is supplied by V/3 (through

auriculotemporal nerve), greater and lesser auricular nerve (from C2, C3 spinal nerves), and Arnold's nerve (from vagus, glossopharyngeal, and facial nerve) (145,146). Based on these studies, substantial activation in the V/2 area might result from snout fixation in the frame, whereas minor changes in the V/1 area are consistent with activation in the FRE group that underwent anesthesia and perfusion. To increase specificity, we examined lidocaine anesthesia's effect on scalp skin (LCFA, LPHYS groups). In this experiment, the scalp skin was infiltrated with 1% lidocaine before incision and dural CFA treatment. Indeed, lidocaine decreased the number of c-Fos IR cells in the V/1 area compared to 2CFA and 2PHYS groups. Growing numbers of studies examined the exact innervation of meninges and its connection to headaches. For example, a study showed that meningeal trigeminal nerve fibers could form collateral branches that leave the skull and innervate extracranial structures. It was suggested that these collateral fibers could transmit sensory information from extracranial stimulation to the dura, which might play a role in meningeal nociception (147). Therefore, surgical incision and craniotomy could induce c-Fos activation in our experimental setting, and these changes might mask the effect of dural stimulation; anesthetizing the scalp can help us accurately examine the effect. To summarize, using the appropriate anesthetic drug, s.c. lidocaine, is crucial to investigate dural treatment's effect in a more precise way. Although the use of the stereotaxic frame cannot be avoided, mapping its effect along the rostrocaudal axis and according to the three branches of the trigeminal nerve, can help the analysis of our experimental results.

After controlling for experimental variables, we examined the effect of CFA applied to the surface of the dura. Our results show that dural CFA treatment over the right parietal hemisphere did not cause any difference in the number of c-Fos IR cells between the left and right dorsal horn of the TNC two hours following dural treatment. Furthermore, we could not find a difference in the number of c-Fos immunopositive cells in the 2CFA group compared to the 2PHYS group. We observed the same tendency even after anesthetizing the scalp with lidocaine; no difference was seen between LCFA and LPHYS groups. Likewise, dural CFA treatment did not cause a change in the number of c-Fos IR cells between 4CFA and 4PHYS groups, nor between the right and left dorsal horns. CFA contains heat-killed *Mycobacterium tuberculosis* in mineral oil, and it is commonly used in inflammatory and neuropathic pain models to induce inflammation and subsequent edema, pain, and hyperalgesia (148). While

CFA causes neuronal activation within a few hours, its effect only peaks after 24-72 hours. This tendency was also demonstrated in the trigeminal system; CFA injection into the parotid gland increased the c-Fos expression after 2, 24, and 72 hours in the TNC (149). When different inflammatory substances were applied on the surface of the dura, sensitization of neural cells occurred in the TNC 2-3 hours after dural treatment (150,151). There is a limited number of studies examining the dural application of CFA. Lukács and her colleagues were among the first to apply CFA on the surface of the dura mater for 20 minutes; they detected increased levels of pERK1/2, CGRP, and IL-1 β levels in the TG compared to the saline-treated group (94). Additionally, a later study found increased number of c-Fos immunopositive cells in the TNC seven days after stimulation of the meninges (152). CFA induces type IV hypersensitivity reaction that can explain delayed onset actions, but short-onset effects have been described as well (148,153). Since CFA's mechanism of action is T-cell-mediated, it needs more time to take effect and might be more variable than other inflammatory agents that directly irritate tissues (154). These phenomena could explain why we could not detect changes in the c-Fos expression two or four hours after the dural stimulation. In addition, we feel it necessary to emphasize that CFA was injected into tissues in most experiments; while we applied CFA for twenty minutes, which might reduce its short-term effects. CFA also contains substances that delay the breakdown of *Mycobacteria*, prolonging its duration of action (153). It was suggested that this feature could be used to model the transformation from episodic migraine to chronic migraine, and CFA administration into the temporomandibular joint might induce a continuous inflammation by releasing neuronal mediators like CGRP, subsequently creating a self-amplifying process (155). This phenomenon could be aligned with repeated migraine attacks in patients, in which sustained neuroinflammation or so-called neurogenic neuroinflammation might develop; Edvinson et al. proposed that CFA treatment could mimic this process (155). Unfortunately, with long-term application of CFA, significant side effects like skin ulceration, focal necrosis, and granuloma were also described (153). Thus, although previous results suggest prolonging experimental endpoints, we decided not to perform further experiments with delayed survival times to avoid long-term complications.

In conclusion, CFA did not cause significant change in the number of c-Fos IR cells in the TNC after two hours or after four hours. Previous experimental results indicate the treatment duration or the survival time might not be long enough to induce c-Fos expression in the second-order

neurons. Even though we did not delay experimental endpoints to ensure we avoided any injury or long-term complication on the dura mater, data suggest that CFA treatment could be used as a model of migraine chronification.

Neurogenic inflammation is hypothesized to play a role in the pathomechanism of migraine, and the use of inflammatory substances like bradykinin, PGE₂, histamine, and 5-HT might be able to model this process (156–158). These agents applied to the dura are known to activate and sensitize trigeminal neurons; therefore, our aim was to examine the effect of dural IS on the number of c-Fos immunopositive cells and to map the somatotopic distribution of the IR cells in the TNC. Markers of activation and sensitization can be observed twenty minutes after stimulation in the primary sensory neurons, while it takes two-three hours to develop sensitization in the secondary neurons; thus, we chose 2.5- and 4-hours survival times in these treatment groups (150,159). In our experiments, IS caused a significant increase in the number of c-Fos positive cells in the TNC compared to SIF two and four hours after dural application. These changes were most prominent at the obex (-1) – (-9) mm rostrocaudal level and in the somatotopic area of the right V/1.

The innervation of the parietal area is mainly provided by the ipsilateral V/1 nerve; accordingly, our results showed significant difference in the number of c-Fos labeled cells in the right and left dorsal horns of the TNC (160). In the past, the IS was often injected into the cisterna magna, and side differences could not be determined between the left and right dorsal horn; this was thought to be the pitfall of this model. When injected into the cisterna magna, substances can spread around the cisterna, and this area also has bilateral innervation; thus, although it might be more effortless and quicker to inject IS into the cisterna, the parietal application enables side comparison and internal control (161). Multiple electrophysiological studies showed that dural inflammatory mediators are able to activate trigeminal neurons; subsequently, we found increased number of c-Fos immunopositive cells not just after two hours but also after four hours (95). It was shown earlier that IS applied on the dura caused increased hyperresponsiveness and receptive field size; furthermore, behavioral studies demonstrated allodynia both in the face and hind paws. These behavioral changes peaked after three hours and returned to baseline after six hours, and this can explain why we found sustained c-Fos activation in the TNC (162).

In summary, IS could induce increased c-Fos labeled cells in the dorsal horn, which was more prominent on the ipsilateral right side. This effect can be more accurately examined when cells are counted according to the somatotopic area of the trigeminal branches. IS is able to cause activation and sensitization in the trigeminal system, which shows a similar time course as the headaches in migraineurs (163,164). Based on these findings, IS applied to the dura mater can be used as a reliable acute migraine model, and it could help us to learn more about pathomechanism and further drug development.

Conclusion

Our results show that NTG and AEA treatment increase SERT expression, but changes in the NTG-induced SERT expression could be prevented by pretreatment with AEA. These findings suggest that NTG not just activates and sensitizes the trigeminal system but also affects the 5-HT system, which plays a crucial role in the pathophysiology of migraine. The endocannabinoid AEA can modulate trigeminal system function; the SERT expression changes by AEA might result from the descending pain modulatory system activation or increased nNOS activity. The combined NTG+AEA treatment attenuated this effect, probably through negative feedback mechanisms. These results confirm the connection between the 5-HT and the endocannabinoid system and suggest the role of 5-HT pathways in cannabinoid-induced analgesia.

IS – applied on the dura mater of rats – activated cells of TNC, which were most prominent in the somatotopic area of the V/1. Surgical procedures could affect and mask the activity changes induced by chemical stimulation of the dura. These results indicate the importance of adequately controlling the experiments in pain research and suggest that chemical stimulation of the dura using IS can be used consistently as a migraine model.

To summarize, our results contribute to understanding the relationship between the 5-HT and the endocannabinoid system and offer a reliable method to examine the trigeminal pain pathway, thus, providing insight into the pathophysiologic processes in migraine.

Acknowledgement

First of all, I would like to express my gratitude to my advisor, Dr. Árpád Párdutz, for his mentorship and giving me the opportunity to work in his lab. I sincerely thank him for his patience, support, and guidance throughout my time in the lab and beyond; I will be forever grateful for it.

I would like to thank Professor László Vécsei and Professor Péter Klivényi for providing me with the opportunity to work in the Department of Neurology.

I wish to thank all of my coworkers in the Department of Neurology. Dr. Zsuzsanna Bohár, Dr. Annamária Fejes-Szabó, and Dr. Gábor Nagy-Grócz introduced the world of neuroscience to me when I was only an undergraduate student, they taught me the nitty-gritty of performing experiments, and kept me enthusiastic about scientific research throughout the years. I am also thankful for Dr. Eleonóra Spekker's help. I want to thank Valéria Vékonyné Széll and Erzsébet Lukács for their assistance and guidance in the lab.

I am grateful to all the people who shaped my view about neuroscience and provided me more learning opportunities, especially Dr. Joanna Spencer-Segal and Dr. Kathryn Hilde.

Finally, I am truly indebted to my family and friends, especially my mom and my brother, for believing in me and encouraging me over the years. Most of all, I am deeply grateful to my husband, without his constant support and love, none of this would have been possible.

References

1. Olesen J. Headache Classification Committee of the International Headache Society (IHS) The International Classification of Headache Disorders, 3rd edition. *Cephalalgia*. 2018 Jan 1;38(1):1–211.
2. Woldeamanuel YW, Cowan RP. Migraine affects 1 in 10 people worldwide featuring recent rise: A systematic review and meta-analysis of community-based studies involving 6 million participants. Vol. 372, *Journal of the Neurological Sciences*. Elsevier; 2017. p. 307–15.
3. Cuvellier JC, Mars A, Vallée L. The prevalence of premonitory symptoms in paediatric migraine: A questionnaire study in 103 children and adolescents. *Cephalalgia*. 2009;29(11):1197–201.
4. Laurell K, Artto V, Bendtsen L, Hagen K, Häggström J, Linde M, et al. Premonitory symptoms in migraine: A cross-sectional study in 2714 persons. *Cephalalgia*. 2016 Sep 1;36(10):951–9.
5. Giffin NJ, Ruggiero L, Lipton RB, Silberstein SD, Tvedskov JF, Olesen J, et al. Premonitory symptoms in migraine: an electronic diary study. *Neurology*. 2003 Mar 25;60(6):935–40.
6. Rasmussen BK, Olesen J. Migraine with aura and migraine without aura: An epidemiological study. *Cephalalgia*. 1992 Aug 7;12(4):221–8.
7. Katsarava Z, Mania M, Lampl C, Herberhold J, Steiner TJ. Poor medical care for people with migraine in Europe – evidence from the Eurolight study. *J Headache Pain*. 2018 Dec 1;19(1):1–9.
8. Ahmed SF arou., Alroughani R, Goadsby PJ. Migraine misdiagnosis as a sinusitis, a delay that can last for many years. *J Headache Pain*. 2013 Dec 12;14(1):97.
9. Linde M, Gustavsson A, Stovner LJ, Steiner TJ, Barré J, Katsarava Z, et al. The cost of headache disorders in Europe: the Eurolight project. *Eur J Neurol*. 2012 May;19(5):703–11.
10. Gooch CL, Pracht E, Borenstein AR. The burden of neurological disease in the United States: A summary report and call to action. Vol. 81, *Annals of Neurology*. John Wiley & Sons, Ltd; 2017. p. 479–84.
11. Doane MJ, Gupta S, Fang J, Laflamme AK, Vo P. The humanistic and economic burden of migraine in Europe: A cross-sectional survey in five countries. *Neurol Ther*. 2020 Dec 1;9(2):535–49.
12. Minen MT, De Dhaem OB, Van Diest AK, Powers S, Schwedt TJ, Lipton R, et al. Migraine and its psychiatric comorbidities. Vol. 87, *Journal of Neurology, Neurosurgery and Psychiatry*. BMJ Publishing Group; 2016. p. 741–9.
13. Breslau N, Davis GC, Andreski P. Migraine, psychiatric disorders, and suicide attempts: An epidemiologic study of young adults. *Psychiatry Res*. 1991;37(1):11–23.
14. Derry CJ, Derry S, Moore RA. Sumatriptan (all routes of administration) for acute migraine attacks in adults - overview of Cochrane reviews. Vol. 2014, *Cochrane Database of Systematic Reviews*. John Wiley and Sons Ltd; 2014.

15. Mayans L, Walling A. Acute migraine headache: Treatment strategies. *Am Fam Physician*. 2018 Feb 15;97(4):243–51.
16. Ha H, Gonzalez A. Migraine headache prophylaxis. *Am Fam Physician*. 2019 Jan 1;99(1):17–24.
17. Andres KH, von Düring M, Muszynski K, Schmidt RF. Nerve fibres and their terminals of the dura mater encephali of the rat. *Anat Embryol (Berl)*. 1987 Jan;175(3):289–301.
18. Mayberg M, Langer RS, Zervas NT, Moskowitz MA. Perivascular meningeal projections from cat trigeminal ganglia: Possible pathway for vascular headaches in man. *Science* (80-). 1981;213(4504):228–30.
19. Olesen J, Burstein R, Ashina M, Tfelt-Hansen P. Origin of pain in migraine: evidence for peripheral sensitisation. *Lancet Neurol*. 2009 Jul 1;8(7):679–90.
20. Burstein R, Jakubowski M, Rauch SD. The science of migraine. *J Vestib Res Equilib Orientat*. 2011;21(6):305–14.
21. Burstein R. Deconstructing migraine headache into peripheral and central sensitization. *Pain*. 2001 Jan;89(2–3):107–10.
22. Russell MB, Olesen J. Increased familial risk and evidence of genetic factor in migraine. *BMJ*. 1995 Aug 8;311(7004):541.
23. Gormley P, Anttila V, Winsvold BS, Palta P, Esko T, Pers TH, et al. Meta-analysis of 375,000 individuals identifies 38 susceptibility loci for migraine. *Nat Genet*. 2016;48(8):856–66.
24. Sutherland HG, Albury CL, Griffiths LR. Advances in genetics of migraine. *J Headache Pain*. 2019 Jun 21;20(1).
25. Gasparini CF, Smith RA, Griffiths LR. Genetic and biochemical changes of the serotonergic system in migraine pathobiology. *J Headache Pain*. 2017 Dec 1;18(1):20.
26. Eikermann-Haerter K, Kudo C, Moskowitz MA. Cortical spreading depression and estrogen. *Headache*. 2007;47(SUPPL. 2):79–85.
27. Ray BS, Wolff HG. Experimental studies on headache - Pain-sensitive structures of the head and their significance in headache. *Arch Surg*. 1940 Oct 1;41(4):813–56.
28. Buzzi MG, Bonamini M, Moskowitz MA. Neurogenic model of migraine. *Cephalalgia*. 1995 Aug 7;15(4):277–80.
29. Bolay H, Reuter U, Dunn AK, Huang Z, Boas DA, Moskowitz MA. Intrinsic brain activity triggers trigeminal meningeal afferents in a migraine model. *Nat Med*. 2002;8(2):136–42.
30. Leo AAP, Morison RS. Propagation of spreading cortical depression. *J Neurophysiol*. 1945 Jan 1;8(1):33–45.
31. Somjen GG. Mechanisms of spreading depression and hypoxic spreading depression-like depolarization. Vol. 81, *Physiological Reviews*. American Physiological Society; 2001. p. 1065–96.
32. Piilgaard H, Lauritzen M. Persistent increase in oxygen consumption and impaired

- neurovascular coupling after spreading depression in rat neocortex. *J Cereb Blood Flow Metab.* 2009 Sep;29(9):1517–27.
33. Hadjikhani N, Sanchez Del Rio M, Wu O, Schwartz D, Bakker D, Fischl B, et al. Mechanisms of migraine aura revealed by functional MRI in human visual cortex. *Proc Natl Acad Sci U S A.* 2001 Apr 10;98(8):4687–92.
 34. Zhang X, Levy D, Kainz V, Nosedá R, Jakubowski M, Burstein R. Activation of central trigeminovascular neurons by cortical spreading depression. *Ann Neurol.* 2011 May;69(5):855–65.
 35. Weiller C, May A, Limmroth V, Jüptner M, Kaube H, Schayck R V., et al. Brain stem activation in spontaneous human migraine attacks. *Nat Med.* 1995;1(7):658–60.
 36. Afridi S, Goadsby PJ. New onset migraine with a brain stem cavernous angioma. *J Neurol Neurosurg Psychiatry.* 2003;74(5):680–2.
 37. Berger M, Gray JA, Roth BL. The expanded biology of serotonin. *Annu Rev Med.* 2009;60:355–66.
 38. Ojima K, Watanabe N, Narita N, Narita M. Temporomandibular disorder is associated with a serotonin transporter gene polymorphism in the Japanese population. *Biopsychosoc Med.* 2007 Jan 10;1:3.
 39. Dahlström A, Fuxe K. Evidence for the existence of monoamine-containing neurons in the central nervous system. I. Demonstration of monoamines in the cell bodies of brain stem neurons. *Acta Physiol Scand.* 1964;Suppl 232:1–55.
 40. Sommer C. Is serotonin hyperalgesic or analgesic? *Curr Pain Headache Rep.* 2006;10:101–6.
 41. Nakajima K, Obata H, Ito N, Goto F, Saito S. The nociceptive mechanism of 5-hydroxytryptamine released into the peripheral tissue in acute inflammatory pain in rats. *Eur J Pain.* 2009 May 1;13(5):441–7.
 42. Sasaki M, Obata H, Kawahara K, Saito S, Goto F. Peripheral 5-HT_{2A} receptor antagonism attenuates primary thermal hyperalgesia and secondary mechanical allodynia after thermal injury in rats. *Pain.* 2006;122(1–2):130–6.
 43. Schmelz M, Schmidt R, Weidner C, Hilliges M, Torebjörk HE, Handwerker HO. Chemical response pattern of different classes of C-nociceptors to pruritogens and algogens. *J Neurophysiol.* 2003 May 1;89(5):2441–8.
 44. Van Bockstaele EJ. Endocannabinoid regulation of monoamines in psychiatric and neurological disorders. *Endocannabinoid Regulation of Monoamines in Psychiatric and Neurological Disorders.* 2013. 1–337 p.
 45. Sicuteri F, Testi A, Anselmi B. Biochemical investigations in headache: increase in the hydroxyindoleacetic acid excretion during migraine attacks. *Int Arch Allergy Immunol.* 1961;19(1):55–8.
 46. Kimball RW, Friedman AP, Vallejo E. Effect of serotonin in migraine patients. *Neurology.* 1960;10(2):107–11.

47. Maneepak M, Le Grand SM, Srikiatkachorn A. Serotonin depletion increases nociception-evoked trigeminal NMDA receptor phosphorylation. *Headache*. 2009 Mar;49(3):375–82.
48. Nicolae Sfetcu. *Health & Drugs: Disease, Prescription & Medication*. 2014.
49. Marziniak M, Mössner R, Schmitt A, Lesch KP, Sommer C. A functional serotonin transporter gene polymorphism is associated with migraine with aura. *Neurology*. 2005 Jan 11;64(1):157–9.
50. Lesch KP, Bengel D, Heils A, Sabol SZ, Greenberg BD, Petri S, et al. Association of anxiety-related traits with a polymorphism in the serotonin transporter gene regulatory region. *Science* (80-). 1996;274(5292):1527–31.
51. Kotani K, Shimomura T, Shimomura F, Ikawa S, Nanba E. A polymorphism in the serotonin transporter gene regulatory region and frequency of migraine attacks. *Headache*. 2002;42(9):893–5.
52. Park E, Hwang YM, Chu MK, Jung KY. Increased Brainstem Serotonergic Transporter Availability in Adult Migraineurs: an [18F]FP-CIT PET Imaging Pilot Study. *Nucl Med Mol Imaging* (2010). 2016 Mar 1;50(1):70–5.
53. Curran T, Peters G, Van Beveren C, Teich NM, Verma IM. FBJ murine osteosarcoma virus: identification and molecular cloning of biologically active proviral DNA. *J Virol*. 1982 Nov;44(2):674–82.
54. Morgan JI, Curran T. Stimulus-transcription coupling in the nervous system: Involvement of the inducible proto-oncogenes fos and jun. *Annu Rev Neurosci*. 1991 Nov 28;14(1):421–51.
55. Hunt SP, Pini A, Evan G. Induction of c-fos-like protein in spinal cord neurons following sensory stimulation. *Nature*. 1987 Aug;328(6131):632–4.
56. Müller R, Bravo R, Burckhardt J, Curran T. Induction of c-fos gene and protein by growth factors precedes activation of c-myc. *Nature*. 1984;312:716–20.
57. Keay KA, Bandler R. Vascular head pain selectively activates ventrolateral periaqueductal gray in the cat. *Neurosci Lett*. 1998 Mar 27;245(1):58–60.
58. Benjamin L, Levy MJ, Lasalandra MP, Knight YE, Akerman S, Classey JD, et al. Hypothalamic activation after stimulation of the superior sagittal sinus in the cat: a Fos study. *Neurobiol Dis*. 2004 Aug 1;16(3):500–5.
59. Boyer N, Dallel R, Artola A, Monconduit LL. General trigeminospinal central sensitization and impaired descending pain inhibitory controls contribute to migraine progression. *Pain*. 2014 Jul;155(7):1196–205.
60. Nozaki K, Moskowitz M a., Boccalini P. CP-93,129, sumatriptan, dihydroergotamine block c-fos expression within rat trigeminal nucleus caudalis caused by chemical stimulation of the meninges. *Br J Pharmacol*. 1992 Jun;106(2):409–15.
61. Bullitt E. Induction of c-fos-like protein within the lumbar spinal cord and thalamus of the rat following peripheral stimulation. *Brain Res*. 1989 Jul 31;493(2):391–7.
62. Hoskin KL, Goadsby PJ. Exposure and isolation of the superior sagittal sinus elicits Fos in the

trigeminal nucleus caudalis and dorsal horn of the cervical spinal cord: How long should you wait? *Brain Res.* 1999 Apr 3;824(1):133–5.

63. Hammond DL, Presley R, Gogas KR, Basbaum AI. Morphine or U-50,488 suppresses fos protein-like immunoreactivity in the spinal cord and nucleus tractus solitarii evoked by a noxious visceral stimulus in the rat. *J Comp Neurol.* 1992;315(2):244–53.
64. Ignarro LJ. After 130 years, the molecular mechanism of action of nitroglycerin is revealed. *Proc Natl Acad Sci U S A.* 2002 Jun 11;99(12):7816–7.
65. Torfgard K, Ahlner J, Axelsson KL, Norlander B, Bertler A. Tissue levels of glyceryl trinitrate and cGMP after in vivo administration in rat, and the effect of tolerance development. *Can J Physiol Pharmacol.* 1991;69(9):1257–61.
66. Bauer JA, Fung HL. Arterial versus venous metabolism of nitroglycerin to nitric oxide: a possible explanation of organic nitrate venoselectivity. *J Cardiovasc Pharmacol.* 1996;28(3):371–4.
67. Sydow K, Daiber A, Oelze M, Chen Z, August M, Wendt M, et al. Central role of mitochondrial aldehyde dehydrogenase and reactive oxygen species in nitroglycerin tolerance and cross-tolerance. *J Clin Invest.* 2004 Feb 1;113(3):482–9.
68. Harrison DG, Bates JN. The nitrovasodilators. New ideas about old drugs. *Circulation.* 1993;87(5):1461–7.
69. Kukovetz WR, Holzmann S. Mechanism of nitrate-induced vasodilation and tolerance - PubMed. *Z Kardiol.* 1983;72(Suppl 3):14–9.
70. Moncada S, Palmer RMJ, Higgs EA. The discovery of nitric oxide as the endogenous nitrovasodilator. Vol. 12, Hypertension. 1988. p. 365–72.
71. Sicuteri F, Del Bene E, Poggioni M, Bonazzi A. Unmasking Latent Dysnociception in Healthy Subjects. *Headache J Head Face Pain.* 1987 Apr 1;27(4):180–5.
72. Thomsen LL, Kruuse C, Iversen HK, Olesen J. A nitric oxide donor (nitroglycerin) triggers genuine migraine attacks. *Eur J Neurol.* 1994 Sep;1(1):73–80.
73. Tegeler CH, Davidai G, Gengo FM, Knappertz VA, Troost BT, Gabriel H, et al. Middle cerebral artery velocity correlates with nitroglycerin-induced headache onset. *J Neuroimaging.* 1996;6(2):81–6.
74. Iversen HK, Holm S, Friberg L, Tfelt-Hansen P. Intracranial hemodynamics during intravenous infusion of glyceryl trinitrate. *J Headache Pain.* 2008 Jun;9(3):177–80.
75. Afridi SK, Kaube H, Goadsby PJ. Glyceryl trinitrate triggers premonitory symptoms in migraineurs. *Pain.* 2004 Aug;110(3):675–80.
76. Maniyar FH, Sprenger T, Monteith T, Schankin C, Goadsby PJ. Brain activations in the premonitory phase of nitroglycerin-triggered migraine attacks. *Brain.* 2014 Jan 1;137(1):232–41.
77. Afridi SK, Matharu MS, Lee L, Kaube H, Friston KJ, Frackowiak RSJ, et al. A PET study exploring the laterality of brainstem activation in migraine using glyceryl trinitrate. *Brain.* 2005

Apr 1;128(4):932–9.

78. Afridi SK, Giffin NJNJ, Kaube H, Friston KJ, Ward NS, Frackowiak RSJJ, et al. A positron emission tomographic study in spontaneous migraine. *Arch Neurol*. 2005 Aug;62(8):1270–5.
79. Tassorelli C, Greco R, Morocutti A, Costa A, Nappi G. Nitric oxide-induced neuronal activation in the central nervous system as an animal model of migraine: mechanism and mediators. *Funct Neurol*. 2001;16(Suppl):69–76.
80. Fanciullacci M, Alessandri M, Figini M, Geppetti P, Michelacci S. Increase in plasma calcitonin gene-related peptide from the extracerebral circulation during nitroglycerin-induced cluster headache attack. *Pain*. 1995;60(2):119–23.
81. Tassorelli C, Joseph SA, Nappi G. Neurochemical mechanisms of nitroglycerin-induced neuronal activation in rat brain: A pharmacological investigation. *Neuropharmacology*. 1997 Oct 1;36(10):1417–24.
82. Tassorelli C, Joseph SA. Systemic nitroglycerin induces Fos immunoreactivity in brainstem and forebrain structures of the rat. *Brain Res*. 1995 Jun 5;682(1–2):167–81.
83. Lambert GA, Donaldson C, Boers PM, Zagami AS. Activation of trigeminovascular neurons by glyceryl trinitrate. *Brain Res*. 2000 Dec 22;887(1):203–10.
84. Pardutz A, Multon S, Malgrange B, Parducz A, Vecsei L, Schoenen J. Effect of systemic nitroglycerin on CGRP and 5-HT afferents to rat caudal spinal trigeminal nucleus and its modulation by estrogen. *Eur J Neurosci*. 2002;15(11):1803–9.
85. Reuter U, Bolay H, Jansen-Olesen I, Chiarugi A, Del Rio MS, Letourneau R, et al. Delayed inflammation in rat meninges: implications for migraine pathophysiology. *Brain*. 2001 Dec 1;124(Pt 12):2490–502.
86. Reuter U, Chiarugi A, Bolay H, Moskowitz MA. Nuclear factor- κ B as a molecular target for migraine therapy. *Ann Neurol*. 2002;51(4):507–16.
87. Párdutz Á, Krizbai I, Multon S, Vecsei L, Schoenen J, Pardutz A, et al. Systemic nitroglycerin increases nNOS levels in rat trigeminal nucleus caudalis. *Neuroreport*. 2000;11(14):3071–5.
88. Pardutz A, Szatmári E, Vecsei L, Schoenen J. Nitroglycerin-induced nNOS increase in rat trigeminal nucleus caudalis is inhibited by systemic administration of lysine acetylsalicylate but not of sumatriptan. *Cephalalgia*. 2004;24(6):439–45.
89. Costa A, Smeraldi A, Tassorelli C, Greco R, Nappi G. Effects of acute and chronic restraint stress on nitroglycerin-induced hyperalgesia in rats. *Neurosci Lett*. 2005 Jul 22;383(1–2):7–11.
90. Greco R, Mangione AS, Siani F, Blandini F, Vairetti M, Nappi G, et al. Effects of CGRP receptor antagonism in nitroglycerin-induced hyperalgesia. *Cephalalgia*. 2013 Dec 23;34(8):594–604.
91. Markovics A, Kormos V, Gaszner B, Lashgarara A, Szoke E, Sandor K, et al. Pituitary adenylate cyclase-activating polypeptide plays a key role in nitroglycerol-induced trigeminovascular activation in mice. *Neurobiol Dis*. 2012 Jan;45(1):633–44.
92. Bates EA, Nikai T, Brennan KC, Fu Y-HH, Charles AC, Basbaum AI, et al. Sumatriptan

- alleviates nitroglycerin-induced mechanical and thermal allodynia in mice. *Cephalalgia*. 2010 Feb;30(2):170–8.
93. Mitsikostas DD, Sanchez Del Rio M, Waeber C, Moskowitz MA, Cutrer FM. The NMDA receptor antagonist MK-801 reduces capsaicin-induced c-fos expression within rat trigeminal nucleus caudalis. *Pain*. 1998 May;76(1–2):239–48.
 94. Lukács M, Haanes K, Majláth Z, Tajti J, Vécsei L, Warfvinge K, et al. Dural administration of inflammatory soup or Complete Freund's Adjuvant induces activation and inflammatory response in the rat trigeminal ganglion. *J Headache Pain*. 2015;16(1):79.
 95. Strassman AM, Raymond SA, Burstein R. Sensitization of meningeal sensory neurons and the origin of headaches. *Nature*. 1996;384(6609):560–4.
 96. Hoffmann J, Neeb L, Israel H, Dannenberg F, Triebe F, Dirnagl U, et al. Intracisternal injection of inflammatory soup activates the trigeminal nerve system. *Cephalalgia*. 2009;29:1212–7.
 97. Hoffmann J, Wecker S, Neeb L, Dirnagl U, Reuter U. Primary trigeminal afferents are the main source for stimulus-induced CGRP release into jugular vein blood and CSF. *Cephalalgia*. 2012;32(9):659–67.
 98. Jakubowski M, Levy D, Kainz V, Zhang X-CC, Kosaras B, Burstein R. Sensitization of central trigeminovascular neurons: Blockade by intravenous naproxen infusion. *Neuroscience*. 2007 Aug 24;148(2):573–83.
 99. Jakubowski M, Levy D, Goor-Aryeh I, Collins B, Bajwa Z, Burstein R. Terminating migraine with allodynia and ongoing central sensitization using parenteral administration of COX1/COX2 inhibitors. *Headache*. 2005 Jul;45(7):850–61.
 100. Burstein R, Jakubowski M. Analgesic Triptan Action in an Animal Model of Intracranial Pain: A Race against the Development of Central Sensitization. *Ann Neurol*. 2004 Jan;55(1):27–36.
 101. Edelmayer RM, Vanderah TW, Majuta L, Zhang E-T, Fioravanti B, De Felice M, et al. Medullary pain facilitating neurons mediate allodynia in Headache-Related pain. *Ann Neurol*. 2009 Feb;65(2):184–93.
 102. Mechoulam R. The Pharmacohistory of Cannabis Sativa. In: Mechoulam R, editor. *Cannabinoids As Therapeutic Agents*. 1986. p. 1–19.
 103. Devane WA, Hanuš L, Breuer A, Pertwee RG, Stevenson LA, Griffin G, et al. Isolation and structure of a brain constituent that binds to the cannabinoid receptor. *Science* (80-). 1992;258(5090):1946–9.
 104. Hanlon EC, Tasali E, Leproult R, Stuhr KL, Doncheck E, De Wit H, et al. Circadian rhythm of circulating levels of the endocannabinoid 2 arachidonoylglycerol. *J Clin Endocrinol Metab*. 2015 Jan 1;100(1):220–6.
 105. Kano M, Ohno-Shosaku T, Hashimoto-dani Y, Uchigashima M, Watanabe M. Endocannabinoid-mediated control of synaptic transmission. *Physiol Rev*. 2009 Jan;89(1):309–80.
 106. Pandey R, Mousawy K, Nagarkatti M, Nagarkatti P. Endocannabinoids and immune regulation. *Pharmacol Res*. 2009 Aug;60(2):85–92.

107. Wenger T, Moldrich G. The role of endocannabinoids in the hypothalamic regulation of visceral function. *Prostaglandins Leukot Essent Fat Acids*. 2002;66(2–3):301–7.
108. Bellocchio L, Cervino C, Pasquali R, Pagotto U. The endocannabinoid system and energy metabolism. *J Neuroendocrinol*. 2008 Jun;20(6):850–7.
109. Katona I, Freund TF. Endocannabinoid signaling as a synaptic circuit breaker in neurological disease. *Nat Med*. 2008 Sep 5;14(9):923–30.
110. Pertwee R, editor. *Cannabinoids*. 2005.
111. Hohmann AG, Briley EM, Herkenham M. Pre- and postsynaptic distribution of cannabinoid and mu opioid receptors in rat spinal cord. *Brain Res*. 1999 Mar 20;822(1–2):17–25.
112. Cabral GA, Raborn ES, Griffin L, Dennis J, Marciano-Cabral F. CB2 receptors in the brain: role in central immune function. *Br J Pharmacol*. 2008 Jan 1;153(2):240–51.
113. Ford ZK, Reker AN, Chen S, Kadakia F, Bunk A, Davidson S. Cannabinoid Receptor 1 Expression in Human Dorsal Root Ganglia and CB13-Induced Bidirectional Modulation of Sensory Neuron Activity. *Front Pain Res*. 2021 Nov 16;2:85.
114. Ständer S, Schmelz M, Metze D, Luger T, Rukwied R. Distribution of cannabinoid receptor 1 (CB1) and 2 (CB2) on sensory nerve fibers and adnexal structures in human skin. *J Dermatol Sci*. 2005 Jun 1;38(3):177–88.
115. Hohmann AG, Kang T, Walker JM. Intrathecal cannabinoid administration suppresses noxious stimulus- evoked Fos protein-like immunoreactivity in rat spinal cord: Comparison with morphine. *Acta Pharmacol Sin*. 1999;20(12):1132–6.
116. Richardson JD, Kilo S, Hargreaves KM. Cannabinoids reduce hyperalgesia and inflammation via interaction with peripheral CB receptors. *Pain*. 1998;75:111–9.
117. Palkovits M, Harvey-White J, Liu J, Kovacs ZS, Bobest M, Lovas G, et al. Regional distribution and effects of postmortal delay on endocannabinoid content of the human brain. *Neuroscience*. 2008 Apr 9;152(4):1032–9.
118. Naidu PS, Booker L, Cravatt BF, Lichtman AH. Synergy between enzyme inhibitors of fatty acid amide hydrolase and cyclooxygenase in visceral nociception. *J Pharmacol Exp Ther*. 2009;329(1):48–56.
119. Huang SM, Bisogno T, Trevisani M, Al-Hayani A, De Petrocellis L, Fezza F, et al. An endogenous capsaicin-like substance with high potency at recombinant and native vanilloid VR1 receptors. *Proc Natl Acad Sci U S A*. 2002 Jun 11;99(12):8400–5.
120. Anand P, Bley K. Topical capsaicin for pain management: therapeutic potential and mechanisms of action of the new high-concentration capsaicin 8% patch. *Br J Anaesth*. 2011 Oct;107(4):490–502.
121. Starowicz K, Makuch W, Osikowicz M, Piscitelli F, Petrosino S, Di Marzo V, et al. Spinal anandamide produces analgesia in neuropathic rats: possible CB(1)- and TRPV1-mediated mechanisms. *Neuropharmacology*. 2012 Mar;62(4):1746–55.
122. Rutkowska M, Gliniak H. The influence of ACEA - A selective cannabinoid CB1 receptor

- agonist on whole blood and platelet-poor plasma serotonin concentrations. *Pharmazie*. 2009;64(9):598–601.
123. Mendiguren A, Pineda J. Effect of the CB 1 receptor antagonists rimonabant and AM251 on the firing rate of dorsal raphe nucleus neurons in rat brain slices. *Br J Pharmacol*. 2009 Nov;158(6):1579–87.
 124. Russo EB. Clinical endocannabinoid deficiency (CECD): can this concept explain therapeutic benefits of cannabis in migraine, fibromyalgia, irritable bowel syndrome and other treatment-resistant conditions? *Neuro Endocrinol Lett*. 2004 Jan 4;25(1–2):31–9.
 125. Cupini LM, Bari M, Battista N, Argirò G, Finazzi-Agrò A, Calabresi P, et al. Biochemical changes in endocannabinoid system are expressed in platelets of female but not male migraineurs. *Cephalalgia*. 2006 Mar 26;26(3):277–81.
 126. Sarchielli P, Pini LA, Coppola F, Rossi C, Baldi A, Mancini ML, et al. Endocannabinoids in chronic migraine: CSF findings suggest a system failure. *Neuropsychopharmacology*. 2007 Jun;32(6):1384–90.
 127. Akerman S, Kaube H, Goadsby PJ. Anandamide is able to inhibit trigeminal neurons using an in vivo model of trigeminovascular-mediated nociception. *J Pharmacol Exp Ther*. 2004 Apr 1;309(1):56–63.
 128. Greco R, Gasperi V, Sandrini G, Bagetta G, Nappi G, MacCarrone M, et al. Alterations of the endocannabinoid system in an animal model of migraine: Evaluation in cerebral areas of rat. *Cephalalgia*. 2010 Mar 1;30(3):296–302.
 129. Willoughby KA, Moore SF, Martin BR, Ellis EF. The biodisposition and metabolism of anandamide in mice. *J Pharmacol Exp Ther*. 1997;282(1):243–7.
 130. Strassman AM, Vos BP. Somatotopic and laminar organization of fos-like immunoreactivity in the medullary and upper cervical dorsal horn induced by noxious facial stimulation in the rat. *J Comp Neurol*. 1993;331:495–516.
 131. Drummond PD. Tryptophan depletion increases nausea, headache and photophobia in migraine sufferers. *Cephalalgia*. 2006 Oct;26(10):1225–33.
 132. Chanrion B, Mannoury La Cour C, Bertaso F, Lerner-Natoli M, Freissmuth M, Millan MJ, et al. Physical interaction between the serotonin transporter and neuronal nitric oxide synthase underlies reciprocal modulation of their activity. *Proc Natl Acad Sci U S A*. 2007 May 8;104(19):8119–24.
 133. Harkin A, Connor TJ, Burns MP, Kelly JP. Nitric oxide synthase inhibitors augment the effects of serotonin re-uptake inhibitors in the forced swimming test. *Eur Neuropsychopharmacol*. 2004 Aug 1;14(4):274–81.
 134. Tassorelli C, Blandini F, Costa A, Preza E, Nappi G. Nitroglycerin-induced activation of monoaminergic transmission in the rat. *Cephalalgia*. 2002 Nov 17;22(3):226–32.
 135. Volfe Z, Dvilansky A, Nathan I. Cannabinoids block release of serotonin from platelets induced by plasma from migraine patients. *Int J Clin Pharmacol Res*. 1985;5(4):243–6.
 136. Lichtman AH, Cook SA, Martin BR. Investigation of brain sites mediating cannabinoid-

- induced antinociception in rats: Evidence supporting periaqueductal gray involvement. *J Pharmacol Exp Ther.* 1996;276(2):585–93.
137. Vaughan CW, Connor M, Bagley EE, Christie MJ. Actions of cannabinoids on membrane properties and synaptic transmission in rat periaqueductal gray neurons in vitro. *Mol Pharmacol.* 2000;57(2):288–95.
 138. Palazzo E, De Novellis V, Petrosino S, Marabese I, Vita D, Giordano C, et al. Neuropathic pain and the endocannabinoid system in the dorsal raphe: Pharmacological treatment and interactions with the serotonergic system. *Eur J Neurosci.* 2006 Oct 1;24(7):2011–20.
 139. Seyrek M, Kahraman S, Deveci MS, Yesilyurt O, Dogrul A. Systemic cannabinoids produce CB1-mediated antinociception by activation of descending serotonergic pathways that act upon spinal 5-HT7 and 5-HT2A receptors. *Eur J Pharmacol.* 2010 Dec 15;649(1–3):183–94.
 140. Carney ST, Lloyd ML, MacKinnon SE, Newton DC, Jones JD, Howlett AC, et al. Cannabinoid regulation of nitric oxide synthase i (nNOS) in neuronal cells. *J Neuroimmune Pharmacol.* 2009 Sep 14;4(3):338–49.
 141. Nagy-Grócz G, Tar L, Bohár Z, Fejes-Szabó A, Laborc KF, Spekker E, et al. The modulatory effect of anandamide on nitroglycerin-induced sensitization in the trigeminal system of the rat. *Cephalalgia.* 2016;36(9):849–61.
 142. Coggeshall RE. Fos, nociception and the dorsal horn. *Prog Neurobiol.* 2005;77(5):299–352.
 143. Erdener SE, Dalkara T. Modelling headache and migraine and its pharmacological manipulation. *Br J Pharmacol.* 2014 Oct;171(20):4575–94.
 144. Svendsen O, Lykkegaard K. Neuronal c-Fos immunoreactivity as a quantitative measure of stress or pain. *Acta Agric Scand A Anim Sci.* 2001;51:131–4.
 145. Greene EC. *Anatomy of the rat.* Anatomy of the rat. Pub. Amer. Philosoph. Soc. Philadelphia.; 1935.
 146. Folan-Curran J, Hickey K, Monkhouse WS. Innervation of the rat external auditory meatus: A retrograde tracing study. *Somatosens Mot Res.* 1994;11(1):65–8.
 147. Schueler M, Messlinger K, Dux M, Neuhuber WL, De Col R. Extracranial projections of meningeal afferents and their impact on meningeal nociception and headache. *Pain.* 2013;154(9):1622–31.
 148. Iadarola MJ, Brady LS, Draisci G, Dubner R. Enhancement of dynorphin gene expression in spinal cord following experimental inflammation: stimulus specificity, behavioral parameters and opioid receptor binding. *Pain.* 1988 Dec;35(3):313–26.
 149. Ogawa A, Ren K, Tsuboi Y, Morimoto T, Sato T, Iwata K. A new model of experimental parotitis in rats and its implication for trigeminal nociception. *Exp brain Res.* 2003;152(3):307–16.
 150. Burstein R, Yamamura H, Malick A, Strassman AM. Chemical stimulation of the intracranial dura induces enhanced responses to facial stimulation in brain stem trigeminal neurons. *J Neurophysiol.* 1998;79(2):964–82.

151. Oshinsky ML, Luo J. Neurochemistry of trigeminal activation in an animal model of migraine. *Headache*. 2006;46(Suppl. 1):S39–44.
152. Lukács M, Warfvinge K, Tajti J, Fülöp F, Toldi J, Vécsei L, et al. Topical dura mater application of CFA induces enhanced expression of c-fos and glutamate in rat trigeminal nucleus caudalis: attenuated by KYNA derivate (SZR72). *J Headache Pain*. 2017;18(1).
153. Osebold JW. Mechanisms of action by immunologic adjuvants. *J Am Vet Med Assoc*. 1982;181(10):983–7.
154. Dvorak AM, Dvorak HF. Structure of Freund's complete and incomplete adjuvants. Relation of adjuvanticity to structure. *Immunology*. 1974 Jul;27(1):99–114.
155. Edvinsson L, Haanes KA, Warfvinge K. Does inflammation have a role in migraine? *Nat Rev Neurol*. 2019 Jul 1;15(8):483–90.
156. Moskowitz MA. The neurobiology of vascular head pain. *Ann Neurol*. 1984 Aug;16(2):157–68.
157. Chen N, Su W, Cui SH, Guo J, Duan JC, Li HX, et al. A novel large animal model of recurrent migraine established by repeated administration of inflammatory soup into the dura mater of the rhesus monkey. *Neural Regen Res*. 2019;14(1):100–6.
158. Arulmani U, Gupta S, MaassenVanDenBrink A, Centurión D, Villalón CM, Saxena PR. Experimental migraine models and their relevance in migraine therapy. *Cephalalgia*. 2006;26(6):642–9.
159. Levy D, Strassman AM. Distinct sensitizing effects of the cAMP-PKA second messenger cascade on rat dural mechanonociceptors. *J Physiol*. 2002;538(Pt 2):483–93.
160. Penfield W, McNaughton F. Dural headache and innervation of the dura mater. *Arch Neurol Psychiatry*. 1940;44(1):43–75.
161. Nozaki K, Moskowitz MA, Boccalini P. CP-93,129, sumatriptan, dihydroergotamine block c-fos expression within rat trigeminal nucleus caudalis caused by chemical stimulation of the meninges. *Br J Pharmacol*. 1992 Jun;106(2):409–15.
162. Edelmayer RM, Vanderah TW, Majuta L, Zhang E-T, Fioravanti B, De Felice M, et al. Medullary pain facilitating neurons mediate allodynia in headache-Related pain. *Ann Neurol*. 2009;65(2):184–93.
163. Jakubowski M, Levy D, Goor-Aryeh I, Collins B, Bajwa Z, Burstein R. Terminating migraine with allodynia and ongoing central sensitization using parenteral administration of COX1/COX2 inhibitors. *Headache*. 2005;45(7):850–61.
164. Lipton RB, Bigal ME, Ashina S, Burstein R, Silberstein S, Reed ML, et al. Cutaneous allodynia in the migraine population. *Ann Neurol*. 2008 Feb;63(2):148–58.

Appendix

I.

METHODOLOGY

Open Access



Trigeminal activation patterns evoked by chemical stimulation of the dura mater in rats

Kludia Flóra Laborc¹, Eleonóra Spekker¹, Zsuzsanna Bohár^{1,2}, Mónika Szűcs³, Gábor Nagy-Grócz^{1,4}, Annamária Fejes-Szabó^{1,2}, László Vécsei^{1,2,5*} and Árpád Párdutz¹

Abstract

Background: Although migraine is one of the most common primary headaches, its therapy is still limited in many cases. The use of animal models is crucial in the development of novel therapeutic strategies, but unfortunately, none of them show all aspects of the disease, therefore, there is a constant need for further improvement in this field. The application of inflammatory agents on the dura mater is a widely accepted method to mimic neurogenic inflammation in rodents, which plays a key role in the pathomechanism of migraine. Complete Freund's Adjuvant (CFA), and a mixture of inflammatory mediators, called inflammatory soup (IS) are often used for this purpose.

Methods: To examine the activation pattern that is caused by chemical stimulation of dura mater, we applied CFA or IS over the right parietal lobe. After 2 h and 4 h (CFA groups), or 2.5 h and 4 h (IS groups), animals were perfused, and c-Fos immunoreactive cells were counted in the caudal trigeminal nucleus. To explore every pitfall, we examined whether our surgical procedure (anesthetic drug, stereotaxic apparatus, local lidocaine) can alter the results under the same experimental settings. c-Fos labeled cells were counted in the second-order neuron area based on the somatotopic organization of the trigeminal nerve branches.

Results: We could not find any difference between the CFA and physiological saline group neither 2 h, nor 4 h after dural stimulation. IS caused significant difference after both time points between IS treated and control group, and between treated (right) and control (left) side. Stereotaxic frame usage had a substantial effect on the obtained results.

Conclusions: Counting c-Fos immunoreactive cells based on somatotopic organization of the trigeminal nerve helped to examine the effect of chemical stimulation of dura in a more specific way. As a result, the use of IS over the parietal lobe caused activation in the area of the ophthalmic nerve. To see this effect, the use of lidocaine anesthesia is indispensable. In conclusion, application of IS on the dura mater induces short-term, more robust c-Fos activation than CFA, therefore it might offer a better approach to model acute migraine headache in rodents.

Keywords: Headache, Migraine, Trigeminal system, Animal model, Inflammatory soup, Complete Freund's adjuvant, C-Fos

* Correspondence: vecsei.laszlo@med.u-szeged.hu

¹Department of Neurology, Faculty of Medicine, Albert Szent-Györgyi Clinical Center, University of Szeged, Semmelweis u. 6, Szeged H-6725, Hungary

²MTA-SZTE Neuroscience Research Group, Szeged, Hungary

Full list of author information is available at the end of the article



© The Author(s). 2020 **Open Access** This article is licensed under a Creative Commons Attribution 4.0 International License, which permits use, sharing, adaptation, distribution and reproduction in any medium or format, as long as you give appropriate credit to the original author(s) and the source, provide a link to the Creative Commons licence, and indicate if changes were made. The images or other third party material in this article are included in the article's Creative Commons licence, unless indicated otherwise in a credit line to the material. If material is not included in the article's Creative Commons licence and your intended use is not permitted by statutory regulation or exceeds the permitted use, you will need to obtain permission directly from the copyright holder. To view a copy of this licence, visit <http://creativecommons.org/licenses/by/4.0/>. The Creative Commons Public Domain Dedication waiver (<http://creativecommons.org/publicdomain/zero/1.0/>) applies to the data made available in this article, unless otherwise stated in a credit line to the data.

Background

According to the Global Burden of Disease Study [1], migraine is the third highest cause of disability worldwide in both men and women. Although many specific drugs are available, the treatment of migraine is limited in many cases [2]. Its exact pathophysiology is still unknown, which makes drug development even more challenging. It is known that during the migraine attack the trigeminal system becomes sensitized and remains overactive, but there are several hypotheses about the initial cause without a clear answer [3]. Finding a reliable animal model would be crucial, though a model which shows all the aspects of the disease is still not available. Use of Complete Freund's Adjuvant (CFA) or inflammatory soup (IS) on the dural surface is a proven useful method to cause trigeminal activation and sensitization in rats and these agents can stimulate neurogenic inflammation [4]. In this model, the activation and sensitization of the second-order sensory neurons occur between 2 and 4 h after application of IS similar to the cutaneous allodynia in migraine patients [5, 6].

The three sensory branches of trigeminal nerve supply the innervation of the dura mater [7, 8] and their somatotopic representation in the brainstem is already well described [9, 10]. However, the effect of chemical stimulation of the dura has never been studied before in regard to the representation of the nerve branches.

Expression of Fos protein is a well-known marker of activation in the trigeminovascular system [11]. In the chemical activation model, c-Fos expression might be induced by many stimuli (anesthetic drug, skin incision, ear bars of the stereotaxic apparatus, meningeal irritation, etc.) [12]. Knowing these effects would be essential for the proper analysis of the specific stimulus, to avoid pitfalls of the model. Thus, the aim of our study is to characterize the neuronal activation using two different inflammatory agents on the dura of rats and to determine the effects of surgery, and other altering factors on the expression of the Fos protein.

Methods

Animals

Forty-eight adult male Sprague-Dawley rats (weight 240–430 g) were used. The animals were raised and housed under standard laboratory conditions, light-dark cycle 12–12 h, regular rat chow and water ad libitum. The procedures used in our study were approved by the Committee of the Animal Research of University of Szeged (I-74-49/2017) and the Scientific Ethics Committee for Animal Research of the Protection of Animals Advisory Board (XI/1098/2018), and followed the guidelines the Use of Animals in Research of the International Association for the Study of Pain and the directive of the European Parliament (2010/63/EU).

Inflammatory substances, drugs

We used two different inflammatory agents on the dura mater: CFA contained dried, inactivated *Mycobacterium tuberculosis* in mineral oil (Sigma-Aldrich, St. Louis, MO, USA) and IS contained 1 mM bradykinin, 100 μ M prostaglandin, 1 mM serotonin, 1 mM histamine, (pH 5.0) in 10 mM HEPES buffer. Control groups received 0.9% physiological saline or synthetic interstitial fluid (SIF) (135 mM NaCl, 5 mM KCl, 1 mM $MgCl_2$, 5 mM $CaCl_2$, 10 mM glucose, in 10 mM HEPES buffer, pH 7.3). Lidocaine (20 mg/mL; Egis, Budapest, Hungary) was diluted with physiological saline to have a final concentration of 10 mg/ml (1%).

Experimental groups

Unstimulated animals

Two groups of animals with no surgery/surgical intervention.

NAT group

Animals were anesthetized and fixed in a stereotaxic apparatus for the same time period as the animals in 2CFA/2PHYS group ($n = 3$).

FRE group

Animals were anesthetized and placed on a heating pad as long as the procedure of the 2CFA or 2PHYS animals was held ($n = 3$).

2PHYS/2CFA; 4PHYS/4CFA groups

Animals underwent surgery, on the dural surface physiological saline (PHYS groups) or CFA (CFA groups) was applied. The survival time was 2 (2PHYS/2CFA) or 4 h (4PHYS/4CFA) after the CFA/saline treatment ($n = 4$, $n = 4$; $n = 3$; $n = 3$).

LCFA/LPHYS groups

Rats in these groups underwent the same procedure as 2CFA and 2PHYS groups, but lidocaine was used to anesthetize the scalp before the incision was made on the head ($n = 2$, $n = 2$).

2SIF/2IS; 4SIF/4IS groups

2.5- or 4-h survival time was chosen to make sure we avoid activation due to the surgery. Animals in these groups had the same surgical procedure as rats in LCFA/LPHYS group, received dural SIF/IS treatment and were perfused after 2.5 h (2SIF/2IS) or 4 h (4IS/4SIF) ($n = 6$ /group) (Fig. 1a).

Procedures

The animals were deeply anesthetized using 4% chloral hydrate (400 mg/kg; intraperitoneal (i.p.)) and placed in a stereotaxic apparatus. The scalp was anesthetized by

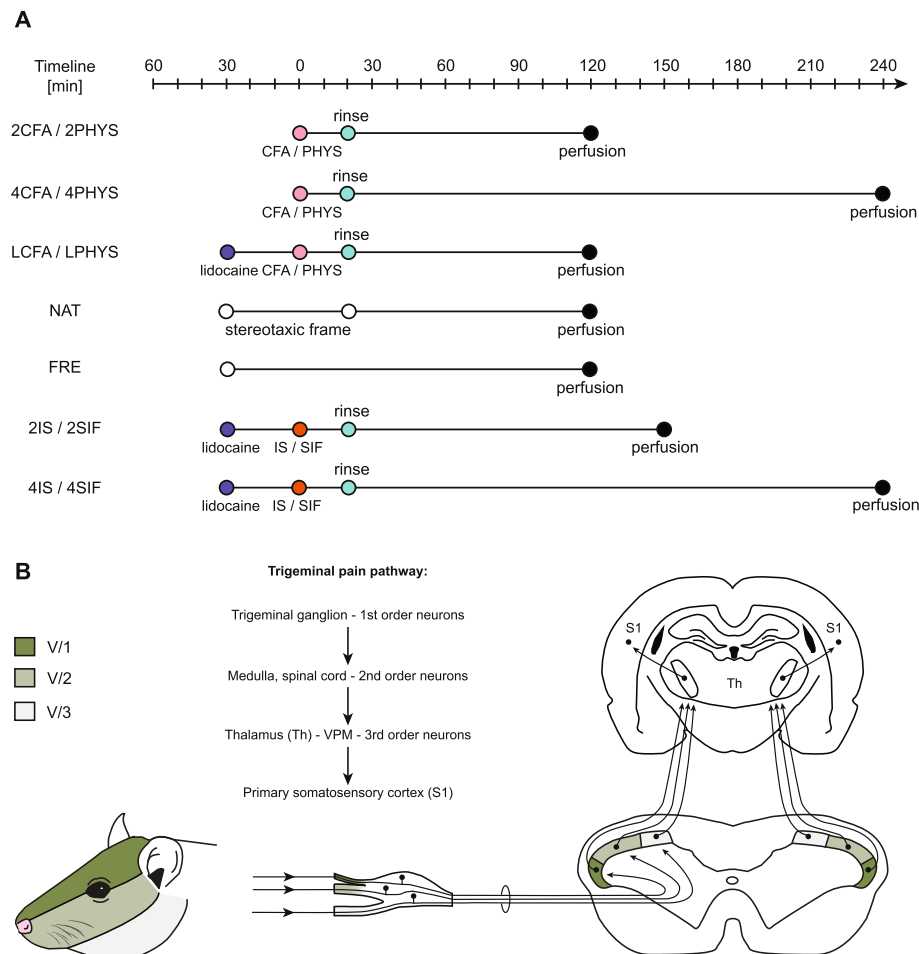


Fig. 1 a: Schematic timeline of the experimental design. The CFA/saline/IS/SIF treatment was considered as "0" timepoint. LCFA, LPHYS, 2IS, 2SIF, 4IS, 4SIF groups received lidocaine before the skin incision. 20 min after dural treatment, the surface of the dura was rinsed off with either saline or SIF. Animals in NAT and FRE groups were only anesthetized and placed in a stereotaxic frame (NAT) or left on a heating pad (FRE) as long as animals in other groups. **b:** Schematic figure of trigeminal pain pathway. Dermatome distribution of the trigeminal nerve divisions of the face. Trigeminal ganglion contains the first-order neurons, second-order neurons are found in the spinal cord and medulla. Schematic figure of the dorsal horn shows the somatotopic representation of the three branches of the trigeminal nerve. The ventral (darkest), intermediate and dorsal part of the dorsal horn considered to be equivalent to the area of the ophthalmic (V/1), maxillary (V/2), and mandibular (V/3) branch. Figure of the coronal brain section represents the third-order neurons in the thalamus (Th) and neurons in the primary somatosensory cortex (S1)

infiltration of lidocaine (dose of 4.5 mg/kg; subcutaneously) in LCFA, LPHYS, 2SIF, 2IS, 4SIF, 4IS groups. A 2 mm × 2 mm hole (5 mm posterior from the bregma and 3 mm lateral of the midline, above the right hemisphere) was carefully drilled with slow speed, using saline for cooling, avoiding any injury of the dura mater. On the dural surface 10 µL CFA (in groups 2CFA, 4CFA, LCFA) or IS (2IS, 4IS) was applied. Control groups received physiological saline (2PHYS, 4PHYS, LPHYS groups) or SIF (in groups 2SIF, 4SIF). To prevent the local spreading of the chemicals, we adjusted the position of the head in the stereotaxic frame, so the dorsal surface of the skull was horizontal. After 20 min the area was washed with either physiological saline or SIF. To prevent drying out of the dura saline or SIF soaked

cotton ball was placed carefully on top. After the surgery animals were kept under anesthesia and placed on a heating pad. The rats were transcardially perfused 2 h (2PHYS, 2CFA, LPHYS, LCFA, NAT, FRE), 2.5 h (2IS, 2SIF) or 4 h (4PHYS, 4CFA, 4IS, 4SIF) after the application of the inflammatory mediators. For the perfusion 50 mL of 0.1 M phosphate-buffered saline (PBS) and 200 mL of 4% phosphate-buffered paraformaldehyde (PFA) was used. The entire brain with the cervical spinal cord was removed, and superficial, angled rostrocaudal cut was made on the ventral, left side of the brainstem and spinal cord. After sectioning this mark allowed us to determine the orientation and the correct rostrocaudal order of the free-floating sections.

Immunohistochemistry

After postfixation (4% PFA overnight) and cryoprotection with 30% sucrose solution (after gradually increased concentration), cryostat sections of 30 μm thickness were cut. Thirty serials of sections were collected into 10 wells starting from one millimeter rostrally to the obex. Every tenth section was used for staining. For the c-Fos immunohistochemistry free-floating sections were blocked using 0.3% H_2O_2 in PBS. After several washes with PBS containing 1% Triton-X-100 (PBS-T), sections were incubated with 10% goat serum in PBS-T for an hour. Incubation with primary antibody for c-Fos (1:2000, sc-52, Santa Cruz Biotechnology, Dallas, TX, USA) was performed on a shaker overnight at room temperature. The reaction was visualized using Vectastain Elite avidin-biotin kit (PK6101, Vector Laboratories, Burlingame, CA, USA) with 3,3'-diaminobenzidine (Sigma-Aldrich, St. Louis, MO, USA) intensified by nickel-ammonium-sulfate. The specificity of the immune reaction was tested by omitting the primary antiserum. The sections were mounted on glass slides and dried overnight, cleared in xylene, and coverslipped.

Counting of immunopositive cells

An observer blind to the procedures counted the immunoreactive cells for c-Fos in laminae I-II of the dorsal horn using Nikon Optiphot-2 light microscope (Nikon, Tokyo, Japan) under 10x objective. The cells were also counted according to the somatotopic representation of the trigeminal nerve branches (based on Strassman and Vos, 1993 [13]). The ventral, intermediate, and dorsal parts of the dorsal horn considered to be equivalent to the area of the ophthalmic (V/1), maxillary (V/2), and mandibular (V/3) branch. (Fig. 1b).

Representative photographs were taken by an AxioImager M2 microscope equipped with AxioCam MRC rev.3 camera (Carl Zeiss, Germany) with a 20x objective.

Statistical analysis

The collected data were analyzed in the 2IS, 2SIF, 4IS, and 4SIF groups. The effects of treatments on c-Fos cell numbers in various distances from the obex between the treated and untreated sides were examined with mixed-design variance of analysis (MIXED-ANOVA) models with distance, treatment, and side as repeated measures (within-subject factor) and group as between-subject factors. $p < 0.05$ was considered statistically significant. Pairwise comparisons were used on estimated marginal means by taking into account the presence or absence of interaction; Holm-Sidak method was performed to adjust p -values. For the statistical analysis, IBM SPSS 24.0 (IBM Corp, Armonk, NY, USA) was used. For all other groups, no statistical analysis was used because of the small sample size and to reduce the number of animals used to a

minimum. Graphs were made in GraphPad Prism 8.0.1, data are showed as mean + SEM on all figures.

Results

Stereotaxic frame

The application of the stereotaxic frame caused bilateral dense, localized increase in the number of immunoreactive (IR) cells in the somatotopic area of the maxillary nerve (maximum cell number (V/2) 24.17 ± 7.96 at obex - 7.5) (Fig. 2a).

Anesthetic effect (chloral hydrate) and perfusion

The effect of chloral hydrate and the perfusion in the trigeminal nerve area was negligible (maximum cell number (V/1) 3.83 ± 1.68 at obex - 0.3, Fig. 2b).

CFA

Dural CFA did not cause noticeable increase in the number of immunoreactive cells compared to physiological saline neither 2 h nor 4 h after administration. There was no difference in the number of cells between the right and left dorsal horns. (Figure not shown.)

However, when the cells were counted based on the trigeminal somatotopy, substantial increase was found in the maxillary nerve area (2CFA, 2PHYS), but no difference was seen between the CFA treated and saline-treated animals (Fig. 3a, b). A slight increase was observed in the ophthalmic nerve area without any difference between the two groups. The labeled cell number was negligible in the mandibular nerve area (Fig. 3a, b).

There was no difference between the 4CFA and 4PHYS groups. The number of c-Fos IR cells was less after 4 h compared to the 2 h group (Fig. 4).

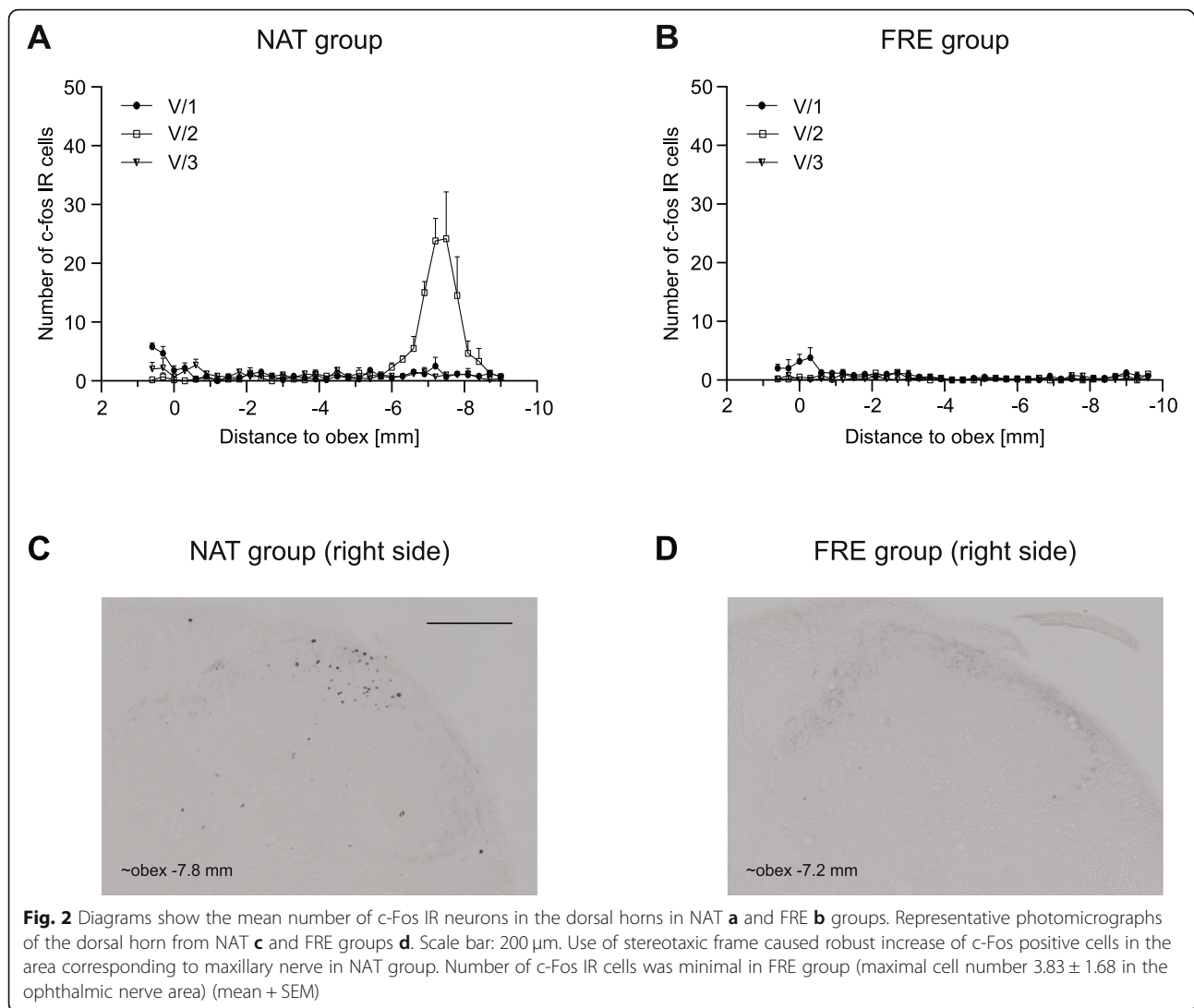
Lidocaine

Subcutaneous lidocaine applied on the scalp decreased the number of c-Fos immunopositive cells compared to 2CFA group, especially in the area of the ophthalmic branch. Dural application of CFA (Fig. 3c) did not cause robust changes compared to saline in this case either (Fig. 3d).

IS

Animals showed significant increase in the number of c-Fos labeled cells in the spinal trigeminal nucleus caudalis both 2.5 h and 4 h after the dural application of IS (Figs. 5 and 6).

In the 2.5 h group, these changes were more prominent in the somatotopic area of the ophthalmic nerve. Two peaks of activation were found among the rostrocaudal axis. The first peak is at the level of the obex which follows the activation pattern of FRE, while the second was at obex (-2) - (-6) mm which in 2IS significantly higher compared to 2SIF. Also, we found significant difference between the right (ipsilateral) and left (contralateral) side at the same rostrocaudal levels. A



substantial peak (at obex $[-6] - [-8]$ mm) can be seen in the sensory area of the maxillary nerve which is consistent with the peak found in NAT and is not different among 2IS and 2SIF. In the mandibular nerve area, the number of labeled cells was negligible without any difference between the groups. The result of the immunohistochemical staining from the 4SIF and 4IS groups is shown in Fig. 6. The activation pattern is comparable to the peak seen in 2IS group after 2.5 h in the V/1 area. The fact that we saw similar activation pattern in the V/1 area suggests sustained stimulation of the ophthalmic nerve. The substantial increase in number of c-Fos IR cells which was seen in the 2SIF and 2IS groups in V/2 cannot be found in the 4-h survival groups. The number of c-Fos positive cells in the V/3 area is negligible. After 4 h there was significant difference between 4SIF and 4IS group which was present both in the dorsal horn and V/1 area (Fig. 6).

Discussion

Fos protein is a widely used marker for locating activated neuronal populations during nociception [14]. C-Fos is an immediate-early gene, its transcription starts within 5 min after the stimulus occurrence [15], and its expression can be already detected at 30 min [16]. Its half-life is 2 h, therefore, it is important to plan the experiment and to establish endpoints according to this time window [17].

Measurement of c-Fos is widely used in headache models, but it is thought to be unspecific since various stimuli might change its expression. In the dural inflammation model, used by our group and many others, surgery (anesthesia, stereotaxic frame – V/1, V/2, skin incision – V/1, etc.) can activate neurons which might interfere with proper data analysis and could be the pitfalls of this method (Fig. 1b).

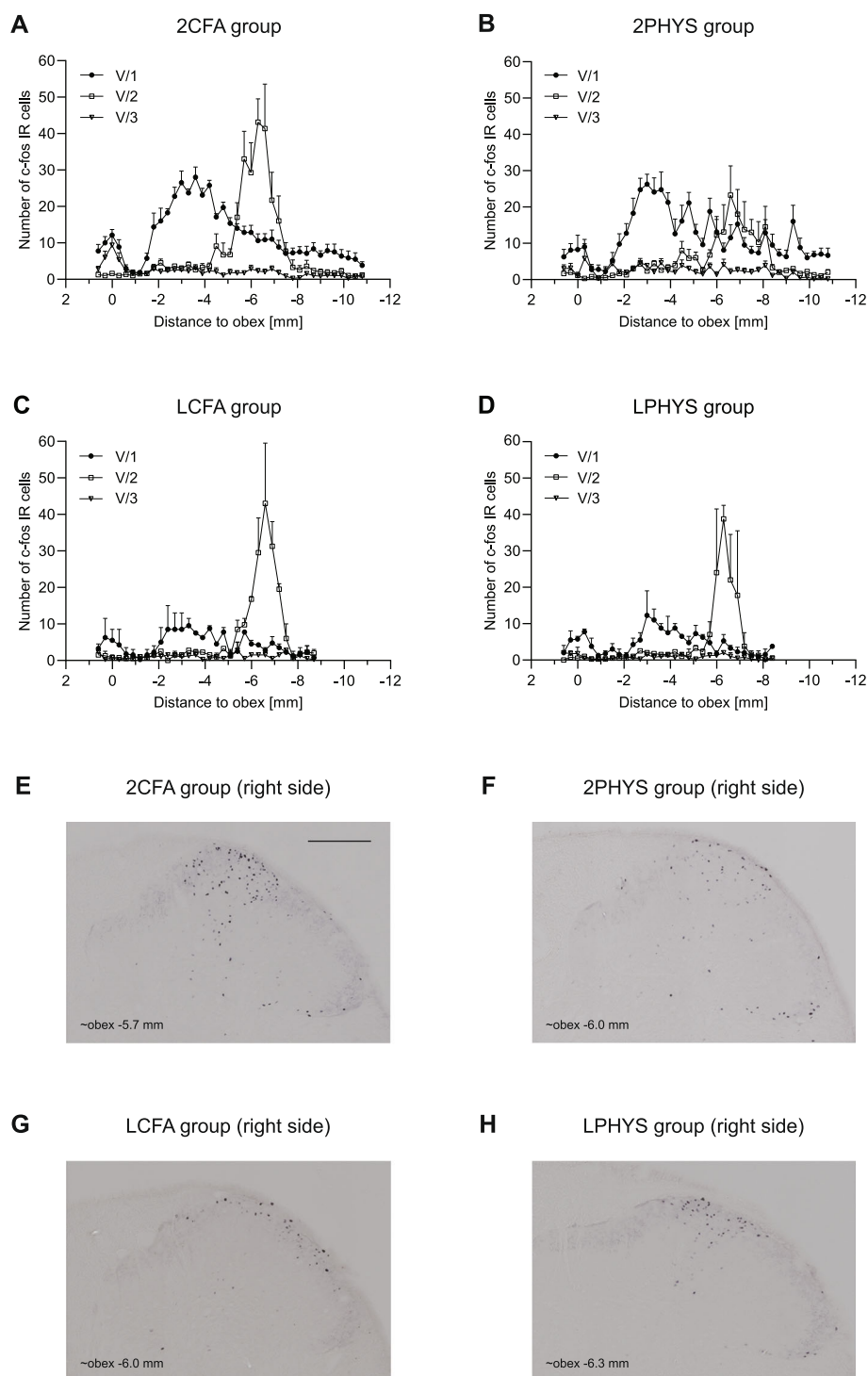


Fig. 3 Diagrams illustrate mean number of c-Fos IR neurons in the dorsal horns 2 h after CFA treatment. The number of the cells is displayed according to somatotopic representation of V/1, V/2, V/3 in 2CFA **a** and 2PHYS **b** groups. Diagrams show the mean number of c-Fos IR cells in LCFA **c** and LPHYS **d** groups. Representative photomicrographs from 2CFA **e**, 2PHYS **f**, LCFA **g**, LPHYS **h** group showing the right dorsal horns. Scale bar: 200 μ m. Lidocaine decreased the number of c-Fos positive cells compared to 2CFA and 2PHYS group especially in the V/1 area of the dorsal horns (mean + SEM)

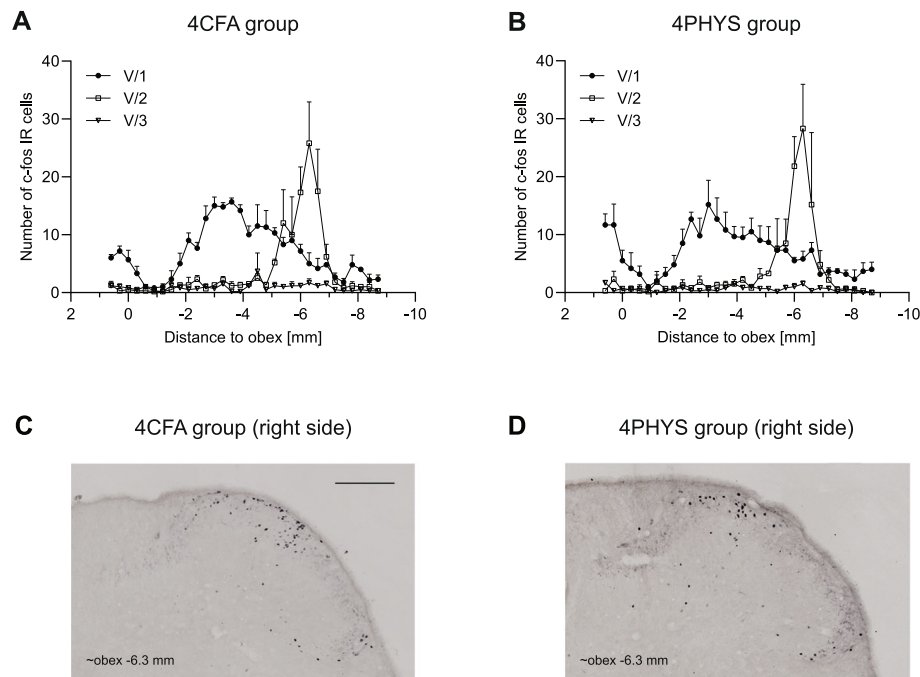


Fig. 4 Diagrams illustrate the number of c-Fos positive neurons (mean + SEM) 4 h after CFA **a** or saline **b** treatment. Representative photomicrographs of the dorsal horns in 4CFA **c**, 4PHYS **d**. Scale bar: 200 μ m. Cells were displayed according to somatotopic area of V/1, V/2, V/3 nerve. No difference was seen between 4CFA **a** and 4PHYS **b** group

To better understand these modifying factors and the pattern of the activated cells, we tested the effect of i.p. anesthetic drug, perfusion, stereotaxic frame, and the anesthesia of the skin and scalp by lidocaine. The expression changes were examined in the spinal trigeminal nucleus caudalis, and the rostrocaudal and somatotopic distribution was also taken into account to increase specificity.

It is known for a long time that urethane can cause activation in the trigeminal system even without any facial stimulation. Strassman and Vos found that not just urethane, but immediate perfusion in pentobarbital anesthesia causes substantial activation in the caudal medulla [13]. Based on this study, we decided to examine the effect of chloral-hydrate anesthesia and perfusion (FRE group). The number of c-Fos IR cells mildly increased in the V/1 area, but no activation was found in the area of V/2 and V/3. The rostrocaudal distribution and the number of c-Fos IR cells were comparable to the previous findings of Strassman and Vos [13].

A stereotaxic frame is essential in cranial surgeries to completely stabilize the head and ensure experimental procedure consistency of each employed animal, but in our experiment, it caused a robust and highly variable activation in the area of the maxillary nerve (NAT group). Animals were held in the frame using three points; ear bars placed in the ear canals and snout were fixed by the front incisors. Innervation of the upper

frontal incisors is provided by the maxillary nerve, which can be responsible for the activation effect seen in the V/2 area [18]. External ear canal is innervated by auriculotemporal nerve (from V/3), greater and lesser auricular nerve (from C2, C3 spinal nerves), Arnold's nerve (from vagus, glossopharyngeal and facial nerve) [19]. As we did not witness any increase in the number of activated cells in the V/3 area, the aforesaid increase in V/2 might be mainly due to the fixation of the snout. The substantial activation found in V/1 area is consistent with the changes seen in FRE group that underwent only anesthesia and perfusion.

In addition, for a more specific analysis of the effects of chemical stimulation of the dura, lidocaine was applied subcutaneously on the scalp (LCFA, LPHYS groups), before the surgical incision and CFA treatment, which decreased the number of c-Fos IR cells in the area of ophthalmic nerve compared to 2CFA and 2PHYS group. Recent tracing studies suggest that intracranial and extracranial structures share afferent fibers, which innervate the dura mater and after penetrating the calvarium they supply the periosteum [20, 21]. Surgical incision of the skin can activate these neurons and can hide the effect of the chemical stimulation of the dura, thus the use of lidocaine is essential when examining dural nociception. The distribution of c-Fos in V/2 area was similar to the NAT group's activation pattern and based on the rostrocaudal appearance and variance, we

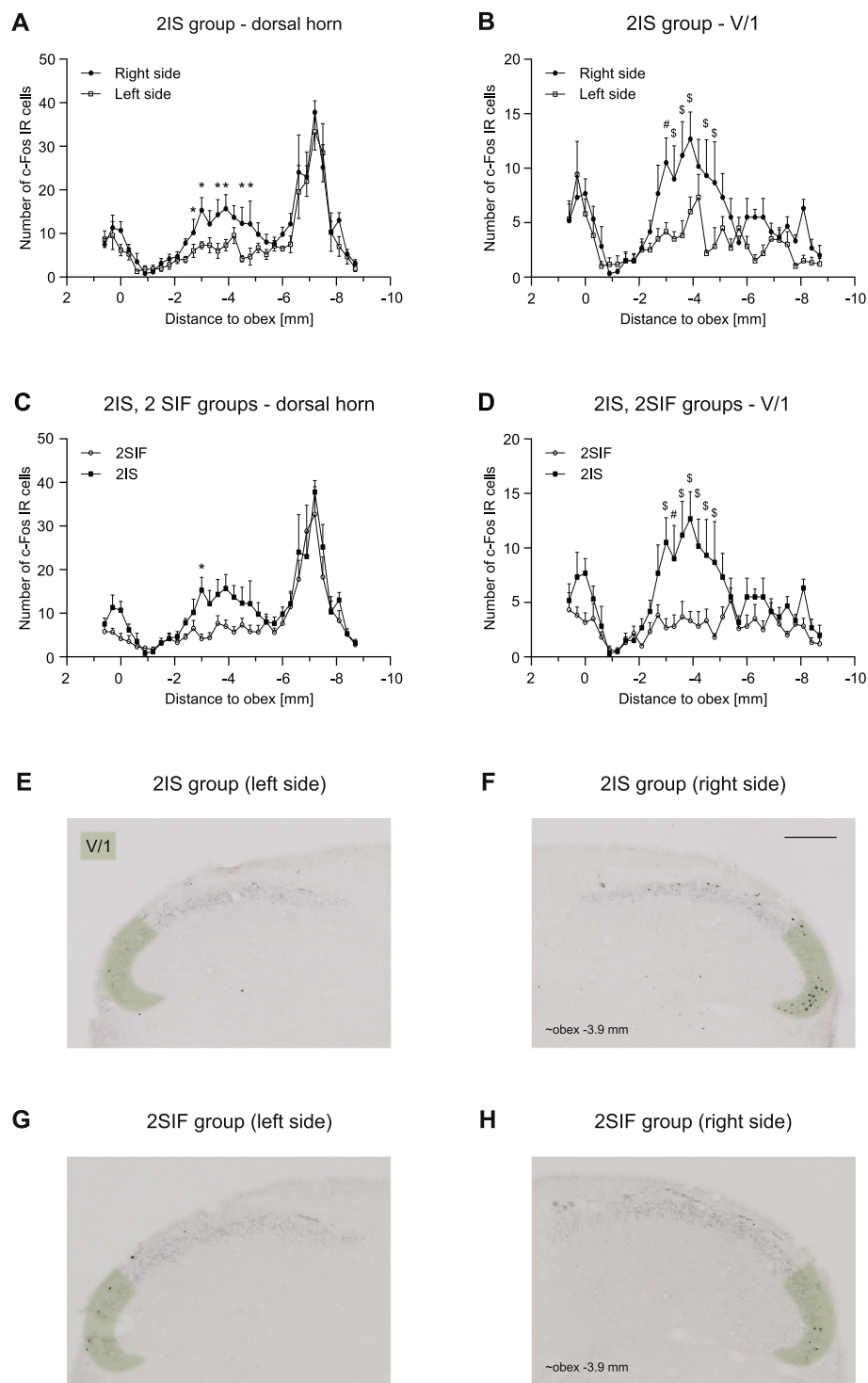


Fig. 5 Diagrams showing c-Fos immunoreactive cells across different levels of TNC (mean + SEM) in the whole dorsal horn **a, c** and the V/1 area **b, d** 2.5 h after IS **a, b, c, d** or SIF **c, d**. Representative photomicrographs showing c-Fos IR cells in the dorsal horns of 2IS **e, f**, 2SIF groups **g, h**. Green highlighting shows the V/1 area in the dorsal horn. Scale bar: 200 μm. We found significant difference between right and left side of the dorsal horn laminae I-II **a**, and the ventral part of the dorsal horn **b**. IS caused significant difference in the number of c-Fos positive cells in the V/1 area **d**. Peak at obex follows the activation pattern of FRE, substantial peak at obex (−6) – (−8) mm is consistent with the increased number of cells found in NAT group (* $p < 0.05$, # $p < 0.01$, \$ $p < 0.001$)

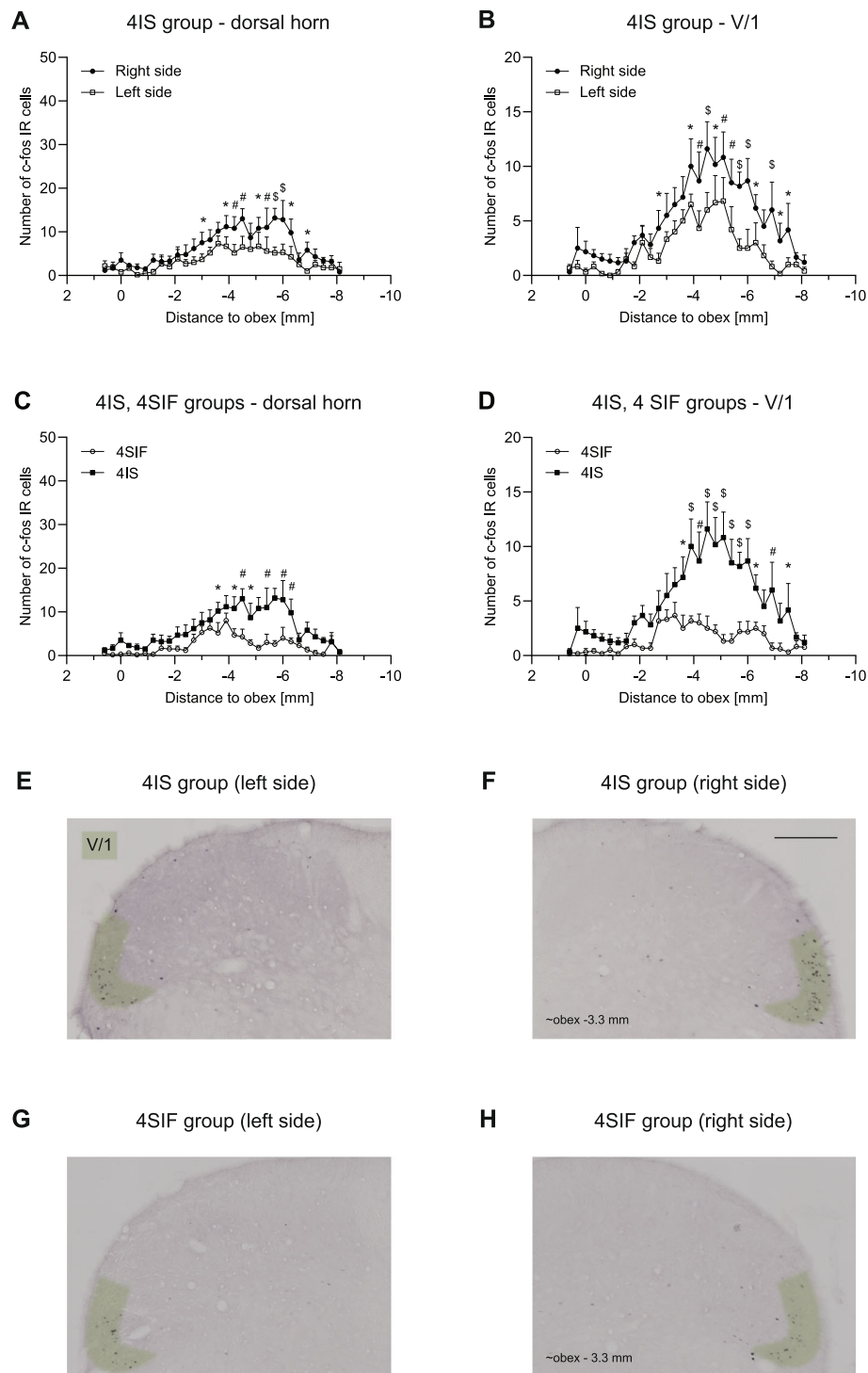


Fig. 6 Diagrams illustrate number of c-Fos positive cells in 4IS, 4SIF groups **a-d**. Photomicrographs showing c-Fos expression in the dorsal horns of 4IS **e, f** and 4SIF groups **g, h**. Green highlighting shows the V/1 area in the dorsal horn. Scale bar: 200 μ m. IS significantly increases the number of c-Fos IR neurons both in the whole dorsal horn **a** and the V/1 area **b**. IS increased the number of c-Fos positive cells compared to SIF in the whole dorsal horn **c** and in the ophthalmic nerve area **d** (mean + SEM; * $p < 0.05$, # $p < 0.01$, \$ $p < 0.001$)

can assume the effect of the stereotaxic frame here as well. These findings might help to identify the effects of various experimental procedures in the future to make data analysis easier.

In this study, we applied two different inflammatory agents on the dura mater, namely CFA and IS. Sub- or intradermal injection of CFA is commonly used in inflammatory and neuropathic pain models: when injected into hind paw, it caused hyperalgesia and edema with rapid onset [22]. While the first effects develop in few hours and peak after 24–72 h, studies also described long-term complications, such as granulomatous inflammation, skin ulceration, focal necrosis [23]. We chose 2-h and 4-h survival time for CFA groups to avoid these long-term effects of the treatment. In our experiments, CFA applied over the right hemisphere, with 2-h survival time, did not cause any difference in the number of c-Fos positive cells between the right and left dorsal horns of the spinal trigeminal nucleus. Moreover, no changes were detected in the number of immunoreactive cells in the CFA treated and saline group either. When lidocaine was used to anesthetize the skin (LCFA and LPHYS groups) before CFA or PHYS treatment, the same outcome was seen, no difference was found among these groups. Even with the longer, 4-h survival time, we could not observe any alterations between the 4CFA and 4PHYS groups either.

Previous electrophysiological studies showed that when inflammatory agents are used on the dural surface, secondary sensitization occurred after the delay of 2–3 h in the spinal trigeminal nucleus [5, 24]. Adjuvants like CFA are frequently used for polyclonal antibody production in animals; thus, they contain substances which slow down the breakdown of Mycobacteria, prolonging its effect [23]. Other studies' results also support the delayed effect of CFA, e.g., its subcutaneous injection can induce swelling and hyperalgesia with peaks around 24 h [22]. In a model of parotitis, CFA was injected into the parotid gland, and increased c-Fos expression was detected in the spinal trigeminal nucleus after 2, 24, 72 h, which peaked at 72 h [25]. Moreover, it is important to emphasize that CFA was applied permanently in these experiments (subcutaneous, intracutaneous application, or injected into the parotid gland), while we rinsed the surface of the dura 20 min after application, which might mitigate its short term effects. The number of studies investigating dural treatment of CFA is limited; Lukács et al. applied CFA on the surface of the dura and rinsed the surface after 20 min, and they described signs of inflammation after 4 and 24 h in the trigeminal ganglion; calcitonin-gene related peptide (CGRP), interleukin-1 β levels were increased compared to saline-treated group [4]. With longer survival time (seven days), they detected increased number of c-Fos positive cells in the spinal

trigeminal nucleus [26]. Based on the studies mentioned above, we can assume that the variances between the site and the mode of application might induce different effects (onset and duration), consequently, in different experiments, various neuronal activation and sensitization patterns were described; the first effects developed over 2, 4 h or more, and in most cases, the peak was between 24 and 72 h. This is consistent with the time course of delayed-type hypersensitivity reaction, which could be the main mechanism of action of the CFA application and can explain the demonstrated variations [27]. In the inflammation pain models, the effects of inflammatory mediators are examined in the neurons of the dorsal root ganglia that are part of the spinothalamic pathway [28], and information processing might be slightly different in the trigeminal system. Hoffman and Matthews found that the proportion of the sympathetic fibers is higher in spinal nerves than trigeminal nerves [29]. The function of the sympathetic nervous system (SNS) in pain processing is not fully understood: it can play a role in the descending inhibition of pain [30], but on the other hand, studies showed that catecholamines might be able to sensitize nociceptors [31]. There is also a link between SNS and immune system; primary and secondary lymphoid organs receive sympathetic innervation [32], and immune cells express adrenergic receptors [33, 34]. In inflammation, immune cells upregulate alpha-1 receptors which can stimulate release of proinflammatory cytokines [35, 36]. The higher proportion of the sympathetic fibers in spinal nerves might be able to stimulate more immune cells which, probably could initiate inflammation faster. The main mechanism of action of the CFA is cell-mediated, this could make it more sensitive to the variances in the autonomic nervous system compared to other inflammatory agents [37]. These phenomena might contribute to our results not showing the activation of the trigeminal system with shorter survival times.

Edvinsson et al. suggested that sustained trigeminal activation produced by dural or temporomandibular CFA administration could model the transformation from episodic to chronic migraine [38]. Nociceptor activation causes release of neuronal mediators like CGRP, which initiate a local inflammatory response [39] and possibly induce continuous activation and sensitization of the trigeminal system [40], creating a self-amplifying process [41]. This can be paralleled by the effect of repeated migraine attacks, which might generate sustained neurogenic inflammation or so-called neurogenic neuroinflammation [38]. As the dural or temporomandibular administration of CFA can cause prolonged activation of the trigeminal system with continuous inflammation [4, 42], it might be able to mimic the chronification process. In our experimental design, it was important to avoid any destruction or injury on the dura mater; thus, we applied CFA for 20 min and sacrificed the animals after a delay of 2 and 4 h to

avoid any long term complications of the application, such as granulomatous infection and focal necrosis, which would appear after a longer delay. It is possible that the time of application or the survival time was too short to activate the secondary sensory neurons in the spinal trigeminal nucleus. As CFA did not cause increase in the number of c-Fos IR cells in the trigeminal system within this time frame, its dural application might be more useful in the investigation of a trigeminal activation with a longer delay.

Sterile inflammation (neurogenic inflammation) can play a role in the pathomechanism of migraine [43], and application of IS on the dura mater is widely used to mimic this process in animals [44, 45]. IS contains inflammatory agents; bradykinin, prostaglandin E_2 , histamine, and serotonin, causing activation of the neurons directly and indirectly through release of other mediators. Activation and sensitization markers can be detected as soon as 20 min after the stimulation in the first-order neurons, and after 2 h in the second-order neurons [5, 46]. We examined the number of c-Fos immunoreactive cells after dural IS in spinal trigeminal nucleus caudalis. Previous mapping studies helped us to learn more about the innervation of the dura mater and the somatotopic representation of the trigeminal nerve [7, 47]. These studies allowed us to be the first to present the effect of chemical stimulation in detail. Compared to SIF, IS caused significant increase in the number of labeled cells was the most prominent in the somatotopic area of the ophthalmic nerve, which is responsible for the somatosensory innervation of the dura mater [48]. The innervation of the supratentorial dura is mostly ipsilateral [48], consequently, we found significant difference between the right (ipsilateral) and left (contralateral) caudal spinal trigeminal nucleus. In several studies, a catheter was placed into the cisterna magna or over the parietal hemisphere [49, 50]. If the mediators are injected to the cisterna magna, side differences cannot be seen because this area has bilateral innervation and the substance spreads around the cisterna [51]. The significant difference in the number of c-Fos IR cells between the IS and SIF groups persists even after 4 h. From earlier studies, it is known that IS can cause activation and sensitization of the trigeminal system: it has been demonstrated that chemical stimulation of the dura caused hyperresponsiveness and increased the receptive field of the TNC neurons [52], and Edelmayer et al. presented that dural IS was able to induce cutaneous allodynia not only in the trigeminal dermatome but also in the hind-paws. In their experiments, withdrawal threshold to von Frey filament stimulation decreased slowly after dural IS application, reached its maximum after 3 h, and returned to baseline after 5–6 h [53]. These findings suggest that the central sensitization and allodynia is an indirect effect of IS and can explain

the persistent activation found throughout our experimental time points.

Application of IS on the dura mater triggers activation and sensitization of the trigeminal system, showing several similarities with migraine. Allodynia is present in ~63% of the patients, in the animal model the time course of the central sensitization is consistent with the cutaneous allodynia seen in patients [54, 55]. Many studies demonstrated that IS evoked activation respond to migraine-specific and non-specific drugs, which supports that the chemical stimulation model has a place in drug development [52, 56]. Though dural application of IS cannot demonstrate all aspects of the disease, based on these findings it can be a valid animal model of migraine.

Our data support that dural application of IS is a relevant animal model of migraine, however, application of CFA can be an alternative method if the longer delay of the latter is taken into account as they recruit leucocytes, which release inflammatory mediators instead of direct neuronal activation.

Conclusion

Counting cells according to the somatotopic organization in the trigeminal system helps the data analysis, chemical stimulation over the parietal lobe has the most prominent effect in the ophthalmic nerve area. Based on other's and our results, somatotopic representation of the scalp and the parietal dura mater overlaps; thus, application of lidocaine is essential to examine the effect of chemical stimulus in a more specific way. In summary, IS applied on the dura mater can serve as an approach to model acute migraine, while dural application of CFA might be used as a long-term trigeminal activation model.

Abbreviations

CFA: Complete Freund's Adjuvant; 2CFA/4CFA: Complete Freund's Adjuvant treated groups; CGRP: Calcitonin-gene related peptide; i.p.: Intraperitoneal; IR: Immunoreactive; IS: Inflammatory soup; 2IS/4IS: Inflammatory soup treated groups; PBS: Phosphate buffered saline; PBS-T: PBS containing 1% Triton-X-100; PFA: Paraformaldehyde; 2PHYS/4PHYS: Physiologic saline treated groups; SIF: Synthetic interstitial fluid; 2SIF/4SIF: Synthetic interstitial fluid treated groups; SNS: Sympathetic nervous system; V/1: Ophthalmic nerve; V/2: Maxillary nerve; V/3: Mandibular nerve

Acknowledgements

We thank Mrs. Valéria Vékony for her technical assistance. We are grateful to Chloé Grieumard and Esmée Burgers for assistance with aspects of experiments.

Authors' contributions

KFL: participated in the design and implementation of experiments, collected data for statistical analysis, interpreted the data and wrote the manuscript. ES: participated in the design and in the implementation of the experiments (4SIF, 4IS groups) and in the critical revision of the manuscript. ZB, GNG: participated in the design and in the implementation of the experiments and in the critical revision of the manuscript. ASF participated in the critical revision of the manuscript. MS participated in the design of the statistical analysis and critical revision of the manuscript. LV participated in the design of the experiments, in the critical revision of the manuscript and in the final approval of the version to be published. ÁP participated in the design of the experiments, the interpretation of the data and the writing and critical

revision of the manuscript. All authors contributed toward drafting and revising the paper and agree to be accountable for all aspects of the work.

Funding

This work was supported by GINOP 2.3.2-15-2016-00034, TUDFO/47138–1/2019-ITM, 20391–3/2018FEKUSTRAT and University of Szeged Open Access Fund, Grant number 4654 programs.

Availability of data and materials

The datasets used and/or analyzed during the current study are available from the corresponding author on reasonable request.

Ethics approval and consent to participate

The procedures used in our study were approved by the Committee of the Animal Research of University of Szeged (I-74-49/2017) and the Scientific Ethics Committee for Animal Research of the Protection of Animals Advisory Board (XI/1098/2018), and followed the guidelines the Use of Animals in Research of the International Association for the Study of Pain and the directive of the European Parliament (2010/63/EU).

Consent for publication

Not applicable.

Competing interests

Not applicable.

Author details

¹Department of Neurology, Faculty of Medicine, Albert Szent-Györgyi Clinical Center, University of Szeged, Semmelweis u. 6, Szeged H-6725, Hungary.

²MTA-SZTE Neuroscience Research Group, Szeged, Hungary. ³Department of Medical Physics and Informatics, Faculty of Medicine, Albert Szent-Györgyi Clinical Center, University of Szeged, Szeged, Hungary. ⁴Faculty of Health Sciences and Social Studies, University of Szeged, Szeged, Hungary.

⁵Interdisciplinary Excellence Center, Faculty of Medicine, University of Szeged, Szeged, Hungary.

Received: 29 May 2020 Accepted: 7 August 2020

Published online: 15 August 2020

References

- Vos T, Allen C, Arora M, Barber RM, Bhutta ZA, Brown A et al (2016) Global, regional, and national incidence, prevalence, and years lived with disability for 310 diseases and injuries, 1990–2015: a systematic analysis for the global burden of disease study 2015. *Lancet*. 388:1545–1602
- Irimia P, Palma JA, Fernandez-Torron R, Martinez-Vila E (2011) Refractory migraine in a headache clinic population. *BMC Neurol* 11(94):11
- Burstein R, Nosedá R, Borsook D (2015) Migraine: Multiple Processes, Complex Pathophysiology. *J Neurosci* 35(17):6619–6629
- Lukács M, Haanes K, Majláth Z, Tajti J, Vécsei L, Warfvinge K et al (2015) Dural administration of inflammatory soup or complete Freund's adjuvant induces activation and inflammatory response in the rat trigeminal ganglion. *J Headache Pain* 16(1):79
- Burstein R, Yamamura H, Malik A, Strassman AM (1998) Chemical stimulation of the intracranial dura induces enhanced responses to facial stimulation in brain stem trigeminal neurons. *J Neurophysiol* 79(2):964–982
- Burstein R, Cutrer MF, Yarnitsky D (2000) The development of cutaneous allodynia during a migraine attack clinical evidence for the sequential recruitment of spinal and supraspinal nociceptive neurons in migraine. *Brain*. 123(8):1703–1709
- Strassman AM, Mineta Y, Vos BP (1994) Distribution of fos-like immunoreactivity in the medullary and upper cervical dorsal horn produced by stimulation of dural blood vessels in the rat. *J Neurosci* 14(6):3725–3735
- Edvinsson JCA, Viganò A, Alekseeva A, Alieva E, Arruda R, De Luca C et al (2020) The fifth cranial nerve in headaches. *J Headache Pain*. 21(1):65
- Renehan WE, Jacquin MF, Mooney RD, Rhoades RW (1986) Structure-function relationships in rat medullary and cervical dorsal horn. II. Medullary dorsal horn cells. *J Neurophysiol* 55(6):1187–1201
- Marfurt CF (1981) The somatotopic organization of the cat trigeminal ganglion as determined by the horseradish peroxidase technique. *Anat Rec* 201(1):105–118
- Mitsikostas DD (2001) Sanchez del Rio M. receptor systems mediating c-fos expression within trigeminal nucleus caudalis in animal models of migraine. *Brain Res Rev* 35:20–35
- Erdener SE, Dalkara T (2014 Oct) Modelling headache and migraine and its pharmacological manipulation. *Br J Pharmacol* 171(20):4575–4594
- Strassman AM, Vos BP (1993) Somatotopic and laminar organization of fos-like immunoreactivity in the medullary and upper cervical dorsal horn induced by noxious facial stimulation in the rat. *J Comp Neurol* 331:495–516
- Coggeshall RE (2005) Fos, nociception and the dorsal horn. *Prog Neurobiol* 77(5):299–352
- Greenberg ME, Ziff EB (1984) Stimulation of 3T3 cells induces transcription of the c-fos proto-oncogene. *Nature*. 311(5985):433–438
- Abbadie C, Besson JM (1992 Jun 1) C-fos expression in rat lumbar spinal cord during the development of adjuvant-induced arthritis. *Neuroscience*. 48(4):985–993
- Svendsen O, Lykkegaard K (2001) Neuronal c-Fos immunoreactivity as a quantitative measure of stress or pain. *Acta Agric Scand A Anim Sci* 51:131–134
- Greene EC. Anatomy of the rat. Anatomy of the rat. Pub. Amer. Philosoph. Soc. Philadelphia; 1935
- Folan-Curran J, Hickey K, Monkhouse WS (1994) Innervation of the rat external auditory meatus: a retrograde tracing study. *Somatosens Mot Res* 11(1):65–68
- Kosaras B, Jakubowski M, Kainz V, Burstein R (2009) Sensory innervation of the calvarial bones of the mouse. *J Comp Neurol* 515(3):331–348
- Schueler M, Messlinger K, Dux M, Neuhuber WL, De Col R (2013) Extracranial projections of meningeal afferents and their impact on meningeal nociception and headache. *Pain*. 154(9):1622–1631
- Iadarola MJ, Brady LS, Draisci G, Dubner R (1988) Enhancement of dynorphin gene expression in spinal cord following experimental inflammation: stimulus specificity, behavioral parameters and opioid receptor binding. *Pain*. 35(3):313–326
- Osebold JW (1982) Mechanisms of action by immunologic adjuvants. *J Am Vet Med Assoc* 181(10):983–987
- Oshinsky ML, Luo J (2006) Neurochemistry of trigeminal activation in an animal model of migraine. *Headache*. 46(Suppl. 1):S39–S44
- Ogawa A, Ren K, Tsuboi Y, Morimoto T, Sato T, Iwata K (2003) A new model of experimental parotitis in rats and its implication for trigeminal nociception. *Exp Brain Res* 152(3):307–316
- Lukács M, Warfvinge K, Tajti J, Fülöp F, Toldi J, Vécsei L et al (2017) Topical dura mater application of CFA induces enhanced expression of c-fos and glutamate in rat trigeminal nucleus caudalis: attenuated by KYNA derivative (SZR72). *J Headache Pain* 18(1)
- Dvorak AM, Dvorak HF (1974 Jul) Structure of Freund's complete and incomplete adjuvants. Relation of adjuvant activity to structure. *Immunology*. 27(1):99–114
- Fehrenbacher JC, Vasko MR, Duarte DB (2012) Models of inflammation: carrageenan- or CFA-induced edema and hypersensitivity in the rat. *Curr Protoc Pharmacol* 56:5.4.1–5.4.7
- Hoffmann KD, Matthews MA (1990) Comparison of sympathetic neurons in orofacial and upper extremity nerves: implications for causalgia. *J Oral Maxillofac Surg* 48(7):720–726
- Millan MJ (2002) Descending control of pain. *Prog Neurobiol* 66:355–474
- Fuchs PN, Meyer RA, Raja SN (2001) Heat, but not mechanical hyperalgesia, following adrenergic injections in normal human skin. *Pain*. 90(1–2):15–23
- Bellinger DL, Millar BA, Perez S, Carter J, Wood C, ThyagaRajan S et al (2008) Sympathetic modulation of immunity: relevance to disease. *Cell Immunol* 252(1–2):27–56
- Bao JY, Huang Y, Wang F, Peng YP, Qiu YH (2007) Expression of α -AR subtypes in T lymphocytes and role of the α -ARs in mediating modulation of T cell function. *Neuroimmunomodulation*. 14(6):344–353
- Grisanti LA, Perez DM, Porter JE (2011) Modulation of immune cell function by α 1-adrenergic receptor activation. *Curr Top Membr* 67:113–138
- Heijnen CJ, Van der Voort CR, Wulffraat N, Van der Net J, Kuis W, Kavelaars A (1996) Functional α 1-adrenergic receptors on leukocytes of patients with polyarticular juvenile rheumatoid arthritis. *J Neuroimmunol* 71(1–2):223–226
- Schlereth T, Birklein F (2008) The sympathetic nervous system and pain. *NeuroMolecular Med* 10(3):141–147
- Huber B, Devinsky O, Gershon RK, Cantor H (1976) Cell-mediated immunity: delayed-type hypersensitivity and cytotoxic responses are mediated by different T-cell subclasses*. *J Exp Med* 143(6):1534–1539

38. Edvinsson L, Haanes KA, Warfvinge K (2019) Does inflammation have a role in migraine? *Nat Rev Neurol* 15(8):483–490
39. Geppetti P, Capone JG, Trevisani M, Nicoletti P, Zagli G, Tola MR (2005 Apr) CGRP and migraine: neurogenic inflammation revisited. *J Headache Pain*. 6(2):61–70
40. Haanes KA, Edvinsson L (2019) Pathophysiological mechanisms in migraine and the identification of new therapeutic targets. *CNS Drugs* 33(6):525–537
41. Párdutz A, Krizbai I, Multon S, Vecsei L, Schoenen J, Párdutz A et al (2000) Systemic nitroglycerin increases nNOS levels in rat trigeminal nucleus caudalis. *Neuroreport*. 11(14):3071–3075
42. Csáti A, Edvinsson L, Vecsei L, Toldi J, Fülöp F, Tajti J et al (2015) Kynurenic acid modulates experimentally induced inflammation in the trigeminal ganglion. *J Headache Pain*. 16:99
43. Moskowitz MA (1984 Aug) The neurobiology of vascular head pain. *Ann Neurol* 16(2):157–168
44. Chen N, Su W, Cui SH, Guo J, Duan JC, Li HX et al (2019) A novel large animal model of recurrent migraine established by repeated administration of inflammatory soup into the dura mater of the rhesus monkey. *Neural Regen Res* 14(1):100–106
45. Arulmani U, Gupta S, MaassenVanDenBrink A, Centurión D, Villalón CM, Saxena PR (2006) Experimental migraine models and their relevance in migraine therapy. *Cephalalgia*. 26(6):642–649
46. Levy D, Strassman AM (2002) Distinct sensitizing effects of the cAMP-PKA second messenger cascade on rat dural mechanonociceptors. *J Physiol* 538(Pt 2):483–493
47. Hunt SP, Pini A, Evan G (1987) Induction of c-fos-like protein in spinal cord neurons following sensory stimulation. *Nature*. 328(6131):632–634
48. Penfield W, McNaughton F (1940) Dural headache and innervation of the dura mater. *Arch Neurol Psychiatr* 44(1):43–75
49. Wieseler J, Ellis A, Sprunger D, Brown K, McFadden A, Mahoney J et al (2010) A novel method for modeling facial allodynia associated with migraine in awake and freely moving rats. *J Neurosci Methods* 185(2):236–245
50. Hoffmann J, Neeb L, Israel H, Dannenberg F, Triebe F, Dirnagl U et al (2009) Intracisternal injection of inflammatory soup activates the trigeminal nerve system. *Cephalalgia*. 29:1212–1217
51. Nozaki K, Moskowitz MA, Boccacini P (1992 Jun) CP-93,129, sumatriptan, dihydroergotamine block c-fos expression within rat trigeminal nucleus caudalis caused by chemical stimulation of the meninges. *Br J Pharmacol* 106(2):409–415
52. Jakubowski M, Levy D, Kainz V, Zhang X-C, Kosaras B, Burstein R (2007) Sensitization of central trigeminovascular neurons: blockade by IV naproxen infusion. *Neuroscience*. 148(2):573–583
53. Edelmayer RM, Vanderah TW, Majuta L, Zhang E-T, Fioravanti B, De Felice M et al (2009) Medullary pain facilitating neurons mediate allodynia in headache-related pain. *Ann Neurol* 65(2):184–193
54. Jakubowski M, Levy D, Goor-Aryeh I, Collins B, Bajwa Z, Burstein R (2005) Terminating migraine with allodynia and ongoing central sensitization using parenteral administration of COX1/COX2 inhibitors. *Headache*. 45(7):850–861
55. Lipton RB, Bigal ME, Ashina S, Burstein R, Silberstein S, Reed ML et al (2008) Cutaneous allodynia in the migraine population. *Ann Neurol* 63(2):148–158
56. Burstein R, Jakubowski M (2004) Analgesic Triptan action in an animal model of intracranial pain: a race against the development of central sensitization. *Ann Neurol* 55(1):27–36

Publisher's Note

Springer Nature remains neutral with regard to jurisdictional claims in published maps and institutional affiliations.

Ready to submit your research? Choose BMC and benefit from:

- fast, convenient online submission
- thorough peer review by experienced researchers in your field
- rapid publication on acceptance
- support for research data, including large and complex data types
- gold Open Access which fosters wider collaboration and increased citations
- maximum visibility for your research: over 100M website views per year

At BMC, research is always in progress.

Learn more biomedcentral.com/submissions



II.



Nitroglycerin increases serotonin transporter expression in rat spinal cord but anandamide modulated this effect



Gábor Nagy-Grócz^{a,b}, Zsuzsanna Bohár^{a,c}, Annamária Fejes-Szabó^a,
Klaudia Flóra Laborc^c, Eleonóra Spekker^c, Lilla Tar^d, László Vécsei^{a,c,*}, Árpád Párdutz^c

^a MTA-SZTE Neuroscience Research Group, University of Szeged, Szeged, Hungary

^b Faculty of Health Sciences and Social Studies, University of Szeged, Szeged, Hungary

^c Department of Neurology, Faculty of Medicine, Albert Szent-Györgyi Clinical Center, University of Szeged, Szeged, Hungary

^d Department of Neurology, University of Ulm, Oberer Eselsberg 45, 89081, Ulm, Germany

ARTICLE INFO

Article history:

Received 24 February 2017

Received in revised form 2 June 2017

Accepted 14 June 2017

Available online 15 June 2017

Keywords:

Migraine
Trigeminal system
Nitroglycerin
Anandamide
Serotonin
Serotonin transporter

ABSTRACT

Migraine is one of the most prevalent neurological diseases, which affects 16% of the total population. The exact pathomechanism of this disorder is still not well understood, but it seems that serotonin and its transporter have a crucial role in the pathogenesis.

One of the animal models of migraine is the systemic administration of nitroglycerin (NTG), a nitric oxide (NO) donor. NO can initiate a central sensitization process in the trigeminal system, which is also present in migraineurs.

Recent studies showed that the endocannabinoid system has a modulatory role on the trigeminal activation and sensitization.

Our aim was to investigate the effect of an endogenous cannabinoid, anandamide (AEA) on the NTG-induced changes on serotonin transporter (5-HTT) expression in the upper cervical spinal cord (C1–C2) of the rat, where most of the trigeminal nociceptive afferents convey.

The animals were divided into four groups. Rats in the first group, called placebo, received only the vehicle solution as treatment. In the second group, they were treated with an intraperitoneal (i.p.) injection of NTG (10 mg/kg). Rats in the third and fourth groups received i.p. AEA (2 × 5 mg/kg) half hour before and one hour after the placebo or NTG treatment. Four hours after placebo/NTG injection, the animals were perfused and the cervical spinal cords were removed for immunohistochemistry and Western blotting.

Our results show that both NTG and AEA alone are able to increase 5-HTT expression in the C1–C2 segments. Combination of NTG and AEA has an opposing effect on this marker, nullifying the effects of non-combined administration, probably by negative feedback mechanisms.

© 2017 Elsevier B.V. All rights reserved.

1. Introduction

Migraine is a chronic neurological disorder characterized by recurrent headaches lasting for 4–72 h and commonly accompanied by nausea, photophobia and phonophobia. This syndrome

affects 16% of the total population (Smitherman et al., 2013). The exact pathomechanism of the disease is not fully known, but it has been suggested that serotonin or 5-hydroxytryptamine (5-HT) has an important role in the migraine attack (Ferrari and Saxena, 1993). In 1961, Sicuteri has shown that the excretion in the urine of 5-hydroxyindoleacetic acid, the principal catabolite of 5-HT, was increased during some attacks of migraine headache (Sicuteri, 1961) and these findings were verified by Curran et al. in 1965 (Curran et al., 1965). Despite these data, the exact role of 5-HT in the pathogenesis of migraine is not fully clear.

Serotonin transporter (5-HTT) removes 5-HT from the synaptic cleft back into the pre-synaptic terminals, mitigating the effect of 5-HT. In patients with familial hemiplegic migraine, Horvath et al. have found low 5-HT levels in the platelets, reduced 5-HT transport

Abbreviations: 5-HT, serotonin; 5-HTT, serotonin transporter; AEA, anandamide; C1–C2, upper cervical spinal cord; CSD, cortical spreading depression; GAPDH, glyceraldehyde 3-phosphate dehydrogenase; i.p., intraperitoneal; nNOS, neuronal nitric oxide synthase; NO, nitric oxide; NTG, nitroglycerin; PBS, phosphate-buffered saline; TBST, Tris-buffered saline containing Tween 20.

* Corresponding author at: Department of Neurology, Faculty of Medicine, Albert Szent-Györgyi Clinical Centre, University of Szeged, Szeged, Semmelweis utca 6, H-6725 Szeged, Hungary.

E-mail address: vecsei.laszlo@med.u-szeged.hu (L. Vécsei).

capacity and low metabolite levels in the cerebrospinal fluid (Horvath et al., 2011). In a neuroimaging study increased 5-HTT availability in the mesopontine brainstem of migraineurs has been detected (Schuh-Hofer et al., 2007). Data show that the vast majority of 5-HTT is localized on the axolemma, in the vicinity of the synapses, and along the axons as well. This distribution suggests that the transporter may play a role not only in the termination of synaptic transmission, but in the general extracellular 5-HT regulation. Intracellularly, it has been demonstrated in low amount in the soma and dendrites (Tao-Cheng and Zhou, 1999; Zhou et al., 1998). Depending on the stimulus, 5-HT uptake and 5-HTT trafficking may be differentially affected, but are often linked with altered 5-HTT basal phosphorylation by Ser/Thr protein kinases (Annamalai et al., 2012; Ramamoorthy et al., 1998).

Nitroglycerin (NTG)-administration is a model of migraine, being able to generate migraine attacks in migraineurs (Sicuteri et al., 1987), and trigger activation and sensitization in the trigeminal system (Di Clemente et al., 2009). It is also well-known, that NTG—a nitric oxide donor (NO)—can initiate trigeminal activation and sensitization in animals as well (Pardutz et al., 2000; Tassorelli and Joseph, 1995). In rats, it has been shown that NTG produced an increase in the area covered by 5-HT-immunoreactive fibres (Pardutz et al., 2002), which suggests that NO influences the 5-HT system.

Cannabis has been sporadically used to reduce nausea and vomiting during chemotherapy and to treat pain, migraine and muscle spasticity (Borgelt et al., 2013). The interactions between the endocannabinoid system and pain perception are intensively studied in several laboratories, but the psychoactive properties of cannabinoids (Crawley et al., 1993) restrict their therapeutic application. On the other hand, a recent retrospective study shows, that medical marijuana is able to decrease the frequency of migraine attacks (Rhyne et al., 2016). The alteration of platelet 5-HT homeostasis was considered to be connected with the pathogenesis of migraine headache (Danese et al., 2014). Research data show a strong interaction between the cannabinoid and 5-HT system in platelets: Δ^1 -tetrahydrocannabinol blocked 5-HT release from the thrombocytes (Volfe et al., 1985), whereas platelet 5-HT uptake was inhibited by various cannabinoids (Velenovska and Fisar, 2007; Volfe et al., 1985). The interaction of cannabinoid and 5-HT systems at the periphery is well documented, but for the better understanding of migraine pathophysiology experimental data are needed about such possible mechanism in the CNS.

Anandamide (AEA) is an extensively studied endocannabinoid, which is effective in the inhibition of trigeminal activation and central sensitization in animals (Greco et al., 2010a; Nagy-Grocz et al., 2016). AEA is an agonist of both cannabinoid 1 and 2 receptors and the transient receptor potential vanilloid type 1 receptor.

The goal of the present study was to investigate the effect of NTG and AEA on the 5-HTT expression levels, in one of the central nervous system structures relevant in migraine: the superficial laminae of the upper cervical spinal cord (C1–C2) with immunohistochemistry and Western blotting.

2. Materials and methods

2.1. Animals

The procedures utilized in this study followed the guidelines for the Use of Animals in Research of the International Association for the Study of Pain and the directive of the European Economic Community (86/609/ECC). They were permitted by the Committee of the Animal Research of University of Szeged (I-74-12/2012) and the Scientific Ethics Committee for Animal Research of the Protection of

Animals Advisory Board (XI./352/2012). Forty-four adult male Sprague-Dawley rats weighing 200–250 g were used. The animals were raised and maintained under standard laboratory conditions, with tap water and regular rat chow available ad libitum on a 12 h dark–12 h light cycle.

2.2. Drug administration

The animals were divided into four groups ($n=6$ per group in the immunohistochemistry, $n=5$ in the Western blot). The animals in the first (placebo) group, received only the vehicle solution as pretreatment. In the second group, the rats were pretreated with an intraperitoneal (i.p.) injection of NTG (10 mg/kg bodyweight, Pohl Boskamp). In the third and fourth groups, rats were given AEA (2×5 mg/kg) injection half hour before and one hour after the placebo or NTG treatment. AEA was dissolved in physiological saline. In the first and second groups, animals were treated with physiological saline instead of AEA.

2.3. Immunohistochemistry

Four hours after the placebo/NTG injection, the rats were perfused transcardially with 100 ml phosphate-buffered saline (PBS, 0.1 M, pH 7.4), followed by 500 ml 4% paraformaldehyde in phosphate-buffer in chloral hydrate (0.4 g/kg bodyweight) anesthesia. The C1–C2 segments of the cervical spinal cord between –5 and –11 mm from the obex, which receive important nociceptive information from the head (Strassman et al., 1993) were removed and postfixed overnight for immunohistochemistry in the same fixative. After cryoprotection, 30 μ m cryostat sections were cut and serially collected from C1–C2 in wells containing cold PBS. The free-floating sections were rinsed in PBS and immersed in 0.3% H_2O_2 in or PBS for 30 min. After several rinses in PBS containing 1% Triton X-100, sections of C1–C2 were kept for two nights at 4 °C in anti-5-HTT antibody (Merck Millipore, ab9726) at a dilution of 1:100 000. The immunocytochemical reaction was visualized by the avidin-biotin kit of Vectastain (PK6101), and nickel ammonium sulphate –intensified 3,3'-diaminobenzidine. The specificity of the immune reaction was controlled by omitting the primary antiserum.

2.4. Western blot analysis

Four hours after the placebo/NTG injection, the animals were perfused transcardially with 100 ml PBS then the dorsal horns of C1–C2 segments were extracted. Until the measurements, the samples were stored –80 °C. The specimens were sonicated in ice cold lysis buffer containing 50 mM Tris-HCl, 150 mM NaCl, 0.1% igeal, 0.1% cholic acid, 2 μ g/ml leupeptin, 2 mM phenylmethylsulphonyl fluoride, 1 μ g/ml pepstatin, 2 mM EDTA and 0.1% sodium dodecyl sulphate. The lysates were centrifuged at 12,000 RPM for 10 min at 4 °C and supernatants were aliquoted and stored at –20 °C until use. Protein concentration was defined with BCA Protein Assay Kit using bovine serum albumin as a standard. Previous to loading, each sample was mixed with sample buffer, and denaturated by boiling for 3 min. Equal amounts of protein samples (20 μ g/lane) were separated by standard SDS polyacrylamide gel electrophoresis on 10% Tris–Glycine gel and electrotransferred onto Amersham Hybond-ECL nitrocellulose membrane (0.45 μ m pore size, GE Healthcare). We used The Page Ruler Prestained Protein Ladder (Thermo Scientific, 10–170 kDa) to define approximate molecular weights. Following the transfer, membranes were blocked for one hour at room temperature in Tris-buffered saline containing Tween 20 (TBST) and 5% non fat dry milk. Then they were incubated in TBST containing 1% non fat dry milk and 5-HTT antibody (Merck Millipore, ab9726, dilution:

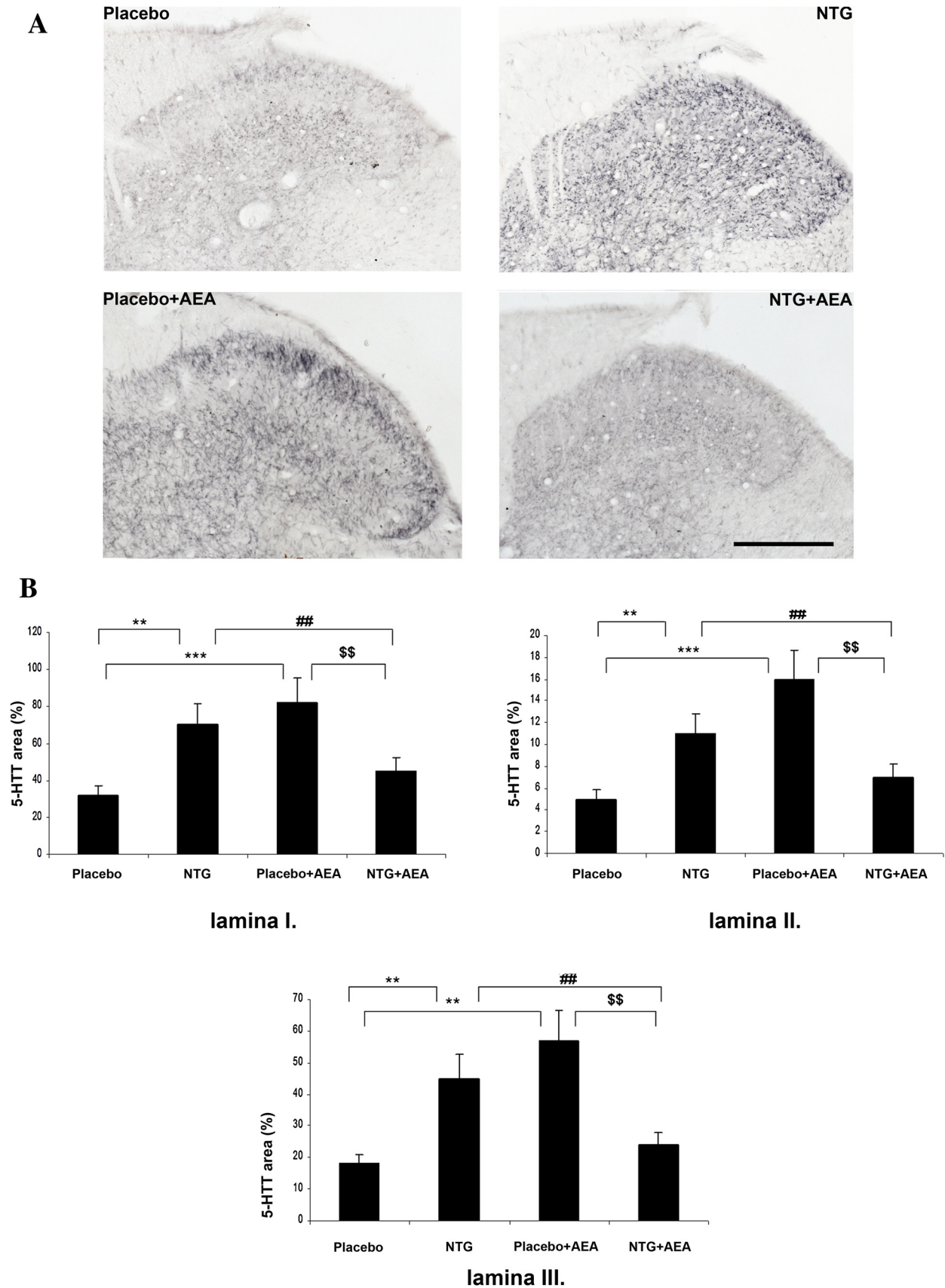


Fig. 1. Summary of immunohistochemistry results I. A. Representative photomicrographs of the 5-HTT expression in the C1–C2 segments from the treatment groups. The expression of 5-HTT is not equal between the measured laminae. Laminae I and III contain higher density of fibres compared to lamina II. B. Changes in area fractions of 5-HTT-immunoreactive fibres in superficial laminae I, II and III of the C1–C2 segments. In the NTG and AEA group, the area covered by 5-HTT was significantly higher than in the placebo group. NTG + AEA treatment abolished this effect. Bars present means \pm SEM. $^{###}p < 0.01$; $^{ss}p < 0.01$; $^{**}p < 0.01$; $^{***}p < 0.001$ Scale bar: 100 μ m.

1:2000, incubation: overnight at 4°C) or glyceraldehyde 3-phosphate dehydrogenase (GAPDH) antibody (Cell Signaling Technologies, 8884, dilution: 1:1000, incubation: overnight at room temperature). Next day, membranes were incubated in TBST containing 1% non fat dry milk and horseradish peroxidase-conjugated anti-rabbit secondary antibody (Santa Cruz Biotechnology; sc-2030) for two hours at room temperature. Protein bands were visualized after incubation of membranes with the

SuperSignal West Pico Chemiluminescent Substrate using Carestream Kodak BioMax Light film.

2.5. Data evaluation

All evaluations were implemented by an observer blind to the experimental groups. The detailed methods were described previously (Nagy-Grocz et al., 2016).

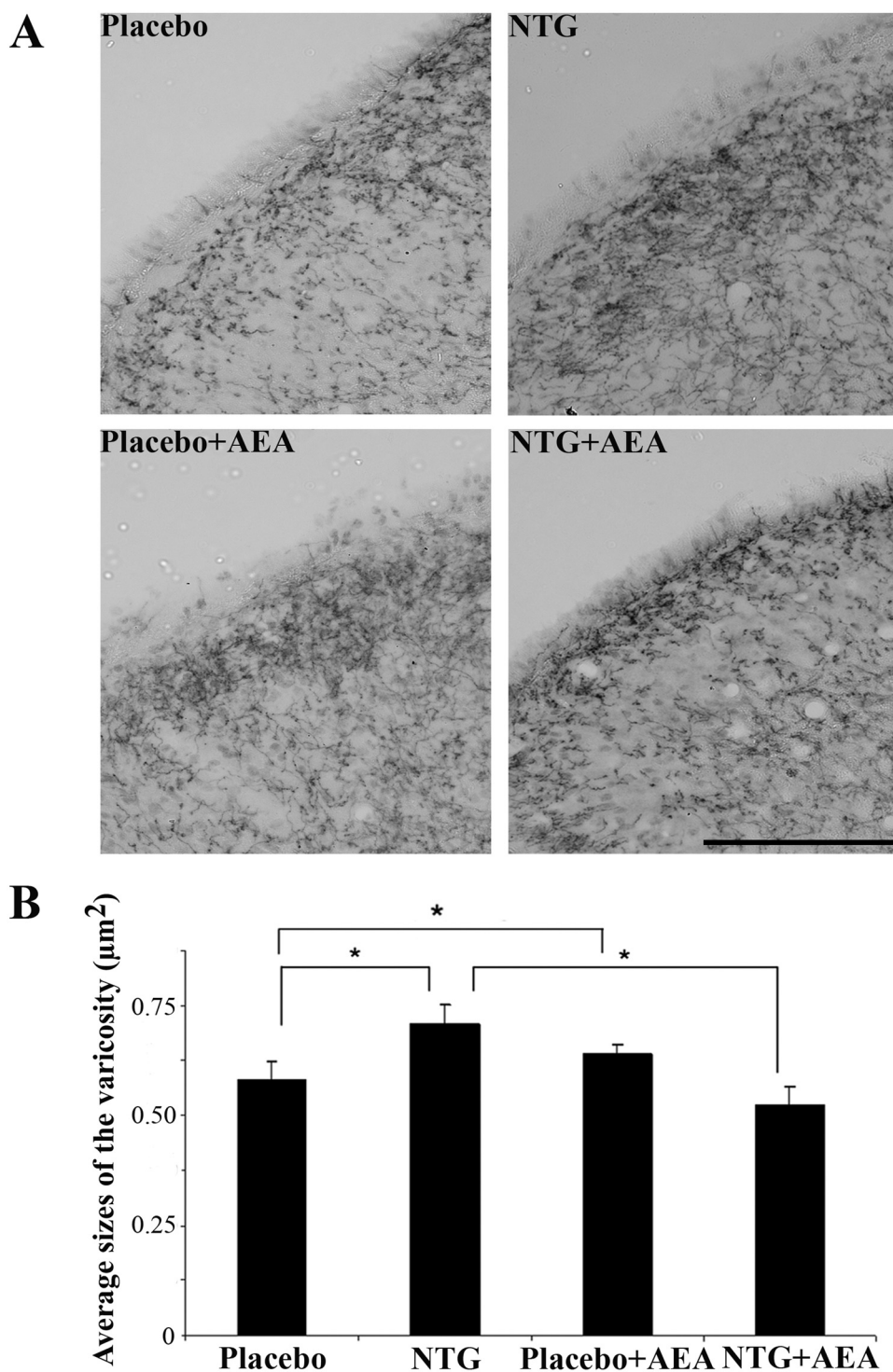


Fig. 2. Summary of immunohistochemistry results II.

A. Representative photomicrographs of the 5-HTT varicose fibres expression in laminae I–III of C1–C2 segments from the treatment groups.

B. Changes in varicosity sizes of 5-HTT in superficial laminae I–III of the C1–C2 segments. In the NTG and AEA group, the varicosity size of 5-HTT was significantly higher than in the placebo group. NTG + AEA treatment reduced this effect. Figure shows means \pm SEM. * $p < 0.05$; Scale bar: 100 μ m.

2.5.1. Immunohistochemistry

The photomicrographs of the stained sections of C1–C2 were taken using Zeiss AxioImager microscope supplied with an AxioCam MRC Rev.3 camera (Carl Zeiss Microscopy, Jena, Germany). The density of the 5-HTT-immunoreactive fibres was analyzed by Image Pro Plus 6.2[®] software (Media Cybernetics). After capturing the images, the borders of laminae I, II and III of the dorsal horn were defined manually as areas of interest (AOI). The background level of the staining intensity was first determined in the recorded gray scale images, which was used as a threshold to segment pixels in the AOI with grey levels above the background, as described in details earlier (Nagy-Grócz et al., 2016). The area innervated by the immunoreactive fibres was expressed as the cumulative number of pixels with densities above the threshold. Finally, the relative area covered by immunoreactive fibres and in the different laminae was calculated as area fractions (%) of the appropriate AOI. To exclude possible errors originating from different staining efficiency in separate experiments, background intensities in indifferent areas on the sections with non-specific staining were measured and used as inter-experimental controls.

Higher magnification photos were also taken to determine the sizes of immunoreactive varicosities by the same digital system using 40 \times objective. For the determination of the cross-sectional areas we selected processes which were in focus and were recognized and measured by the program as single objects. Measurements were carried out as above.

2.5.2. Western blot analysis

For densitometric analyses, films were scanned and quantified using Java ImageJ 1.47 v analysis software (National Institutes of Health). GAPDH served as a control to ensure loading of equivalent amounts of sample proteins and measured protein levels of 5-HTT were normalized to GAPDH.

2.6. Statistical analysis

Statistical analysis of measurements were performed in SPSS Statistics software (Version 20.0 for Windows, SPSS Inc.) by one-way analysis of variance followed by the Fishers Least Significant Difference post hoc test, with $p < 0.05$ taken as statistically significant. Normality was tested with Shapiro-Wilk test. Group values are reported as means \pm S.E.M.

3. Results

3.1. NTG and AEA raise 5-HTT expression in the C1–C2, but the combined treatment inhibits this effect—immunohistochemistry data

On microscopic investigation (20 \times objective) of transverse sections of the C1–C2 segments, there were abundant 5-HTT-positive fibres in the superficial layers (I–III) of the dorsal horn. In animals sacrificed four hours after i.p. NTG-injection the 5-HTT-immunoreactive area was significantly higher in each layers compared to the placebo-treated group ($p < 0.01$). This effect has

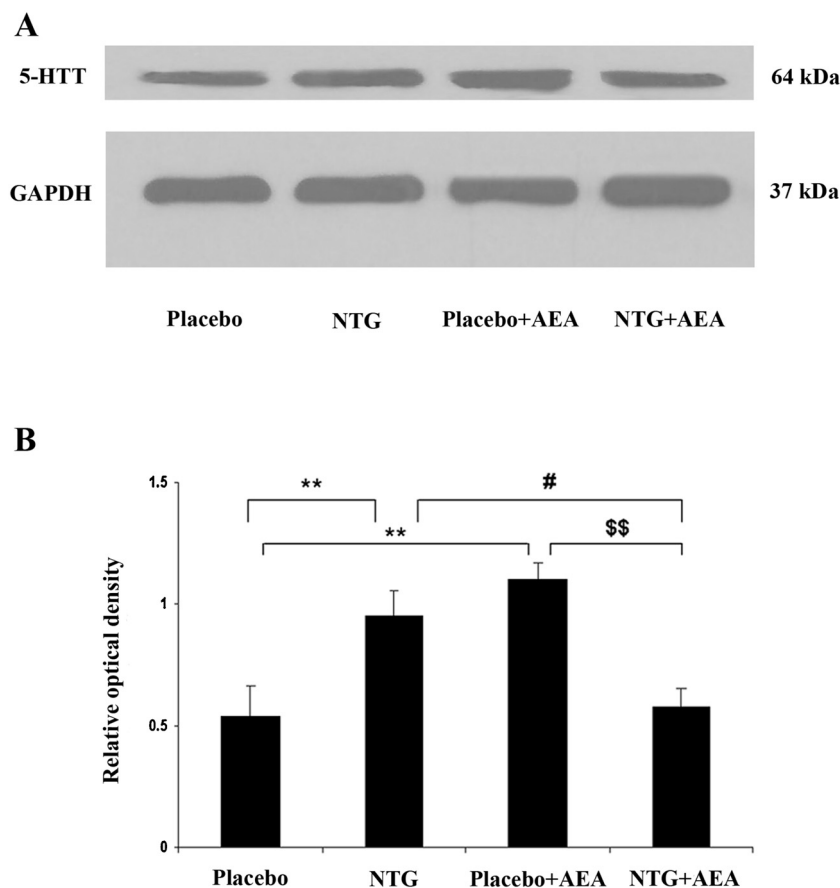


Fig. 3. Summary of Western blot data. A. Western blots of 5-HTT and GAPDH expression in the C1–C2. B. The quantitative analysis shows that in the NTG and AEA groups, the relative optical density of 5-HTT specific bands was significantly higher than in the placebo group. NTG + AEA treatment abolished this effect. # $p < 0.05$; \$\$ $p < 0.01$; ** $p < 0.01$.

been experienced also in the AEA-treated animals ($p < 0.01$; $p < 0.001$). It is interesting that, in the combined NTG + AEA treated group the 5-HTT area fractions were significantly decreased ($p < 0.01$) as compared either with the NTG or the AEA treated groups (lamina I: $F(3,20) = 26.556$; $p = 2 \times 10^{-6}$; lamina II: $F(3,20) = 92.104$; $p = 2.62 \times 10^{-10}$; lamina III: $F(3,20) = 45.300$; $p = 4.81 \times 10^{-8}$) (Fig. 1).

3.2. NTG and AEA also enhance the sizes of the 5-HTT varicose fibres in the C1–C2, but the combined treatment reduces this effect—immunohistochemistry data

On higher magnification ($40\times$ objective), the microscopic examination of the sections revealed numerous immunoreactive processes. The average size of the fiber varicosity was significantly higher in the NTG or AEA treated animals compared to the placebo-treated group ($p < 0.05$). In the combined NTG + AEA treated group, the sizes was reduced ($p < 0.05$) as compared to the NTG or the AEA treated groups ($F(3,20) = 12.071$; $p = 9.9 \times 10^{-5}$) (Fig. 2).

3.3. NTG and AEA increase 5-HTT expression in the C1–C2, but the combined administration attenuates this effect—western blot data

Western blot analysis of the C1–C2 region confirmed the results obtained by 5-HTT immunohistochemistry. The characteristic band of 5-HTT was visualized at 64 kDa. Densitometric analysis showed that, in the NTG and AEA treated groups 5-HTT bands were significantly increased ($p < 0.01$) as compared with the placebo-treated group. After the combined NTG + AEA treatment the bands were significantly decreased ($p < 0.05$; $p < 0.01$) as compared either with the NTG or the AEA treated groups ($F(3,16) = 8.088$; $p = 2 \times 10^{-3}$) (Fig. 3).

4. Discussion

Despite the fact that the role of 5-HT in the migraine pathogenesis is generally accepted, the exact molecular mechanism of its effect is far from being clearly understood. One of the key molecules of 5-HT signaling mechanisms is its membrane transporter 5-HTT, which is responsible for the cellular internalization of the released transmitter, thereby terminating its effect.

In our present study, we found an increase in 5-HTT and processes expression after the NTG administration in rat C1–C2 segments, where most of the trigeminal nociceptive afferents terminate. Our western blot data demonstrate that the endocannabinoid AEA has similar effect; its administration increases the 5-HTT expression.

From functional point of view the observed changes, i.e. the increased transport of 5-HT may indicate a decrease in the serotonergic activity in these brain areas. These observations are in line with previous neuroimaging and molecular biology studies. By using neuroimaging methods (SPECT-images coregistered with MRI-scans) (Schuh-Hofer et al., 2007) it was shown that there is an increased availability of 5-HTT in brainstem in migraine patients during the interictal period. The recent PET-study also confirms that the 5-HTT availability is crucial in the pathomechanisms of migraine (Park et al., 2016). The limitation of the complete comparison of our results with the clinical studies is that the human observations are examining migraine during the interictal period opposite the NTG model of migraine, which is the ictal model of migraine. On the other hand, clinical and experimental data from several laboratories clearly indicate that the 5-HTT gene is one of the genetically contributing factors of migraine (Murphy et al., 2001). In migraine patients with and without aura it has been shown an altered allelic division of the 5-HTT (Ogilvie et al., 1998).

Our data give more emphasis on the role of the transporter in the regulation of 5-HT levels and provide further evidences for the crosstalk existing between serotonergic and NO systems (Miller and Hoffman, 1994; Zhu et al., 2004). By using proteomic methods Chanrion et al. showed that the 5-HTT interacts with the nNOS and they concluded that this physical association may make reciprocal modulation possible (Chanrion et al., 2007). It was also shown that the application of L-NAME (a nonspecific nNOS inhibitor) reduces the vascular abnormalities which are induced by the CSD-triggered 5-HT depletion, suggesting that NO production has a pivotal role in the CSD caused 5-HT depletion (Saengjaroenatham et al., 2015). In addition, Harkin et al. showed that inhibition of NO synthase could be used as a strategy to raise the clinical efficacy of serotonergic antidepressants, enhancing the activity of the drug (Harkin et al., 2004).

A previous study found an increase in the 5-HT-IR fibres in C1–C2 of rats in the NTG-model, which may indicate a reduced release of 5-HT from the terminals (Pardutz et al., 2002). Our present data suggests that NTG may increase 5-HT reuptake and may reduced its levels in the synaptic cleft. In addition, the increased 5-HTT varicosity may suggest a raised 5-HT turnover, as well. This data is in accordance with the HPLC results of Tassorelli and her group, which was shown that NTG can decrease the levels of 5-HT in rats medullary segments (Tassorelli et al., 2002). It has been observed, that the depletion of tryptophan (precursor of 5-HT) is positively correlated with the severity of the headache in migraineurs (Drummond, 2006), and for that reason the decreased level of 5-HT is a crucial factor in the trigeminal activation and the pathomechanism of migraine.

According to our data the endocannabinoid AEA had an effect on the 5-HTT too, it increased its expression. Literature data show that AEA regulates the expression of several genes and some of its effect is receptor (CB1) dependent, but receptor independent actions have also been reported (Correa et al., 2008; Mestre et al., 2011; Sancho et al., 2003). One can not exclude the possibility of some indirect action, because it is known that endocannabinoids are able to raise NO production by upregulating the nNOS activity (Carney et al., 2009). It is therefore possible that the increase of 5-HTT expression is due to the increase of NO after the administration of AEA. The possible role of the endocannabinoid system in the descending modulation of the trigeminal complex was characterized by Akerman and his group. They showed that CB1 receptor activation is able to inhibit the trigeminal nociceptive pathway and AEA is involved in the modulation of the descending trigemino-vascular nociception (Akerman et al., 2013, 2004). In our previous study, we investigated the effect of AEA on the markers of sensitization and inflammation in the NTG model (Nagy-Grocz et al., 2016). Taken together, AEA was able to inhibit the NTG induced changes, suggesting that AEA would have beneficial effect of migraine pathophysiology, while the interaction with the serotonergic axis might be more complex.

It was quite unexpected that in animals treated with NTG + AEA we could not detect changes in 5-HTT expression. The present data do not permit us to explain all aspects of this phenomenon, but we can not exclude the possibility of a negative feed-back mechanism, since both NTG and AEA increase cGMP and NO levels (Carney et al., 2009). It is also worth considering, that administration of NTG increases the activity of enzymes, which break down endogenous endocannabinoids in the midbrain of rats (Greco et al., 2010b), suggesting, that NTG is able to influence the endocannabinoid pathway.

On the other hand, we do not exclude that the combined treatment may act at gene expression level, and the accelerated induction of 5-HTT synthesis and the rapid reversability of expression may result in a recovery to the control level by 4 h.

Further experiments are needed to reveal the molecular background of this interesting observation.

5. Conclusion

The present study has demonstrated that NTG and AEA alone, and in a combined treatment are able to modulate 5-HTT expression. These findings suggest a complex interaction between the serotonergic and endocannabinoid system on the NTG-induced trigeminal activation and sensitization phenomenon, which are important during migraine attack.

Conflict of interest

We declare that we have no conflict of interest.

Authors contribution

GNN: participated in the design and implementation of experiments, statistical analysis, interpreted data and wrote the manuscript, ZSB, AFSZ, KFL, ES, LT: participated in the implementation of the experiments, statistical analysis LV: participated in the design of the experiments, in the final approval of the version to be published, AP: participated in the conception and design of the experiments, the interpretation of the data and writing, all authors: critical revision of the manuscript.

Acknowledgements

This work was supported by the Hungarian Brain Research Program [Grant No. KTIA_13_NAP-A-III/9]; the EUROHEADPAIN [FP7-Health 2013-Innovation; Grant No. 602633] and GINOP-2.3.2-15-2016-00034. Gábor Nagy-Grócz was supported through the ÚNKP-ÚNKP-16-3 New National Excellence Program of the Ministry of Human Capacities. Dr. Árpád Párdutz was supported by the Bolyai Scholarship Programme of the Hungarian Academy of Sciences. We are indebted to Mrs. Valéria Vékony for histotechnical assistance.

References

- Akerman, S., Kaube, H., Goadsby, P.J., 2004. Anandamide is able to inhibit trigeminal neurons using an in vivo model of trigeminovascular-mediated nociception. *J. Pharmacol. Exp. Ther.* 309, 56–63.
- Akerman, S., Holland, P.R., Lasalandra, M.P., Goadsby, P.J., 2013. Endocannabinoids in the brainstem modulate dural trigeminovascular nociceptive traffic via CB1 and triptan receptors: implications in migraine. *J. Neurosci.* 33, 14869–14877.
- Annamalai, B., Mannangatti, P., Arapulisamy, O., Shippenberg, T.S., Jayanthi, L.D., Ramamoorthy, S., 2012. Tyrosine phosphorylation of the human serotonin transporter: a role in the transporter stability and function. *Mol. Pharmacol.* 81, 73–85.
- Borgelt, L.M., Franson, K.L., Nussbaum, A.M., Wang, G.S., 2013. The pharmacologic and clinical effects of medical cannabis. *Pharmacotherapy* 33, 195–209.
- Carney, S.T., Lloyd, M.L., MacKinnon, S.E., Newton, D.C., Jones, J.D., Howlett, A.C., Norford, D.C., 2009. Cannabinoid regulation of nitric oxide synthase I (nNOS) in neuronal cells. *J. Neuroimmune Pharmacol.* 4, 338–349.
- Chanrion, B., Mannoury la Cour, C., Bertaso, F., Lerner-Natoli, M., Freissmuth, M., Millan, M.J., Bockaert, J., Marin, P., 2007. Physical interaction between the serotonin transporter and neuronal nitric oxide synthase underlies reciprocal modulation of their activity. *Proc. Natl. Acad. Sci. U. S. A.* 104, 8119–8124.
- Correa, F., Docagne, F., Clemente, D., Mestre, L., Becker, C., Guaza, C., 2008. Anandamide inhibits IL-12p40 production by acting on the promoter repressor element GA-12: possible involvement of the COX-2 metabolite prostamide E(2). *Biochem. J.* 409, 761–770.
- Crawley, J.N., Corwin, R.L., Robinson, J.K., Felder, C.C., Devane, W.A., Axelrod, J., 1993. Anandamide, an endogenous ligand of the cannabinoid receptor, induces hypomotility and hypothermia in vivo in rodents. *Pharmacol. Biochem. Behav.* 46, 967–972.
- Curran, D.A., Hinterberger, H., Lance, J.W., 1965. Total plasma serotonin, 5-hydroxyindoleacetic acid and p-hydroxy-m-methoxymandelic acid excretion in normal and migrainous subjects. *Brain* 88, 997–1010.
- Danese, E., Montagnana, M., Lippi, G., 2014. Platelets and migraine. *Thromb. Res.* 134, 17–22.
- Di Clemente, L., Coppola, G., Magis, D., Gerardy, P.Y., Fumal, A., De Pasqua, V., Di Piero, V., Schoenen, J., 2009. Nitroglycerin sensitises in healthy subjects CNS structures involved in migraine pathophysiology: evidence from a study of nociceptive blink reflexes and visual evoked potentials. *Pain* 144, 156–161.
- Drummond, P.D., 2006. Tryptophan depletion increases nausea, headache and photophobia in migraine sufferers. *Cephalalgia* 26, 1225–1233.
- Ferrari, M.D., Saxena, P.R., 1993. On serotonin and migraine: a clinical and pharmacological review. *Cephalalgia* 13, 151–165.
- Greco, R., Gasperi, V., Maccarrone, M., Tassorelli, C., 2010a. The endocannabinoid system and migraine. *Exp. Neurol.* 224, 85–91.
- Greco, R., Gasperi, V., Sandrini, G., Bagetta, G., Nappi, G., Maccarrone, M., Tassorelli, C., 2010b. Alterations of the endocannabinoid system in an animal model of migraine: evaluation in cerebral areas of rat. *Cephalalgia* 30, 296–302.
- Harkin, A., Connor, T.J., Burns, M.P., Kelly, J.P., 2004. Nitric oxide synthase inhibitors augment the effects of serotonin re-uptake inhibitors in the forced swimming test. *Eur. Neuropsychopharmacol.* 14, 274–281.
- Horvath, G.A., Selby, K., Poskitt, K., Hyland, K., Waters, P.J., Coulter-Mackie, M., Stockler-Ipsiroglu, S.G., 2011. Hemiplegic migraine, seizures, progressive spastic paraparesis, mood disorder, and coma in siblings with low systemic serotonin. *Cephalalgia* 31, 1580–1586.
- Mestre, L., Inigo, P.M., Mecha, M., Correa, F.G., Hernangomez-Herrero, M., Loria, F., Docagne, F., Borrell, J., Guaza, C., 2011. Anandamide inhibits Theiler's virus induced VCAM-1 in brain endothelial cells and reduces leukocyte transmigration in a model of blood brain barrier by activation of CB(1) receptors. *J. Neuroinflammation* 8, 102.
- Miller, K.J., Hoffman, B.J., 1994. Adenosine A3 receptors regulate serotonin transport via nitric oxide and cGMP. *J. Biol. Chem.* 269, 27351–27356.
- Murphy, D.L., Li, Q., Engel, S., Wichems, C., Andrews, A., Lesch, K.P., Uhl, G., 2001. Genetic perspectives on the serotonin transporter. *Brain Res. Bull.* 56, 487–494.
- Nagy-Grócz, G., Tar, L., Bohar, Z., Fejes-Szabo, A., Laborc, K.F., Spekter, E., Vecsei, L., Párdutz, A., 2016. The modulatory effect of anandamide on nitroglycerin-induced sensitization in the trigeminal system of the rat. *Cephalalgia* 36 (9), 849–861.
- Ogilvie, A.D., Russell, M.B., Dhali, P., Battersby, S., Ulrich, V., Smith, C.A., Goodwin, G.M., Harmar, A.J., Olesen, J., 1998. Altered allelic distributions of the serotonin transporter gene in migraine without aura and migraine with aura. *Cephalalgia* 18, 23–26.
- Párdutz, A., Krizbai, I., Multon, S., Vecsei, L., Schoenen, J., 2000. Systemic nitroglycerin increases nNOS levels in rat trigeminal nucleus caudalis. *Neuroreport* 11, 3071–3075.
- Párdutz, A., Multon, S., Malgrange, B., Párdutz, A., Vecsei, L., Schoenen, J., 2002. Effect of systemic nitroglycerin on CGRP and 5-HT afferents to rat caudal spinal trigeminal nucleus and its modulation by estrogen. *Eur. J. Neurosci.* 15, 1803–1809.
- Park, E., Hwang, Y.M., Chu, M.K., Jung, K.Y., 2016. Increased brainstem serotonergic transporter availability in adult migraineurs: an [(18)F]FP-CIT PET imaging pilot study. *Nucl. Med. Mol. Imaging* 50, 70–75.
- Ramamoorthy, S., Giovanetti, E., Qian, Y., Blakely, R.D., 1998. Phosphorylation and regulation of antidepressant-sensitive serotonin transporters. *J. Biol. Chem.* 273, 2458–2466.
- Rhine, D.N., Anderson, S.L., Gedde, M., Borgelt, L.M., 2016. Effects of medical marijuana on migraine headache frequency in an adult population. *Pharmacotherapy* 36 (5), 505–510.
- Saengjaroentharn, C., Supornsilpchai, W., Ji-Au, W., Srikiatkachorn, A., Maneesri-Grand, S., 2015. Serotonin depletion can enhance the cerebrovascular responses induced by cortical spreading depression via the nitric oxide pathway. *Int. J. Neurosci.* 125, 130–139.
- Sancho, R., Calzado, M.A., Di Marzo, V., Appendino, G., Munoz, E., 2003. Anandamide inhibits nuclear factor-kappaB activation through a cannabinoid receptor-independent pathway. *Mol. Pharmacol.* 63, 429–438.
- Schuh-Hofer, S., Richter, M., Geworski, L., Villringer, A., Israel, H., Wenzel, R., Munz, D.L., Arnold, G., 2007. Increased serotonin transporter availability in the brainstem of migraineurs. *J. Neurol.* 254, 789–796.
- Sicuteri, F., Del Bene, E., Poggioni, M., Bonazzi, A., 1987. Unmasking latent dysnociception in healthy subjects. *Headache* 27, 180–185.
- Sicuteri, F., 1961. Introduction of serotonin antagonists in therapy. *Clin. Ther.* 21, 394–423.
- Smitherman, T.A., Burch, R., Sheikh, H., Loder, E., 2013. The prevalence, impact, and treatment of migraine and severe headaches in the United States: a review of statistics from national surveillance studies. *Headache* 53, 427–436.
- Strassman, A.M., Vos, B.P., Mineta, Y., Naderi, S., Borsook, D., Burstein, R., 1993. Fos-like immunoreactivity in the superficial medullary dorsal horn induced by noxious and innocuous thermal stimulation of facial skin in the rat. *J. Neurophysiol.* 70, 1811–1821.
- Tao-Cheng, J.H., Zhou, F.C., 1999. Differential polarization of serotonin transporters in axons versus soma-dendrites: an immunogold electron microscopy study. *Neuroscience* 94, 821–830.
- Tassorelli, C., Joseph, S.A., 1995. Systemic nitroglycerin induces Fos immunoreactivity in brainstem and forebrain structures of the rat. *Brain Res.* 682, 167–181.

- Tassorelli, C., Blandini, F., Costa, A., Preza, E., Nappi, G., 2002. Nitroglycerin-induced activation of monoaminergic transmission in the rat. *Cephalalgia* 22, 226–232.
- Velenovska, M., Fisar, Z., 2007. Effect of cannabinoids on platelet serotonin uptake. *Addict. Biol.* 12, 158–166.
- Volfe, Z., Dvilansky, A., Nathan, I., 1985. Cannabinoids block release of serotonin from platelets induced by plasma from migraine patients. *Int. J. Clin. Pharmacol. Res.* 5, 243–246.
- Zhou, F.C., Tao-Cheng, J.H., Segu, L., Patel, T., Wang, Y., 1998. Serotonin transporters are located on the axons beyond the synaptic junctions: anatomical and functional evidence. *Brain Res.* 805, 241–254.
- Zhu, C.B., Hewlett, W.A., Feoktistov, I., Biaggioni, I., Blakely, R.D., 2004. Adenosine receptor, protein kinase G, and p38 mitogen-activated protein kinase-dependent up-regulation of serotonin transporters involves both transporter trafficking and activation. *Mol. Pharmacol.* 65, 1462–1474.